Mathematical model of the industrial kitchen steam condenser

Rafał Robert Wieczorek

Thesis to obtain the Master of Science Degree in

Energy Engineering and Management

Supervisors: Prof. Pedro Jorge Martins Coelho
Dr. Arkadiusz Ryfa

Examination Committee

Chairperson: Prof. Francisco Manuel da Silva Lemos
Supervisor: Prof. Pedro Jorge Martins Coelho
Member of the Committee: Prof. Viriato Sérgio de Almeida Semião

June 2018

Acknowledgments

After an intensive period of seven months, today is the day: writing this note of thanks is the finishing touch on my dissertation. It has been a period of intense learning for me, not only in the scientific arena but also on a personal level. I would like to reflect on the people who have supported and helped me so much throughout this period.

I would first like to thank my supervisors Prof. Pedro Jorge Martins Coelho at Instituto Superior Tecnico in Lisbon and Dr Arkadiusz Ryfa at Silesian University of Technology in Gliwice. I want to thank you both for your cooperation and guidance which let me successfully complete my dissertation. I would like to particularly thank Prof. Pedro Jorge Martins Coelho for great reliance on me at the beginning and Dr Arkadiusz Ryfa for providing me with the tools that I needed to choose the right direction and accomplish the goal.

I would also like to thank two much bigger teams. First of all, the Retech company for their collaboration and references I was given to conduct my research. Last but not least words of thanks I would like to target at the KIC Innoenergy. This dissertation has been developed as well as many more activities thanks to Clean Fossil and Alternative Fuels Energy MSc program which I have a great pleasure to be part of.

Thank you very much, everyone.

Abstract

The numerical simulation of a top hood steam condenser (*THSC*) is reported in the present thesis. A *THSC* supports the daily work of a large-scale mass cooking oven, and its main goal is to prevent the accumulation of water vapour in the air released to the kitchen. A secondary goal of the *THSC* is to reduce the unpleasant smells and to avoid increased humidity that may lead to mist appearance. The operation of a *THSC* depends on its geometry and working conditions: temperature and humidity of the air in the kitchen, flow rate of steam flowing from the oven to the *THSC*. The main goal of the present study is to develop a mathematical model to simulate the behaviour of the steam condenser implemented in Visual Basic for Application. It is based on the combination of a single pipe CFD model and on global mass and energy balances for the *THSC*. The predictions are validated against available experimental data. The developed *THSC* model requires much less computing time and human effort to produce satisfactory solutions in comparison with a fully developed CFD model, and allows the user to investigate the behaviour of the *THSC* under various operating conditions, and to perform an analysis of the effect of possible configuration changes. Among the studied modifications, the reduction of the number of pipes, which has no impact on the condensation efficiency, is recommended. This improvement minimizes the cost of the *THSC* and can be carried out with presently used ovens.

Keywords: top hood steam condenser, Fluent, Visual Basic for Application, CFD simulation, working conditions

Resumo

Este trabalho descreve a simulação numérica de um condensador de vapor (top hood steam condenser - *THSC*). O condensador apoia o trabalho diário de um forno e tem como principal objetivo impedir a acumulação de vapor água na cozinha. Os objetivos secundários são a redução de odores desagradáveis e o impedimento do aumento da humidade que pode levar ao aparecimento de névoa. A operação do condensador depende da sua geometria e condições de funcionamento: temperatura e humidade do ar na cozinha, caudal de vapor escoado do forno/fogão para o condensador. O objetivo principal deste estudo é o desenvolvimento de um modelo matemático para simular o comportamento do condensador, implementado em Visual Basic. Este modelo baseia-se na combinação de um modelo de CFD para um único tubo e em balanços globais de massa e energia para o condensador. As previsões são validadas por comparação com dados experimentais disponíveis. O modelo desenvolvido requer muito menos tempo de cálculo para obter soluções satisfatórias comparativamente a um modelo completo de CFD, permite ao utilizador investigar o comportamento do condensador para diferentes condições de funcionamento e analisar o efeito de possíveis alterações geométricas. Entre as modificações estudadas, recomenda-se a diminuição do número de tubos, o que não afeta a eficiência da condensação. Este melhoramento irá minimizar os custos do condensador e pode ser efetuado com os fogões atualmente utilizados.

Palavras chave: top hood steam condenser, Fluent, Visual Basic for Application, simulação computacional de dinâmica de fluidos, condições de funcionamento

Contents

ABSTRACT ..... **V**

RESUMO ..... **VII**

LIST OF FIGURES ..... **XI**

LIST OF TABLES ..... **XIII**

LIST OF ACRONYMS ..... **XV**

NOMENCLATURE ..... **XVI**

1. INTRODUCTION **1**

1.1. RELATED WORK 2

1.2. OBJECTIVES 3

1.3. THESIS STRUCTURE 5

2. TOP HOOD STEAM CONDENSER **6**

3. MODEL **7**

3.1. Geometry *8*

3.2. Mesh *8*

3.3. Fluent model setup *9*

3.4. Turbulence model selection *12*

3.5. Analytical model of the pipe heat transfer *16*

3.6. Fin efficiency analysis *24*

3.7. Pipe equation *25*

3.8. THSC model development *27*

3.8.1. Heat losses *27*

3.8.2. Distribution of air and steam *30*

3.8.3. Correction factors *30*

3.8.4. Description of THSC model operations *32*

3.8.5. Validation *35*

3.8.6. Technological modifications *37*

4. ANALYSIS OF THSC WORK **41**

5. CONCLUSIONS **51**

APPENDIX A **57**

APPENDIX B **63**

List of Figures

FIGURE 1 TOP-SIDE, TOP AND SIDE VIEW OF THSC 6

FIGURE 2 GEOMETRY OF THE PIPE IN DM WITH DIMENSIONS (LEFT) AND EDGE SIZING LOCATION (RIGHT) 8

FIGURE 3 INITIAL (LEFT) AND BENCHMARK (RIGHT) MESHES GENERATED FOR THE PIPE 9

FIGURE 4 LOCATION OF BOUNDARY CONDITIONS IN ANSYS FLUENT FOR SINGLE PIPE MODEL 11

FIGURE 5 AIR (LEFT), FIN&AIR (MIDDLE), OUTLET (RIGHT) CROSS-SECTION SURFACES 12

FIGURE 6 NON-PHYSICAL RESULTS FOR MESH VII 14

FIGURE 7 TEMPERATURE AT OUTFLOW (TOP LINE) AND CROSS-SECTION (BOTTOM LINE) IN: BENCHMARK, MESH XII, MESH III, MESH IV 15

FIGURE 8 VELOCITY AT OUTFLOW (TOP LINE) AND CROSS-SECTION (BOTTOM LINE) IN: BENCHMARK, MESH XII, MESH III, MESH IV .. 16

FIGURE 9 FLOWCHART OF ITERATION FOR STEAM HEAT TRANSFER COEFFICIENT 17

FIGURE 10 TEMPERATURE AT CROSS-SECTIONS T3H3A5M3S4 20

FIGURE 11 VELOCITY AT CROSS-SECTION (MIDDLE RIGHT) AND OUTFLOW (RIGHT) T3H3A5M3S4 20

FIGURE 12 CORRELATION BETWEEN POWER AND MASS FLOW RATE OF AIR 21

FIGURE 13 CORRELATION BETWEEN POWER AND ANGLE OF AIR FLOW RATE 22

FIGURE 14 CORRELATION BETWEEN POWER AND AIR HUMIDITY 22

FIGURE 15 CORRELATION BETWEEN POWER AND STEAM TEMPERATURE 23

FIGURE 16 CORRELATION BETWEEN POWER AND AIR TEMPERATURE 23

FIGURE 17 SURFACES OF HEAT LOSS IN THSC 28

FIGURE 18 SURFACES OF WALL CONDENSATION IN CONDENSATION CHAMBERS OF THSC 29

FIGURE 19 INPUT DATA FOR EPS CALIBRATION 30

FIGURE 20 COMPARISON OF POWER OUTPUT FOR THSC MODEL AND FLUENT WITHOUT CORRECTION FACTORS (TOP) AND WITH THEM (BOTTOM) 31

FIGURE 21 FLOWCHART OF THSC MODEL 32

FIGURE 22 TEMPERATURE RESULTS FROM THSC MODEL VS MEASUREMENTS 36

FIGURE 23 RH RESULTS FROM THSC MODEL VS MEASUREMENTS 36

FIGURE 24 CONDENSATE RESULTS FROM THSC MODEL VS MEASUREMENTS 37

FIGURE 25 THSC MODEL - ENLARGED STEAM PASSAGE 37

FIGURE 26 TEMPERATURE RESULTS FROM THSC MODEL VS MEASUREMENTS – 1ST AND 8TH TIER SWITCHED OFF 38

FIGURE 27 TEMPERATURE RESULTS FROM THSC MODEL VS MEASUREMENT - 1ST AND 2ND TIER SWITCHED OFF 39

FIGURE 28 RH RESULTS FROM THSC MODEL VS MEASUREMENT - 1ST AND 8TH TIER SWITCHED OFF 39

FIGURE 29 RH RESULTS FROM THSC MODEL VS MEASUREMENTS - 1ST AND 2ND TIER SWITCHED OFF 40

FIGURE 30 CONDENSATE RESULTS FROM THSC MODEL VS MEASUREMENTS – 1ST AND 8TH TIER SWITCHED OFF 40

FIGURE 31 CONDENSATE RESULTS FROM THSC MODEL VS MEASUREMENTS – 1ST AND 2ND TIER SWITCHED OFF 41

FIGURE 32 THSC WORK ANALYSIS - GRAPH OF INFLUENCE OF RH 43

FIGURE 33 THSC WORK ANALYSIS - GRAPH OF INFLUENCE OF TEMPERATURE 44

FIGURE 34 THSC WORK ANALYSIS - GRAPH OF INFLUENCE OF STEAM FLOW RATE (ROWS 1-9) 46

FIGURE 35 THSC WORK ANALYSIS - GRAPH OF INFLUENCE OF STEAM FLOW RATE (ROWS 10-18) 47

FIGURE 36 WORKSHEET "INPUT_OUTPUT" IN THE THSC MODEL - INPUTS 57
FIGURE 37 WORKSHEET "INPUT_OUTPUT" IN THE THSC MODEL - OUTPUTS 57
FIGURE 38 WORKSHEET "COMPLEMENTARY_DATA" IN THE THSC MODEL - SAMPLE DETAILED DATA FOR RIGHT SECTION OF THSC . 58
FIGURE 39 WORKSHEET "SAVES" IN THE THSC MODEL - PARAMETERS FOR CALCULATION..... 58
FIGURE 40 GUI1 - INITIAL DATA FOR TOP HOOD STEAM CONDENSER 59
FIGURE 41 GUI1 - HELP 59
FIGURE 42 GUI2 - USER-DEFINED OPTIONS..... 60
FIGURE 43 WARNING COMMUNICATES - CHOICE WINDOW (LEFT) AND ERROR WINDOW (RIGHT)..... 60
FIGURE 44 GUI2 - HELP 61
FIGURE 45 GUI4 - RESULTS..... 62

List of Tables

TABLE 1 VELOCITIES, TEMPERATURES, FLUX VALUES AND EDGE SIZING FOR MESH I-IV 13

TABLE 2 Y* VALUES FOR MESH I-IV 13

TABLE 3 VELOCITIES, TEMPERATURES, FLUX VALUES AND EDGE SIZING FOR I-IV, XII, XIII MESHES AND BENCHMARK 15

TABLE 4 CONVECTIONAL HEAT TRANSFER COEFFICIENT ITERATION 17

TABLE 5 MODEL CASES 19

TABLE 6 POWER OUTPUT FROM FLUENT SIMULATION FOR ALL CASES 24

TABLE 7 HEAT TRANSFER COEFFICIENT FOR PLANE TUBE 25

TABLE 8 COMPARISON OF EMPIRICAL PIPE EQUATION VARIANTS 26

TABLE 9 HEAT LOSS TO THE SURROUNDING THROUGH EXTERNAL WALLS 28

TABLE 10 HEAT PROVIDED THROUGH THE WALLS IN CONDENSATION CHAMBERS OF THSC 29

TABLE 11 CORRECTION FACTORS FOR THSC MODEL 31

TABLE 12 VALIDATION DATA OF THSC MODEL UNDER DEFAULT WORKING CONDITION 35

TABLE 13 THSC WORK ANALYSIS – INCREASE OF RH OF AIR 42

TABLE 14 THSC WORK ANALYSIS - OUTFLOW RESULTS FOR CHANGE OF RH 42

TABLE 15 THSC WORK ANALYSIS - INCREASE OF AIR TEMPERATURE 43

TABLE 16 THSC WORK ANALYSIS - OUTFLOW RESULTS FOR CHANGE OF TEMPERATURE 44

TABLE 17 THSC WORK ANALYSIS - INCREASE OF STEAM FLOW RATE 45

TABLE 18 THSC WORK ANALYSIS - OUTFLOW RESULTS FOR CHANGE OF STEAM FLOW RATE 46

TABLE 19 THSC WORK ANALYSIS - INCREASE OF STEAM FLOW RATE (MIXTURE OF AIR/WATER MIST APPEARANCE) 47

TABLE 20 THSC WORK ANALYSIS - OUTFLOW RESULTS FOR CHANGE OF STEAM FLOW RATE (MIXTURE OF AIR/WATER MIST APPEARANCE) 47

TABLE 21 THSC WORK ANALYSIS - INPUT DATA FOR PIPES MODIFICATION 48

TABLE 22 THSC WORK ANALYSIS - OUTFLOW RESULTS FOR CHANGE OF PIPES WITH EQUAL DISTRIBUTION OF STEAM 48

TABLE 23 THSC WORK ANALYSIS - OUTFLOW RESULTS FOR CHANGE OF PIPES WITH INTERNAL FORMULA FOR DISTRIBUTION OF STEAM 49

TABLE 24 THSC WORK ANALYSIS - OUTFLOW RESULTS FOR CHANGE OF PIPES IN RIGHT SECTION WITH INTERNAL FORMULA FOR DISTRIBUTION OF STEAM 49

TABLE 25 SET OF ALL MESHES AND BENCHMARK 63

List of Acronyms

BSL	Baseline (turbulence k-ω model)
CFD	Computational Fluid Dynamics
DM	Design Modeler
EES	Engineering Equation Solver
Eps	Correction factors in THSC
EWT	Enhanced Wall Treatment
FOU	First Order Upwind
GGNB	Green-Gauss Node Based
GUI	Guideline Userform Interface
LSCB	Least Squares Cell Based
RH	Relative Humidity
SWT	Standard Wall Treatment
THSC	Top Hood Steam Condenser
VBA	Visual Basic for Application

Nomenclature

latin	
A	the angle (α) at which the air inflow the pipe, °
A_{fin}	area of a single fin, m^2
A_s	area of the pipe, m^2
$C_{1\varepsilon}, C_{2\varepsilon}, C_{3\varepsilon}$	Constants, -
c_{pl}	specific heat of liquid, J/kg-K
D_e	external diameter of the pipe, m
D_f	the share of steam mass flow rate directed to the right section of *THSC,* -
D_i	internal diameter of the pipe, m
E	total energy, J
f	friction coefficient, -
g	gravitational acceleration, m/s^2
G_b	generation of turbulence kinetic energy due to buoyancy, -
G_k	generation of turbulence kinetic energy due to mean velocity gradients, -
G_ω	generation of ω, -
$H\ (RH)$	relative humidity of air, -
h_{air_in}	heat transfer coefficient of air inside collecting chamber, W/m^2-K
h_{air_out}	heat transfer coefficient of air outside *THSC,* W/m^2-K
h_{finned}	heat transfer coefficient inside finned tube, W/m^2-K
h_{plane}	heat transfer coefficient inside plane tube, W/m^2-K
h_S	enthalpy of steam for $T_{steam}, (S)$, kJ/kg
h_{steam}	heat transfer coefficient of steam, W/m^2-K
h_{fg}	enthalpy of vaporization, J/kg
h_{fg}^*	modified latent heat of vaporization, J/kg
h_j	sensible enthalpy of species j, J/kg
$\vec{J_i}$	diffusion flux of species i, kg/m^2-s
J_j	diffusion flux of species j, kg/m^2-s
k	kinetic energy per unit mass, J/kg
k	thermal conductivity of the wall, W/m-K
k_{eff}	effective conductivity, W/m-K
k_l	thermal conductivity of the liquid, W/m-K
L	length of the pipe, m
$\dot{m}_{air,i}, (M)$	mass flow rate of the air flowing through the i pipe in *THSC,* kg/s,
$\dot{m}_{cond}$	mass flow rate of steam condensed on the walls of condensation chambers in *THSC,* kg/s
$\dot{m}_{cond,i}$	mass flow rate of steam condensed on the i pipe in *THSC,* kg/s
M_{H2O}, M_{da}	molar mass of water and dry air, $kg_{H2O}/kmol_{H2O}$, $kg_{da}/kmol_{da}$
$\dot{m}_{steam}$	total steam mass flow rate, kg/s
$\dot{m}_{steam\_left,i}$	mass flow rate of steam left to be condensed on the i pipe in *THSC,* kg/s
N	number of tubes, -
n_{fin}	number of fins, -
Nu	Nusselt number, -
p	static pressure, Pa
p_o	air pressure, hPa
$p_{sat}, p_{sat,out,L}$	saturation pressure for $T, T_{out,L}$, hPa
Pr	Prandtl number, -
Q_{CFD}	power output of pipe from CFD model, W

Q_{gain}	heat gain from walls of condensation chambers, W
Q_{lost}	heat loss through the *THSC* walls, W
Q_{pipe}	power output of pipe from formula in *THSC,* W
Re	Reynolds number, -
t	Time, s
T	temperature of the air, K
T_{air_in}	temperature of air inside collecting chamber, K
T_{air_out}	temperature of air outside *THSC,* K
$t_{bfinned}$	area-weighted temperature just for the pipe interface base, K
t_f	average temperature of the fluid in tube, K
t_{fin}	fin thickness, m
t_{finned}	area-weighted average-wall temperature at pipe interface for whole area with fins, K
t_{fluid}	mass-weighted average-static temperature at interior of the pipe for fluid, K
$T_{out,L}$	temperature of mixed air flow rates at the outflow of collecting chamber, K
T_{sat}	saturation temperature, K
T_s	surface temperature, K
$T_{steam,}\ (S)$	temperature of the steam, K
t_w	temperature of the wall in tube, K
T_{wall_air}	temperature of side and top external wall, K
T_{wall_steam}	temperature of backside external wall, K
u_i	velocity magnitude on x_i coordinate, m/s
Y_k	dissipation of k due to turbulence, -
Y_M	contribution of fluctuating dilatation in compressible turbulence to overall dissipation rate, -
Y_{i}	local mass fraction of ith species, -
Y_{ω}	dissipation of ω due to turbulence, -
greek	
Γ	effective diffusivity, -
δ	thickness of the wall, m
ε	turbulent dissipation rate, m^2/s^3
ε	emissivity of the wall surface, -
ε	coefficient for gases, -
$\varepsilon_T, \varepsilon_A, \varepsilon_S, \varepsilon_H$	correction factors with respect to: T, A, S, H, -
η_{fin}	efficiency of the fin, -
μ	dynamic viscosity, Pa-s
μ_l	viscosity of the liquid, kg/m-s
ρ	Density, kg/m^3
ρ_l	density of the liquid, kg/m^3
ρ_v	density of the vapour, kg/m^3
σ	turbulent Prandtl number for k and ε, -
σ	Stefan-Boltzmann constant, W/m^2-K^4
$\vec{v}$	velocity, m/s
$\bar{\bar{\tau}}$	stress tensor, Pa
$\bar{\bar{\tau}}_{eff}$	effective stress tensor, Pa
ω	specific dissipation rate, s^{-1}

1. Introduction

A condenser is a device designed to change the phase of a working fluid from vapour to liquid during the condensation process [1]. It is rather used among other subparts of the technological cycle than separately. The condenser is a heat exchanger putting media of different phases and temperatures into indirect contact so that the energy can easily flow. It can be divided according to size, construction and working medium. Nevertheless, society may associate it mainly with power engineering sector and air conditioning. In reality, condensers are developed and exist in a great amount of non-power producing appliances. One of them, named *top hood steam condenser* (*THSC*), is connected with large-scale mass cooking ovens used in gastronomy.

Invention and technological progress of *THSC*, as well as other heat exchangers, would not be possible without the continuous creation of prototypes and their verification by measurements. However, at the time of economical reasoning such an approach is not sufficient from the investment point of view [2]. To assure the cost limiting, before the production of the first prototype a model of the particular device is created. Similarly, for existing solutions, a model constitutes the grounds for improvements and cost decrease. For both situations, feedback prevents over-scaling and insufficient work of the heat exchanger. That is why nowadays the program-based designing and physical constructing are equally needed for final results. In general, when creating the model two approaches may be chosen. The first way is to make a highly complex model with full numerical computational fluid dynamics (CFD) analysis [3]. Deciding on this, there would be a price to pay for the very detailed solution. Namely, such a model needs a relatively big amount of time and computational effort. Alternatively, there is another way that consists of developing a simple mathematical model that relies only on balance equations (e.g. of mass and energy like in the case of *THSC)* generating a much faster response.

A *top hood steam condenser* is the crucial element of ovens, both in a kitchen and at industrial level, where various types of food are prepared [4]. Thanks to it the air outside the oven is free of high humidity and fog, which are unhealthy. This increased humidity without condenser may appear outside as a result of the food preparation process during which hot air accumulates water. Furthermore, food preparation results in smells production that may be unpleasant. The same *THSC* helps in absorbing them guaranteeing a neutral scent of the nearby air. Since the operating conditions of the *THSC* depend on varying conditions inside the oven as well as in the kitchen, the essential step is to analyze its work. The condensers can be cooled down with either water or air [5]. As the connection of water to *THSC* is not desired by the manufacturer (since it is treated as an operating disadvantage) [4] only air cooling is taken into consideration. When looking at air-cooled condenser the obvious configuration is that steam condensates inside the tubes while air flows at the outside. Then, the outside surface is finned to facilitate the heat flow [6]. Such designs are deeply studied and described. The analyzed condenser is, however, a unique construction. Namely, in *THSC* the air flows inside the internally finned tubes which are surrounded by the steam. This kind of pipe has not been analyzed in the literature yet. Moreover, the pipe of such a construction is rarely met on the market, which makes the company strongly dependent on one of the subcontractors. Having in mind the condenser is already on sale and the pipe is an underbelly of a whole device, the Retech company is highly interested in the improvement of *THSC*

production process. According to the relatively big number of pipes mounted in *THSC,* the suspicion appears that it is over-scaled and that the number of pipes may be reduced. If so, then minimizing the number of pipes in each condenser would lead to a decreased pipes stock and improved accounting liquidity of the Retech company.

The Retech company declares an interest in the model that can present the performance of *THSC* under various working conditions with respect to the actual geometry of their device. In addition, the model is aimed to foresee trends of *THSC* behaviour for structural changes. It is pointed out that the crucial issue is the calculation time and availability of the software for the company employees. Even though CFD model of whole *THSC* can fully foresee its performance, the computational power and price of the software are not attractive to the company. The ease of use and fast response of the model are agreed to characterize its work at the price of a simplified way of calculated results [4]. Therefore, to address all requirements a mathematical model implemented in Excel is proposed.

1.1. Related work

Searching for heat exchangers in the literature allows one find that those devices are commonly used in a wide range of applications, from power production in power units to chemical processing or air-conditioning and heating systems in households. The device facilitates the exchange of heat between two fluids differing in temperature but, in comparison to mixing chambers, it does not allow them to mix. Heat transfer in heat exchangers usually consists of two phenomena like convection in each fluid and conduction through the wall separating the two fluids [1]. A vast range of applications requires different types of hardware that operate with different configurations of heat transfer equipment. The devices are matched with requirements within the specified constraints that, in consequence, result in numerous types of heat exchanger designs.

Heat exchangers may be classified by their degree of compactness, by flow arrangement, or by construction. According to the first category, compactness of heat exchangers is expressed by the ratio of heat transfer surface area to unit volume (called area density). Within this classification compact device is the one that comprises large heat transfer keeping small volume (area density greater or equal than 700 m^2/m^3). Furthermore, both flows can either run side by side (e.g. in double-pipe), be in counterflow (with cold and hot streams flowing in opposite directions) or in crossflow (having two flow streams normal to each other) with respect to flow arrangement. Finally, in classification by construction one can distinguish heat exchangers in the form of double-pipe (fluids flow inside the internal pipe and through the annular space between the two pipes) or shell-and-tube (from one U-tube bundle up to a several hundred tubes packed in the shell) [5]. Apart from this, an innovative type of plate and frame (or just plate) heat exchanger with the widespread use or regenerative type with the alternate passage of the cold and hot fluids through a porous mass with high storage capacity can be found. To reflect specific applications, heat exchangers are often given specific names like condenser – most important type of heat exchanger with respect to the area of interest of this thesis.

Most condensers used for both home and industrial appliances are air-cooled exchangers or shell-and-tube exchangers [6]. In the former, usually the ambient air as coolant is blown across the tubes

by fans and condensing vapor flows inside a bank of finned tubes. Other types of equipment are less frequently used (double-pipe, plate-and-frame, direct contact condensers). Mentioned fins are mounted optionally but, assuming good condensate drainage (right fin spacing), condensing coefficients for finned tubes tend to be substantially higher than for plain ones [7]. That is why usually in air-cooled steam condensers the fins appear to increase heat transfer surface area compensating far less specific heat value for air as the cooling medium. Moreover, it can be said that generally finned heat exchangers are used when liquid flows inside the tubes while the second fluid is a gas. When plate-type exchangers are concerned they are described as un-finned, finned on one side only or finned on both the process-air side and the cooling air-side (provided always that in close-circuit appliances the process-air side is never finned because of the obstruction risk with respect to deposition of impurities) [8]. When reading articles about the phenomenon of heat transfer it is easy to come to a conclusion that neither tried theoretical sources nor modern experimental study [9] considers the situation in which air-cooled condenser consists of internally finned tubes.

Even though, analyzed *THSC* can be classified as compact, air-cooled heat exchanger with mixed cross-flow configuration, there is no such a construction mentioned in the literature. In other words, steam condenser with fins mounted inside the tubes where air flows is a unique conception for this device. Usually, according to literature, air-cooled steam condenser works with hot process fluid flowing through a bank of finned tubes while ambient air is blown across the tubes impelled by one or more fans. Therefore, it is clear the air that exhibits a heat transfer coefficient lower by two-three orders of magnitude than that of water needs enlarged contact area to intensify the heat transfer on the internal side of the tubes. The lack of corresponding examples in literature results in two main conclusions. Unfortunately, the work of this thesis cannot be based on already developed references, which makes it more complicated; results and conclusions cannot be easily compared to work of other authors. On the other hand, such a situation makes this work a real research work which is a more challenging task. What is more, afterthoughts from this work are unique at the moment of the document creation, which makes them even more attractive.

1.2. Objectives

Since the following thesis is made in cooperation with the industry – Retech company, the goals standing behind it are correlated mainly with the needs of this company. As it is mentioned in an introduction above, production of *THSC* carries nowadays relatively high level of reliance on subcontractors because of the internally finned pipes. The rareness of this type of pipes influences the cost of the condenser and finally the cost of the *THSC* itself. Unfortunately, *THSC* on its own is only a subpart of another Retech product on sale. That is why the company cannot fully resign from this product but looks for improvements of their *THSC* design. Here, one can find the first general aim of this work – to find the way or tool helping in the process of improvement.

Nevertheless, it is necessary to understand the way how the *THSC* works. Since the most important thing is the quality of the released air, it has to be defined which input parameters influence the performance of the condenser and, more important, what kind of values should be identified for

verification of the right operation of *THSC*. The answer for the latter is the humidity, temperature and carried smells (or to be strict the lack of last in the outlet air). To keep a comfortable atmosphere in the kitchen, the *THSC* has to firstly filter the air from food fragrances. Secondly, it must limit the temperature and humidity increase preventing the accumulation of humidity in the room where the oven is located and, in consequence, the creation of mould. That is why output parameters like temperature and relative humidity of the released air have to be anticipated with respect to given inputs. Moreover, the user has to be informed about the appearance of a mixture of air/water mist at the outlet of *THSC,* which disqualifies its work as a condenser [4].

According to the fact the *THSC* is on sale in only one variant at the moment, it is crucial to verify what is the exact range of feasible working conditions under which its performance is right. This information answers the question about possible applications and limits which cannot be exceeded. On the other hand, there is a suspicion that considered the design of *THSC* is highly over-scaled in many appliances and generates unreasonable investment cost. That is why it should be allowed to check what is the margin for optimization for various set of working conditions. In the framework of the thesis, it is verified whether the *THSC* model can predict the behaviour of the device also when implementing the structural changes – testing another prototype. In other words, the model aims to reflect the *THSC* performance with actual design and when reducing the surface area of heat exchange. Thanks to that, not only extreme working conditions can be tested but also customized versions of *THSC*. Knowing what to do to help in improvements, namely which aspects have to be analyzed, permits to have time to consider how this should be done.

In this part, the main goal is to create the model that allows Retech employees to analyze independently the work of *THSC*. As mentioned previously, theoretically the most straightforward solution would be to create the numerical model of the whole *THSC*. Nevertheless, fully developed CFD model of *THSC* involves an enormous number of elements and complicated mesh. It requires a huge amount of time not only to calculate the results but also to be prepared after any change of geometry. To make any adjustments in the model one has to know exactly what to change in the setup. Since Retech company is not interested in either buying the license for CFD software, which is costly, or ordering consecutive researches from outsourcing companies, a mathematical model seems to be a better solution. However, since mass and energy balances made to the entire device is not enough to reflect the performance of *THSC* it is decided that those two approaches meet halfway. Namely, a numerical model of the single pipe is performed to describe the behaviour of the condenser itself for various air/steam values. Then, feedback from this analysis is integrated into the mathematical model that consists of mass and energy balances of several subsections of *THSC.* This simplified *THSC* model is designed to generate a quick response for a wide range of inputs. The other reason standing behind the project is the availability of the Microsoft Office.

Thanks to CFD model of the single pipe the representative number of case differing by working condition is performed. Having the results, it is possible to answer the question whether this model is necessary at all or tabular efficiencies for externally finned pipes can be used. Since a possible number of cases is infinite the analyzed ones are chosen to cover the widest feasible area of change. Results

of the CFD simulations for the single pipe are used as a base for a development of the single pipe thermal response model. In the form of the empirical equation, the model of the single pipe is combined with global mass and energy balances to create one final air-cooled steam condenser model. After this integration, and since the goal is to have reliable feedback, a major step is to validate the predictions of the *THSC* model against data from measurements [10].

While fulfilling this goal further activities may focus on refining the *THSC* model from the point of view of its future service by Retech company employees. The *THSC* model is created in the form of black box keeping in mind there should be no need of interfering with the code or demand for advanced knowledge. The aim is to make the programme as user-friendly as possible. Therefore, its operation is controlled by conditions which not only eliminate mistakes but also activate reports informing the user in the event of an exceptional situation. In order to provide easy access and service, *THSC* model is implemented with the use of Graphical User Interface (GUI) in Excel file with an intuitive interface based on Visual Basic language.

It should be emphasized that the CFD model for *THSC* would give more accurate results than the present mathematical model. Nevertheless, building consecutive prototypes, as well as advanced numerical models, is not fast enough and what is more important generates costs that can be avoided by the manufacturer. That is why for the preliminary analyzes Retech company is willing to receive the mathematical model providing quick and rough analysis of the *THSC* work without demand for high computational power and huge investment. According to that, the main goal of the thesis is to answer the question whether a relatively simple model which can be used independently by Retech company is able to reflect the performance of *THSC*.

1.3. Thesis structure

The whole thesis consists of a few stages of work in different softwares and connected with separate duties. To achieve the goals, the study is organized in the following chapters. Apart from the introduction, thesis consists of four more chapters. In chapter 2, the *top hood steam condenser* construction is described and its way of work is illustrated. Chapter 3 presents the whole preparation process and description of the *THSC* model. Sections 3.1 and 3.2 describe the process of building the geometry and mesh necessary to create a single pipe model. Sections 3.3 and 3.4 introduce the model settings in Fluent as well as the selection of activated models. Section 3.5 describes the choice of parameters as well as their influence on the power of the pipe described in numerical model. Section 3.6 verifies the legitimacy of using above model to describe the operation of a single pipe in relation to the usage of available tabular values, illustrating the efficiency of externally finned pipes. Section 3.7 focuses on creating an empirical equation describing the work of a single pipe. The entire section 3.8 describes the creation of the final *THSC* model taking into account heat losses, flow rates distribution and necessary correction factors calibrating its performance. Finally, in the same subchapter, a flowchart is presented depicting the work of the model itself. The prepared *THSC* model is validated and used for verification of a new prototype. In chapter 4, the *THSC* work under different operating conditions and

settings is analyzed using *THSC* model. The last chapter 5 gathers conclusions and afterthoughts from work.

2. Top Hood Steam Condenser

When analyzing the construction of *THSC*, two parts should be distinguished: cold (blue) and hot (red) in Figure 1. The former includes the air inlet (1) with filters (2) and a fan (3). The hot part consists of distribution chamber (4) and two condensation sections: the left (5) and right (6) where each consists of 24 pipes. Below the left condensation chamber there are two steam channels (7). In addition, there can be also distinguished two heated air collecting chambers on the sides of condensation sections respectively (8-9) and the mixing chamber (10) located above the distribution chamber and condensation sections. Last two locations are air outflow (11) and condensate runoff (12).

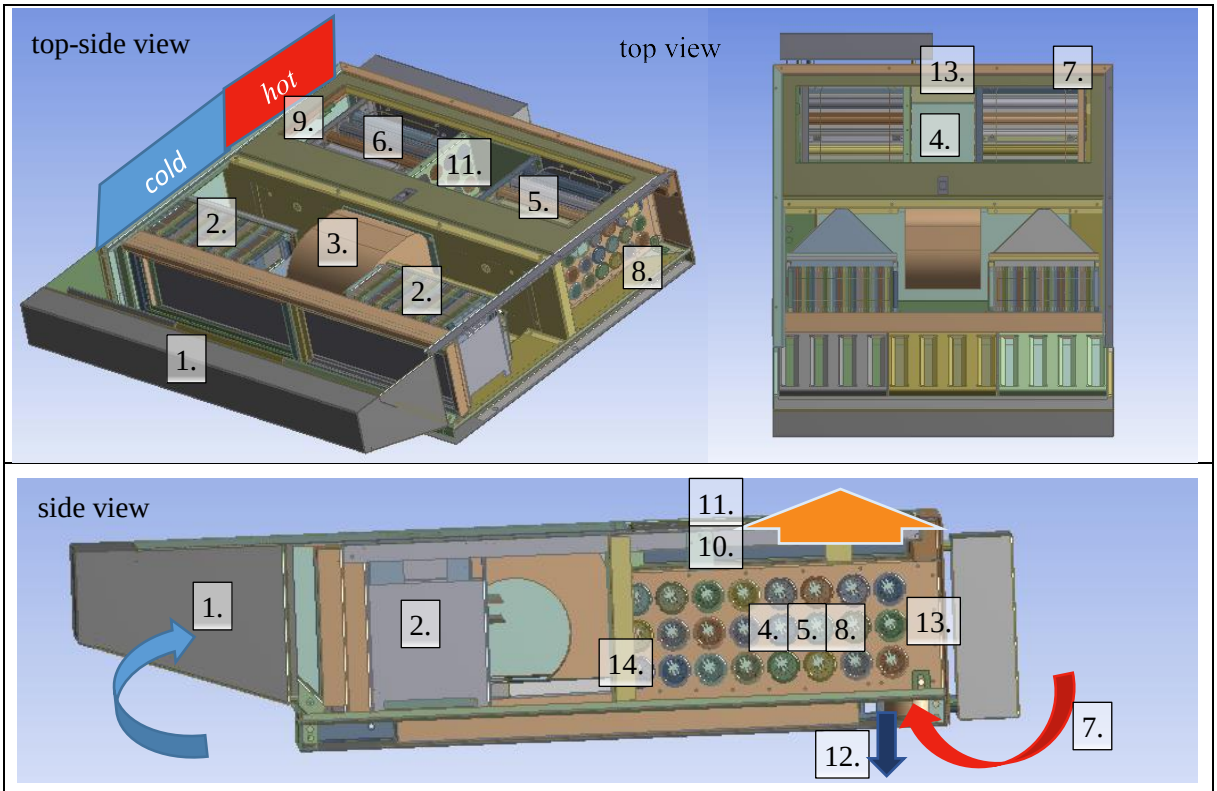

1. Air inflow (blue arrow)	6. Right condensation section	11. Air outflow (orange arrow)
2. Air filters	7. Steam inflow (red arrow)	12. Condensate (navy arrow)
3. Fan	8. Left air collecting chamber	13. Steam passage
4. Distribution chamber	9. Right air collecting chamber	14. Vents
5. Left condensation section	10. Mixing chamber	

Figure 1 Top-side, top and side view of THSC

To describe the principle of operation of the *THSC* it is reasonable to start from the cold part of the condenser. The atmospheric air is sucked in (1) and flows through the filters (2) and a fan (3) to the distribution chamber (4) where it spreads between 48 pipes divided equally on the right (6) and left (5) sections of *THSC*. The air absorbs there the heat from the condensing steam flowing between the pipes, perpendicularly to them. The already warmed air leaving the tubes comes to the collecting chambers behind the appropriate sections and passes over them to the mixing chamber (10) from where it is

directly released through the air outflow (12) to the surroundings of the device. The steam enters the *THSC* via steam channels (7) and is divided between two condensation sections. To the left section (5) steam comes directly while to the right one (6) it goes through the narrow steam passage (13). After the condensation process, the appearing condensate flows down to the oven through the condensate runoff (12). If some of the steam does not condensate passing through all 8 columns of the pipes then it is sucked by the fan through the small vents (14) installed on the wall that separates cold and hot part of *THSC*. That amount of steam then is mixed with air from the inflow.

3. Model

The *THSC* model consists of two parts. First of all, a CFD model of a single pipe is prepared to estimate the dependence of the condensation on various working condition. The second part is the mass and energy balances for different parts of *THSC* i.e. left section of the THSC, the right one, collecting chambers and finally the mixing chamber of the condenser. Therefore, the creation of the final model consists of a few stages working with mainly Fluent, Engineering Equation Solver (EES) and VBA in Excel. In the following subchapters, the whole process is described starting from CFD model for a single pipe from *THSC* through building the matrix of solutions and verifying the parameters up to their implementation and final *THSC* model creation.

Having all the necessary dimensions available on complex CFD assembly drawing the model of a single pipe in the whole condenser does not have to be created from the scratch [4]. Although, the geometry of the single pipe can be copied directly from the mentioned drawing, it is decided to build up a new one. Assembly drawings consist of many detailed dimensions and parts separated in the way which let the constructor know how to manufacture and assemble the final products. That information is good to have in mind but unessential for numerical purposes. In consequence, that drawing is organized with respect to a different approach.

To ensure good quality of the results it is decided to build a fully structural hexahedral mesh through the pipe [3]. This decision has to be made before the creation of the geometry as it influences all the initial steps starting from a sketch in DM and ending on edge sizing of the elements in Mesher. It means single solid part of the pipe, as well as the single volume of air inside it, is divided into much smaller hexahedral subparts to prevent the creation of non-structural or mixed mesh which is easier to be built but worse from the quality of solution point of view.

The second reason is having much smaller parts it is possible to specify more precisely where the model has denser mesh and where not necessary. This is crucial when the amount of mesh elements has to be limited like in this project. To solve the mass and energy balances mentioned mesh is condensed both inside and nearby the fins where intense heat exchange took place (a temperature gradient is higher between neighouring points) while in the core of the pipe the same mesh can stay thinner (the same gradient is lower).

3.1. Geometry

Before drawing the geometry of the single pipe in Design Modeler all the necessary dimensions and features related to this pipe have to be found in documentation [4], see Figure 2. First of all, it is checked that the 0.95 mm thick pipe (1) is made of steel and has 285.6 mm of length (2). Along the pipe of 28 mm internal diameter (3), there are 12 fins mounted evenly around the circumference. Each of the 1mm thick fin (4) has 6.25 mm of length (5). Additionally, fins end at the top with a curvature of 0.5 mm diameter and at the base the filletings on both sides are 0.6 mm diameter. According to last two dimensions at this stage of mesh building, an important simplification is assumed. All the top and bottom curvatures of the fins are neglected and fins are assumed to be square. It can be done since from the heat transfer point of view the change is negligible. On the other hand, numerically, for the mesh creation and Fluent calculation, such an assumption drastically improves the feasibility of the solution. It is related to the fact that when some small curvatures were left the software would have problems with meshing close to them influencing the quality of the final mesh [3]. The final effect of the geometry can be seen in Figure 2 below.

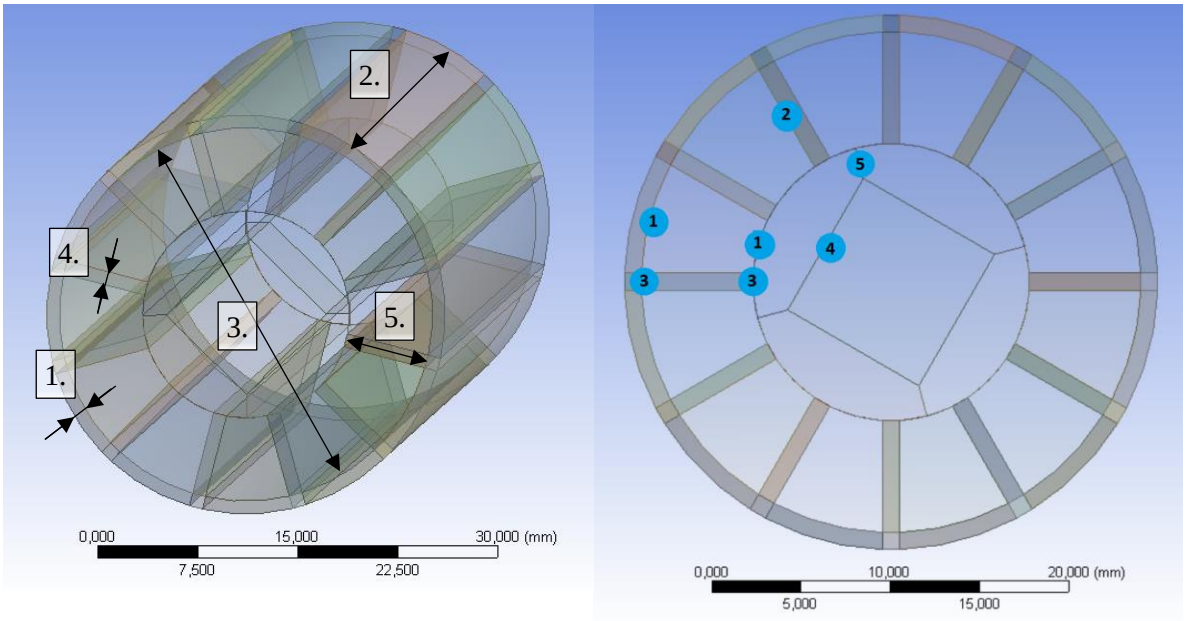

Figure 2 Geometry of the pipe in DM with dimensions (left) and edge sizing location (right)

Although the geometry of the pipe is symmetrical, the pipes are installed in the *THSC* perpendicularly to the outlet of the fan. In consequence, the air flows through the pipes of *THSC* in a non-symmetrical way under different angles. Since there is no certain information how the air flow rate will deflect inside the pipe, at this stage of model preparation the only way is to take the geometry of the whole pipe instead of a repeatable pipe fragment.

3.2. Mesh

Before the analysis, another assumption related to the mesh is set. This time it is the academic campus version of Ansys that should be used. This results in the mesh that should consist of not more than half of a million elements (512,000 elements). The goal is to have the reliable and fast model. Such

a demanding condition results in validation of mesh in each subpart of the geometry. In consequence, the number of the elements is decreased, for example in the middle of the pipe where heat transfer between neighboring layers of the air is not that important. On the other hand, next to the fins the same number is increased. Since a number of the elements along the pipe is to be decreased, edge sizing is additionally used with the bias factor. It provides denser mesh at the inlet where the flow rate is more irregular in comparison to the outflow.

To eliminate doubts whether the solution depends on the number of elements and keep the limitation, it is decided to generate one much bigger mesh. This mesh consisting of 2 million elements is validated and assumed as a benchmark for coarser ones. To implement the benchmark mesh in Fluent without any limitation one of the university clusters is used. Initially, meshes I-IV with various meshes are created (presented in next chapter in Tables 1-2). Based on the results two models, namely I and II are rejected as they produced unfeasible results in terms of velocity and temperature. On the basis of models III and IV, the new models with changed edge sizing and using bias factor are prepared. The aim of this is to find the mesh which is the combination of III and IV models with results close enough to benchmark (right view in Figure 3) to accept the model as the final one.

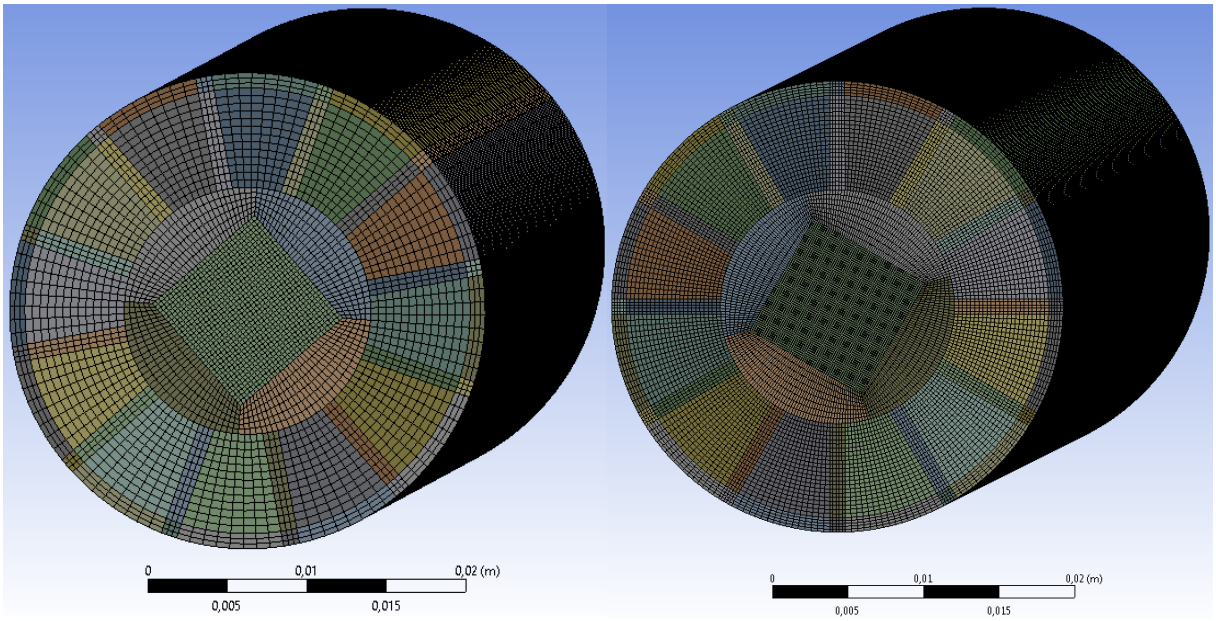

Figure 3 Initial (left) and benchmark (right) meshes generated for the pipe

3.3. Fluent model setup

To generate solutions for a single pipe model ANSYS Fluent software is used. Going through the Setup it is decided to use a Steady Flow Solver with turned off gravity as for the gas it has no significant influence. Since the flow of air involves heat transfer ANSYS Fluent solves not only conservation equations for mass and momentum but also for the energy.

According to the fact that in this case there is not source of mass taken into account the equation for mass conservation applied in Fluent is as follows (1).

$$\nabla \cdot (\rho \vec{v}) = 0 \tag{1}$$

ρ – density kg/m^3, $\vec{v}$ – velocity m/s

Similarly, in case of momentum conservation equation, there is not either source of the momentum or gravitational body force. That is why formula of the equation is given as (2).

$$\nabla \cdot (\rho \vec{v} \vec{v}) = -\nabla \mathrm{p} + \nabla \cdot (\bar{\bar{\tau}}) \tag{2}$$

p – static pressure Pa, $\bar{\bar{\tau}}$ – stress tensor Pa

For the energy in ANSYS Fluent, keeping in mind that there is no volumetric heat source included, the equation used for calculation is given in the following form of equation (3). In this equation k_{eff} – depends on turbulent thermal conductivity related to the used turbulence model. Since the model is pressure-based the reference temperature for enthalpy is 298.15 K.

$$\nabla \cdot \left(\vec{v}(\rho E + p)\right) = \nabla \cdot \left(k_{eff} \nabla \mathrm{T} - \sum_j h_j \overrightarrow{J_j} + (\bar{\bar{\tau}}_{eff} \cdot \vec{v}) \right) \tag{3}$$

$\bar{\bar{\tau}}_{eff}$ – effective stress tensor Pa, E – total energy J, k_{eff} – effective conductivity W/m-K, T – temperature K, h_j – sensible enthalpy of species j J/kg, J_j – diffusion flux of species j kg/m^2-s

When describing the viscosity model it is worth to mention that two turbulence models are tested, namely k-ε and k-ω. For the former one Standard, k-ε model with Standard Wall Functions is activated without taking into account any user-defined source terms. To obtain the turbulence kinetic energy and rate of dissipation following transport equations (4-5) are used.

$$\frac{\partial}{\partial x_i}(\rho k u_i) = \frac{\partial}{\partial x_j}\left[\left(\mu + \frac{\mu_t}{\sigma_k}\right)\frac{\partial k}{\partial x_j}\right] + G_k + G_b - \rho\varepsilon - Y_M \tag{4}$$

$$\frac{\partial}{\partial x_i}(\rho \varepsilon u_i) = \frac{\partial}{\partial x_j}\left[\left(\mu + \frac{\mu_t}{\sigma_\varepsilon}\right)\frac{\partial \varepsilon}{\partial x_j}\right] + C_{1\varepsilon}\frac{\varepsilon}{k}(G_k + C_{3\varepsilon}G_b) - C_{2\varepsilon}\rho\frac{\varepsilon^2}{k} \tag{5}$$

k – kinetic energy per unit mass J/kg, ε – turbulent dissipation rate m^2/s^3, u_i – velocity magnitude on x_i coordinate m/s, μ – dynamic viscosity Pa-s, σ – turbulent Prandtl number for k and ε, G_k – generation of turbulence kinetic energy due to mean velocity gradients, G_b – generation of turbulence kinetic energy due to buoyancy, Y_M – contribution of fluctuating dilatation in compressible turbulence to overall dissipation rate, $C_{1\varepsilon}, C_{2\varepsilon}, C_{3\varepsilon}$ – constants

Since not this but the k-ω model is used, the transport equations for Standard k- ω Model with Standard Wall Functions is used to obtain turbulence kinetic energy and its rate of dissipation as shown (6-7).

$$\frac{\partial}{\partial x_i}(\rho k u_i) = \frac{\partial}{\partial x_j}(\Gamma_k \frac{\partial k}{\partial x_j}) + G_k - Y_k \tag{6}$$

$$\frac{\partial}{\partial x_i}(\rho \omega u_i) = \frac{\partial}{\partial x_j}\Gamma_\omega \frac{\partial \omega}{\partial x_j} + G_\omega - Y_\omega \tag{7}$$

ω – specific dissipation rate s^{-1}, Γ – effective diffusivity, G_ω – generation of ω, Y_k – dissipation of k due to turbulence, Y_ω – dissipation of ω due to turbulence

Because in the air there is also a water-vapor included, species model is activated with species conservation equation without any user-defined sources. That is why the formula for species transport is given as (8).

$$\nabla \cdot (\rho \vec{v} Y_i) = -\nabla \cdot \vec{J_i} \tag{8}$$

Y_i – local mass fraction of i[th] species, $\vec{J_i}$ – diffusion flux of species i kg/m^2-s

Having the models chosen next step is to specify properties of the materials. Constant values are used since within the analyzed range changes there are not significant variations to be taken into account. Thus, for pipe made of steel, density, specific heat and thermal conductivity are taken respectively equal to: 8030 kg/m^3, 502.48 J/kg-K, 16.27 W/m-K.

To set the boundary conditions for the pipe, first the wall condition is set for external, inlet and outlet walls as well as the pipe interface. The external wall is the one and only having the convection boundary condition (dark red color – (1) in Figure 4). Initially h_{steam} – heat transfer coefficient is set at the level of 9000 W/m^2-K with respect to preliminary analytical calculation in EES and free stream temperature equals to the steam one which is 373 K. Analytical calculations prove that assumption of temperature boundary condition instead of convective one influences the heat flux transferred through the pipe. For the inlet and outlet wall, the insulation has to be set by choosing the zero heat flux (red color – (2) in Figure 4). For a plane of air at the inlet (green color – (3) in Figure 4) with 25 mm hydraulic diameter given [1] initially the velocity condition is set. This calculated hydraulic value is necessary since it differs from the dimension of the pipe because of the fins which influence the results. In addition, the velocity of the air and the turbulent intensity are specified as 10 m/s and 10% respectively. There is no data allowing for verification of the velocity profile thus, it is assumed uniform. The flow rate of the air initially is normal to the boundary (α=0° in Figure 4). For the same boundary condition, the temperature is specified as 300 K while at the outlet only the outflow is set with no other specification. Outflow condition is enough in single pipe model since, differently from CFD model, for the whole *THSC* [10] in the single pipe model the pressure drop at the outlet of the pipe does not influence the air flow rate distribution and final results. Values such as the temperature of air and steam as well as the direction of the flow rate are changed further when calculating various cases of single pipe model to know the correlation between them and the power of the single pipe.

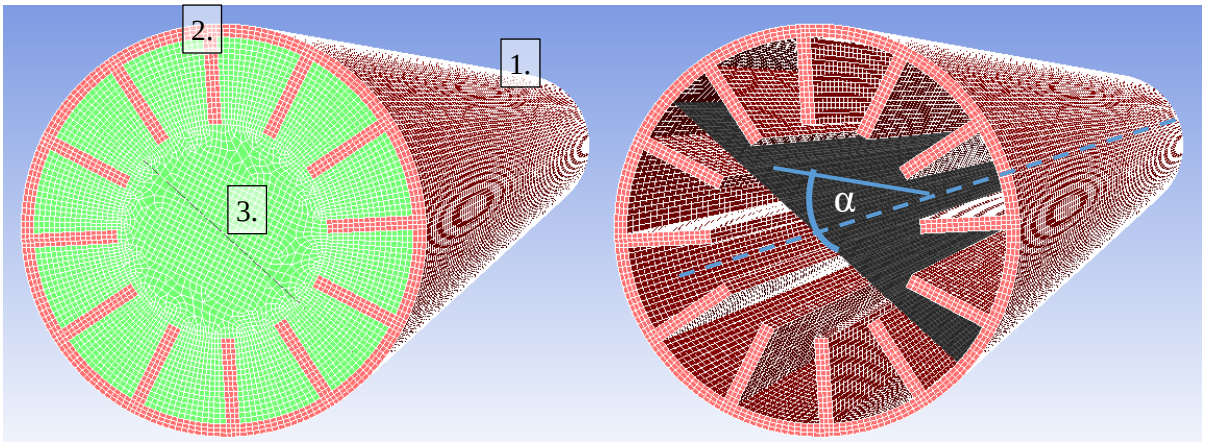

Figure 4 Location of boundary conditions in ANSYS Fluent for single pipe model

When the boundary conditions are set the methods are specified in the Solution. At the beginning, the First Order Upwind (FOU) option is chosen with the Green-Gauss Node Based (GGNB) Gradient. Though they are not the proper ones they let the solution to initially converge. It happens like that since the values for succeeding cells are calculated based on the relation of precedent cell. Afterwards, the GGNB Gradient with Second Order Upwind (SOU) option is set. At that time, for each cell calculation, all the neighboring elements are taken into account.

3.4. Turbulence model selection

As it is mentioned before two turbulence models are tested: k-ε and k-ω. First one is dedicated for flows with high Reynolds number like in this case (about 17,000 for 10 m/s). Depending on the parameter Y* dissimilar approaches for the subdivisions of the near-wall region can be applied. Either Standard Wall Treatment (SWT), for which the correctness of the results can be assumed when the mentioned parameter is not lower than 11.225 or the Enhanced Wall Treatment (EWT) where Y* must not be higher than 1.

Four meshes (labelled I-IV) with various element density are generated. Below, in Table 1, a comparison of edge sizings between all four meshes can be observed (numbers in the brackets correspond to right view in Figure 2). Meshes from I to III are built similarly using face meshing for all 53 elements on the base of the pipe. That guarantees the square elements have the regular and repeatable shape. The only difference between them is the number of elements generated in particular bodies. Enough number of elements between the fins (right view (1) in Figure 2) in those models results in too dense mesh inside the pipe. Such a huge density in the core of the flow is unnecessary since there is no big change happening there. Differently from these three meshes, the face meshing in the IV mesh covers all the same elements except 4 arcs inside. Thanks to that the edge sizing for two opposite edges of those quadrants can differ. Then some triangular elements might appear there but it is an acceptable sacrifice. In consequence, the number of inner elements can be significantly reduced separately from air-between-fins-spaces where this amount matters a lot.

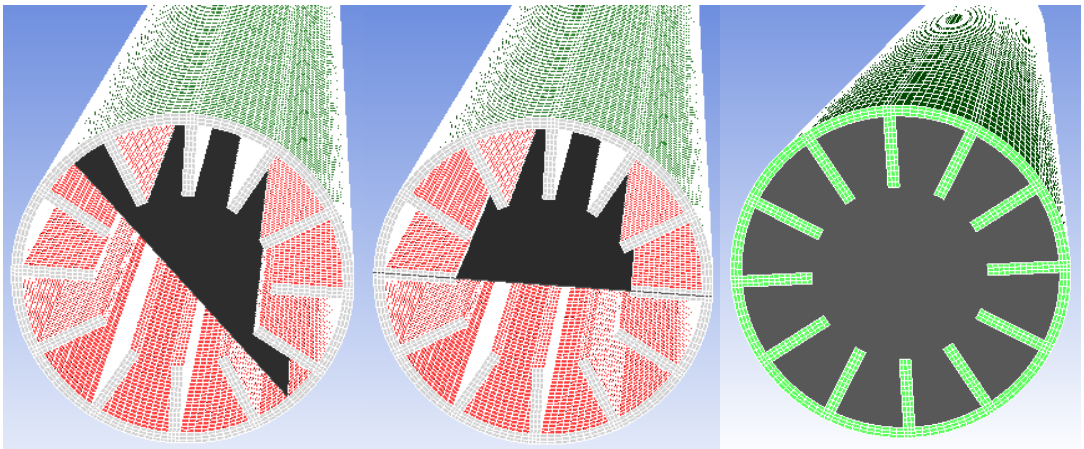

Figure 5 Air (left), Fin&air (middle), Outlet (right) cross-section surfaces

Verification of the results is conducted comparing the temperature and velocity in two ways: values for surface integrals at the outlet and in macroscopic way contours at cross-section planes. Even though the net values for total heat transfer and mass flow rate in fluxes confirm convergence of the

models, the results for surface integrals are not identical. The received temperatures and velocities are compared in Table 1 below. The potential reason of those discrepancies is noticed further in macroscopic comparison of temperature and velocity profiles. Surfaces are presented in the Figures 5.

Table 1 Velocities, temperatures, flux values and edge sizing for mesh I-IV

K- ε models					
mesh name		**IV**	**III**	**II**	**I**
surface integrals					
report type	**surface***	**velocity values [m/s]**			
mass-weighted average	air cross-section	10.93	10.62	10.56	10.57
	fin&air cross-section	12.02	11.45	11.26	10.55
	outlet air	10.78	10.74	10.71	10.65
report type	**surface***	**temperature values [K]**			
mass-weighted average	air cross-section	309.00	309.08	310.21	309.87
	fin&air cross-section	305.31	306.88	309.58	312.69
	outlet air	333.93	329.91	332.22	331.66
fluxes					
mass flow rate net results [kg/s]		-8.67E-19	-1.82E-17	-7.81E-18	6.94E-18
total heat transfer rate net results [W]		-8.40E-11	-2.27E-12	9.71E-11	-2.31E-11
edge sizing**		**number of elements**			
air top/bottom between fins (1)		16	6	8	8
air between fins side (2)		23	10	12	13
fin top/bottom side (3)		4	2	3	3
inside square side (4)		40	24	33	33
between arcs side (5)		8	4	6	6
pipe side (along the pipe)		200	100	110	120

*cross-sections showed in Figure 5, ** numbers corresponds to the right view in Figure 2

For all cases, there is a problem: the generated mesh would be either too dense or too sparse. As it can be seen in values from the Table 2 neither SWT nor EWT are proper. Though the k-ε model is mostly the first choice for Fluent in this case according to a limited number of elements the results do not fit a specified range of values what is an obstacle.

Table 2 Y values for mesh I-IV*

K- ε models					
mesh name		**IV**	**III**	**II**	**I**
report type	**surface**	**Y* values**			
facet minimum	pipe interface shadow	7.62	8.24	8.83	10.43
facet maximum		16.53	20.57	20.08	26.41
facet average		10.39	12.34	12.43	16.16

Therefore, it is decided to switch from k-ε model to k-ω one in which results do not depend on the Y* parameter and which avoids numerical instability. Having the viscous model changed the rest of the settings and steps are repeated for a new simulation like before. In total, 13 meshes are analyzed: I-IV corresponds to the previous ones with the k-ε model. Comparing them to the benchmark meshes I

and II are rejected according to relatively incorrect results. Meshes III and IV are better but not satisfactory enough. That is why meshes V-XIII are newly generated taking the feedback from III and IV as a starting point. Meshes V-X are denser along the pipe at the price of a smaller number of elements in cross-section. Meshes XI-XII are modified with opposite approach giving up a high number of elements along the pipe to make the mesh denser in cross-section.

All the meshes are correct according to the results from fluxes and both mass and energy balances. However, simulations V-XI generated non-physical results in some number of cells. Namely, just behind the inlet where the boundary condition is set to 300 K the temperature in some elements is below this value. The sample situation from one of the models can be observed below in Figure 6.

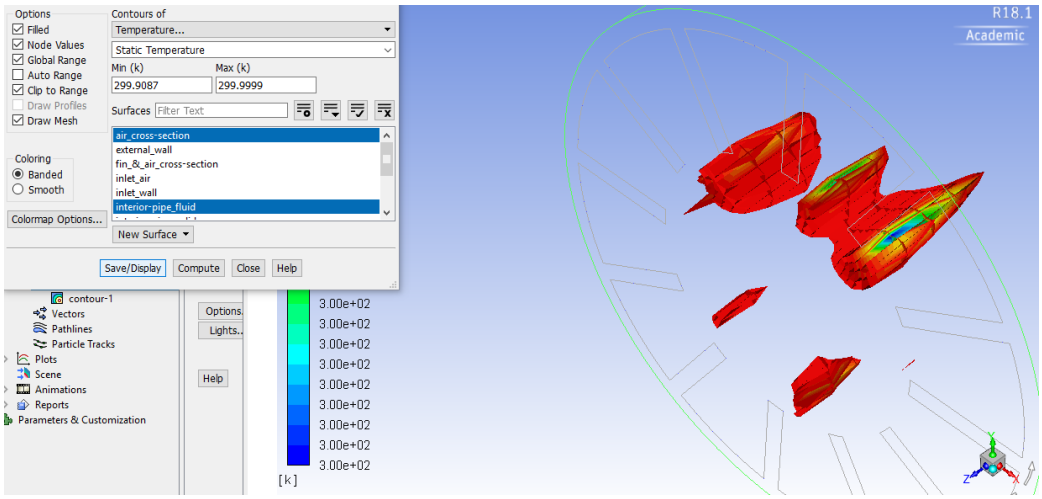

Figure 6 Non-physical results for mesh VII

Not being sure about the source of such a numerical discrepancy and having in mind it might undermine the model validity all models with such results are rejected. Since such a behaviour is not observed for the last two meshes, where the number of elements is coarser in cross-section, the final choice is between the two of them. Comparing models XII and XIII with III and IV it turns out that decreasing the number of elements alongside and having denser mesh between fins indicate a better quality of the results. The reduced number of elements along the pipe comparing XII and XIII does not improve the quality of the results with respect to the benchmark. Therefore, it is decided mesh XII (orange in Table 3) is satisfactory enough comparing to benchmark to be the final one. The results of the analysis for all meshes and benchmark are shown in Appendix B while error-free ones are gathered in Table 3. Moreover, in Figures 7-8, three meshes are compared macroscopically with the benchmark.

Table 3 Velocities, temperatures, flux values and edge sizing for I-IV, XII, XIII meshes and benchmark

K- ω models								
mesh name		**benchmark**	**I**	**II**	**III**	**IV**	**XII**	**XIII**
surface integrals								
report type	**surface***	**velocity values [m/s]**						
mass-weighted average	air cross-section	11.03	10.68	10.72	10.73	11.02	11.22	11,27
	fin&air cross-section	11.09	10.38	11.28	11.55	12.15	11.97	12,17
	outlet air	11.28	10.91	10.99	11.02	11.07	11.14	11.17
report type	**surface***	**temperature values [K]**						
mass-weighted average	air cross-section	309.27	311.23	311.31	310.15	309.67	308.36	308,30
	fin&air cross-section	311.32	316.11	311.64	307.86	305.97	306.12	305,23
	outlet air	331.11	333.54	334.09	331.05	334.06	331.27	331.28
fluxes								
mass flow rate net results [kg/s]		3.7E-17	-1.7E-17	0.0E+00	0.0E+00	6.9E-18	-2.6E-18	-1.4E-17
total heat transfer rate net results [W]		-4.8E-13	6.2E-12	-1.2E-11	-1.6E-12	-2.6E-11	4.7E-12	6.2E-12
edge sizing**		**number of elements**						
air top/bottom between fins (1)		16	6	8	8	10	14	16
air between fins side (2)		23	10	12	13	14	16	16
fin top/bottom side (3)		4	2	3	3	3	3	3
inside square side (4)		40	24	33	33	20	20	20
between arcs side (5)		8	4	6	6	6	6	6
pipe side (along the pipe)		200	100	110	120	100	95	88

*cross-sections showed in Figure 5, ** numbers corresponds to the right view in Figure 2

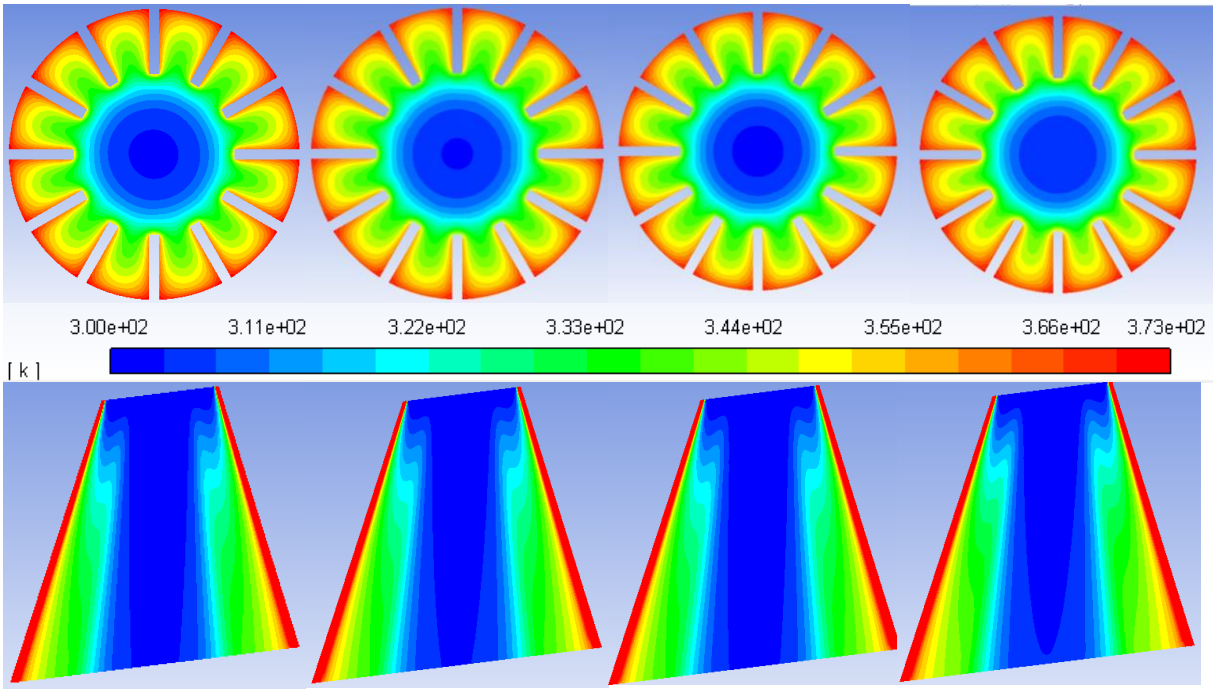

Figure 7 Temperature at outflow (top line) and cross-section (bottom line) in: benchmark, mesh XII, mesh III, mesh IV

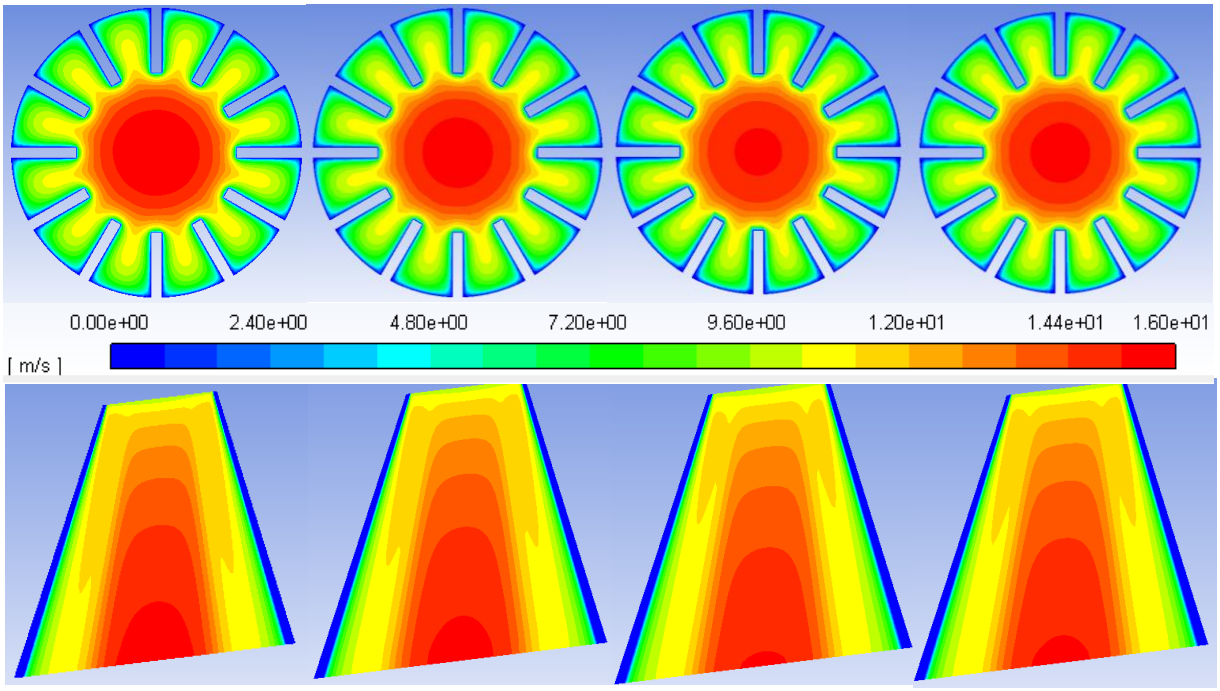

Figure 8 Velocity at outflow (top line) and cross-section (bottom line) in: benchmark, mesh XII, mesh III, mesh IV

3.5. Analytical model of the pipe heat transfer

The model XII described in the previous chapter is the final one and thus it is used further when generating an input data for the analytical model. Having the model ready, to simulate next the various states under which the pipe can be during *THSC* work, it has to be decided which parameters may change. The first factor, which may matter is h_{steam} – the convection heat transfer coefficient outside the pipe for steam condensation [11]. The final value is calculated iteratively using the written code in Engineering Equation Solver and Fluent final model. Mentioned EES software is used since it is a dedicated engineering tool for complicated calculations, making it course the iterative process, that eliminates the problem of equations transformation [12]. What is even more important in this case is that it has built-in thermodynamic tables from which necessary parameters can be read-in. The procedure of computing h_{steam} consists of a few steps starting from assumption for h_{steam} in Fluent. For given h_{steam} the power and wall temperature are obtained. The latter is used in EES to calculate the new h_{steam} for horizontal tubes in vertical tier [13] and power from equations (9-11). The new h_{steam} is applied in Fluent as a new assumption.

$$h_{horiz,N\ tubes} = 0.729 \cdot \left[\frac{g \cdot \rho_l \cdot (\rho_l - \rho_v) \cdot h_{fg}^* \cdot k_l^3}{\mu_l \cdot (T_{sat} - T_s) \cdot N \cdot D_e}\right]^{1/4} \quad (9)$$

$$h_{fg}^* = h_{fg} + 0.68 \cdot c_{pl} \cdot (T_{sat} - T_s) \quad (10)$$

$$Q = h_{horiz} \cdot A_s \cdot (T_{sat} - T_s) \quad (11)$$

g – gravitational acceleration m/s^2, ρ_l – density of the liquid kg/m^3, ρ_v – density of the vapour kg/m^3, h_{fg}^* - modified latent heat of vaporization J/kg, k_l – thermal conductivity for the liquid W/m-K, μ_l – viscosity of the liquid kg/m-s, T_{sat} – saturation temperature K, T_s – surface temperature K, N – number of tubes, D_e – external diameter of the pipe m, h_{fg} – enthalpy of vaporization J/kg, c_{pl} – specific heat of liquid J/kg-K, A_s – area of the pipe m^2

Analogically the convectional heat transfer coefficient and wall temperature are shared between two softwares until noticing no change in values of power output. The procedure is shown in the Figure 9.

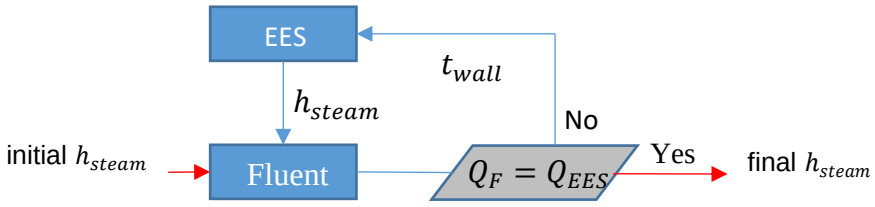

Figure 9 Flowchart of iteration for steam heat transfer coefficient

Final h_{steam} for which both EES and Fluent give comparable values is at the level of 30230 W/m^2-K. Nevertheless, the difference in power is relatively negligible throughout the range which eliminates h_{steam} as a crucial parameter to be changed. From now on the h_{steam} is equal to the last reached value. All the steps can be seen in Table 4.

Table 4 Convectional heat transfer coefficient iteration

EES			Fluent		
Temperature of the wall	h_{steam}	Q	Temperature of the wall	h_{steam}	Q
K	W/m2K	W	K	W/m2K	W
372.14	22367	518.1			
372.65	28046	263.3	372.65	22367	210.0
372.72	29671	222.5	372.72	28046	210.3
372.74	30230	210.4	372.74	29671	210.3
			372.74	30230	210.3

Furthermore, it is decided to take into consideration five parameters which may influence the pipe performance, which are: *T* – the temperature of air, *H* – relative humidity of air, *A* – the angle at which the air inflow the pipe (0° when normal to the boundary and 90° for parallel to the boundary as shown in Figure 4), *M* – mass flow rate of the air flowing through the pipe and finally *S* – temperature of the steam. Even though it is clear the number of possible configuration is infinite, matrix of solution is built on the basis of representative cases in limited amount. Such a decision results from the limited time and computational power for each simulation. The reasoning behind the choice of specific cases is to select widest possible distribution of the parameters within chosen variants. Furthermore, to have some step pattern it is decided that mostly one factor is changed while the others stay constant. It guarantees observation of tendency when varying one variable only. Even if for each given factor there were chosen 5 representative values to be checked the number of variants would be 5^5=3125 which gives roughly almost 1.5 years to calculate 4-hour long simulations. That is why, it is decided to choose the base variant with 20 more modified versions. Each variant is named on the basis of the parameter and the number representing the value e.g. T3H3A4M3S4 – stands for the base model described further.

The basic variant is assumed according to the measurements [4] as the most representative one with average or most probable values. It means the case in which the 30°C air of 60% relative humidity enters the pipe at an angle 45° to the central axis of the pipe. The air flow rate assumed as

average is equal to 1/48 of the measured mass flow rate flowing through *THSC* which is 0.003958 kg/s (corresponds to the velocity of 10 m/s and Re=17006) while the steam temperature is 100°C [10]. When setting these parameters in Fluent except air mass flow rate and its temperature the other ones have to be given indirectly. For the air humidity, one more time the EES software with its tables is used to calculate the mass fraction of water for given temperature. The angle value is put in the form of Cartesian coordinates while the steam temperature is set as a temperature of the wall. All those values are specified in the form of boundary conditions.

Then, choosing the modification it is assumed that when changing one parameter the others remain the same as in base variant. In the end, three more specific sets of values are specified. Two of them assume two opposite extreme conditions for heat exchange in the pipe while the last one is randomly chosen with all values not set previously. When it comes to air temperature it is assumed the values may vary from T1 – 20°C to T6 – 40°C. Other temperatures of the air should not appear in the kitchen where people work. In case of air humidity, the range H1 – 40 to H6 – 100 percent as well as the angle of air flow rate A1 – 10° to A6 – 80° is much wider. Both factors can strongly vary what prevent from limiting the range. Nevertheless, it should be highlighted that specific perpendicular arrangement of the pipes towards the main air inflow [4] eliminate the possibility of small angle values and flow parallel to pipe axis. More probable are the high values which still taking turbulence and swirl into account cannot be taken for granted. In the case of air flow rate values are specified intuitively starting from M1 – half of default mass flow rate (equal to 0.003958 kg/s and related to 10 m/s velocity and Re=17006) up to M5 – double basic value (equal to 0.007917 kg/s and related to 20 m/s and Re=34014). At the end the temperature of the steam is decreased from S4 – 100°C up to S1 – 90°C since the air may appear together with the steam which causes lower saturation temperature.

Statistically, the values of all parameters should appear the same amount of times except the basic ones which can be seen in major part. All the cases are gathered together in Table 5 where orange background highlights unchanged factors with respect to the basic case while the white color points out the varying one.

Table 5 Model cases

Variant name	parameter				
	air temperature	air humidity	air inlet angle	air mass flow rate	steam temperature
	°C	%	°	kg/s	°C
T3H3A4M3S4	30	60	45	0.003958	100
T1H3A4M3S4	20	60	45	0.003958	100
T2H3A4M3S4	25	60	45	0.003958	100
T5H3A4M3S4	35	60	45	0.003958	100
T6H3A4M3S4	40	60	45	0.003958	100
T3H1A4M3S4	30	40	45	0.003958	100
T3H2A4M3S4	30	50	45	0.003958	100
T3H5A4M3S4	30	80	45	0.003958	100
T3H6A4M3S4	30	100	45	0.003958	100
T3H3A1M3S4	30	60	10	0.003958	100
T3H3A3M3S4	30	60	30	0.003958	100
T3H3A5M3S4	30	60	60	0.003958	100
T3H3A6M3S4	30	60	80	0.003958	100
T3H3A4M1S4	30	60	45	0.001979	100
T3H3A4M4S4	30	60	45	0.005937	100
T3H3A4M5S4	30	60	45	0.007916	100
T3H3A4M3S1	30	60	45	0.003958	90
T3H3A4M3S2	30	60	45	0.003958	94
T6H6A5M1S1	40	100	60	0.001979	90
T1H1A2M5S4	20	40	20	0.007916	100
T4H4A6M2S3	32	70	80	0.002968	98

The procedure of generating solutions for each of the cases is similar to the previously described for the k-ω model. The only exception takes place in the T3H3A6M3S4 and T4H4A6M2S3 variant where convergence problems appear. Therefore, to prevent such problems those calculations are initialized from the beginning with applied Baseline k-ω (BSL) turbulence model with curvature correction activated. Though chosen BSL model is similar to standard k-ω, it consists of blending function. It activates standard k-ω model in the near-wall region and transformed k-ε one far away from the surface. In addition, the curvature correction sensitizes model to the effects of streamline curvature.

Since all cases differed from each other it is hard to present each of them in this work. Therefore, it is decided to show a sample result T3H3A5M3S4 in which the angle is 60°. First of all, one can see the temperature and velocity distribution on the same planes which are used to present both k-ε and k-ω models (Figures 7-8). Views in Figures 10-11 show the flow inside a pipe is no longer symmetrical with respect to the pipe axis, which in consequence gives unequal heat transfer along the pipe. That is why the velocity and temperature profiles are somehow moved in comparison to those from previous Figures.

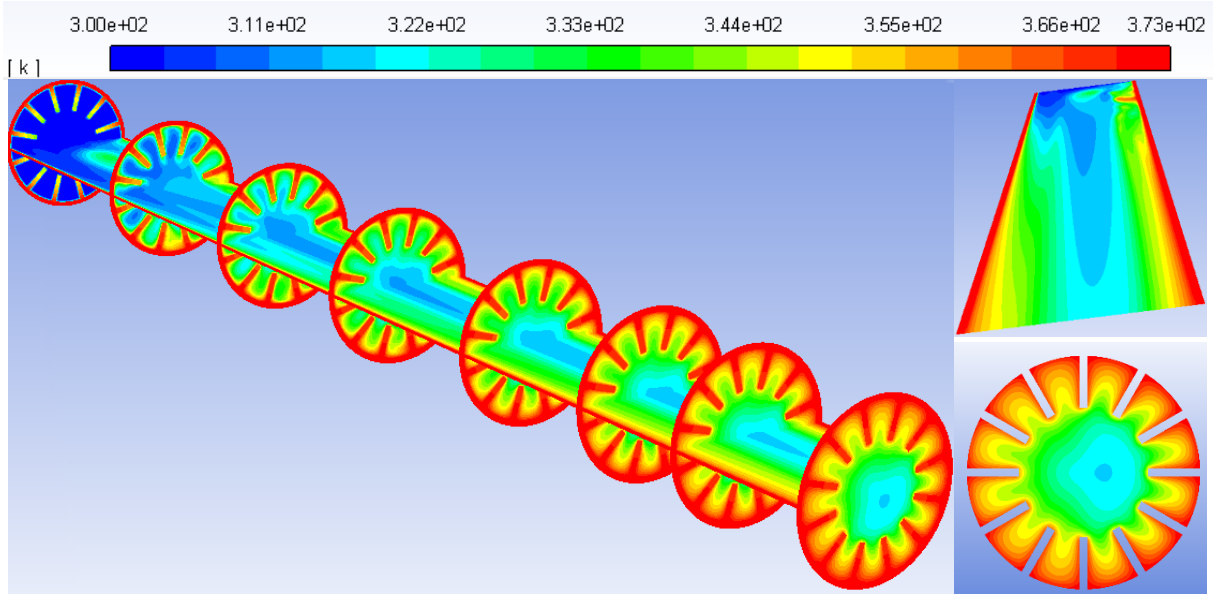

Figure 10 Temperature at cross-sections T3H3A5M3S4

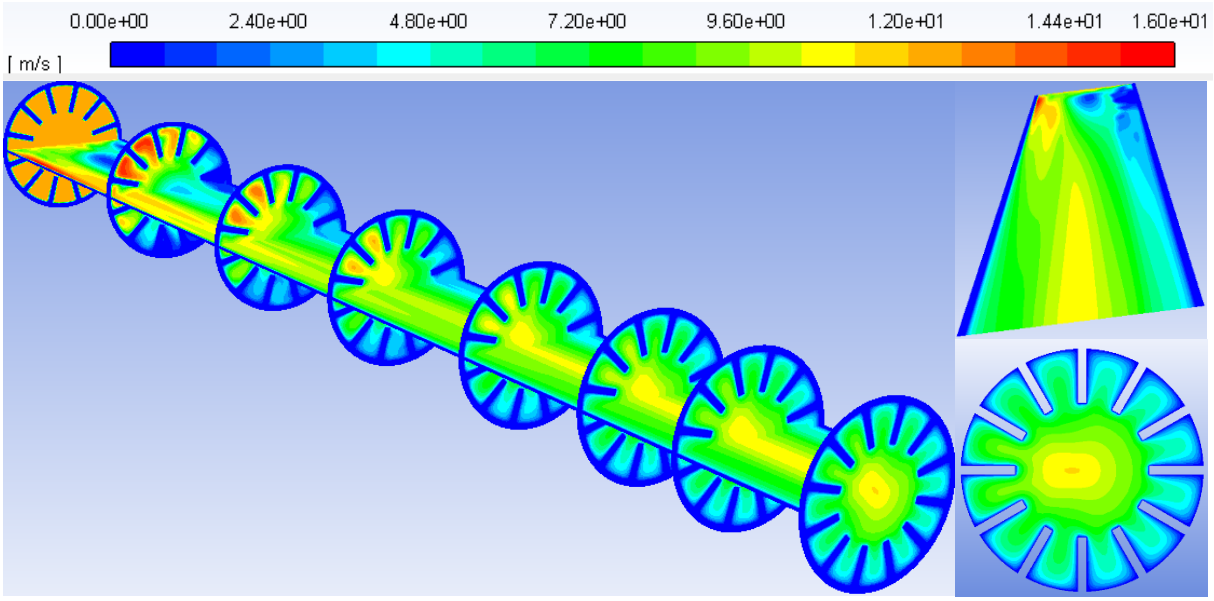

Figure 11 Velocity at cross-section (middle right) and outflow (right) T3H3A5M3S4

It can be said the inflowing air in this case enters the pipe towards the left side from the shown perspective and bounces to the opposite one. In time, until the outflow both velocity and temperature values spread out more and more evenly. Nevertheless, the trend of velocity decrease from the core of the flow to the walls corresponds to the opposite change in a temperature increase from external walls to the core. It happens like this since the lower the speed of medium the more heat is absorbed and accumulated in one place increasing the temperature and impairing the heat transfer rate. Even though, unequally loaded walls may mean the pipe does not work evenly on the whole perimeter, it can be seen further in Table 6 that unsymmetrical flow and appearing swirling terms give the higher power output.

Having all the models finished it is possible to analyze the influence of each factor on the power of the pipe. It is decided to develop an empirical equation as such approach allows for encompassing all analyzed parameters on the power of the pipe. Since the empirical equation has to define the

correlation between each parameter and power they are analyzed separately. To visualize the changes, cases are grouped and presented in a graphical way. For each of the graph, the trend line with the equation is generated using the Excel file.

The strongest influence and biggest increase in power can be noticed when changing the mass flow rate of the air. The tendency of the change, in this case, is quadratic and the direction of change is straightforward. The more air goes through the pipe the more heat it can take from the steam which is seen in the power increase. Such a relation is logical and takes place not only for air since the final amount of heat taken by any medium depends on multiplication of both specific heat and amount of the medium itself [5]. The measured points with the trend line can be seen in Figure 12. What is more, it is checked that for the values of mass flow rate greater than 0.0167 kg/s the trendline give inversed results with decreasing power which is unacceptable and limited in consequence.

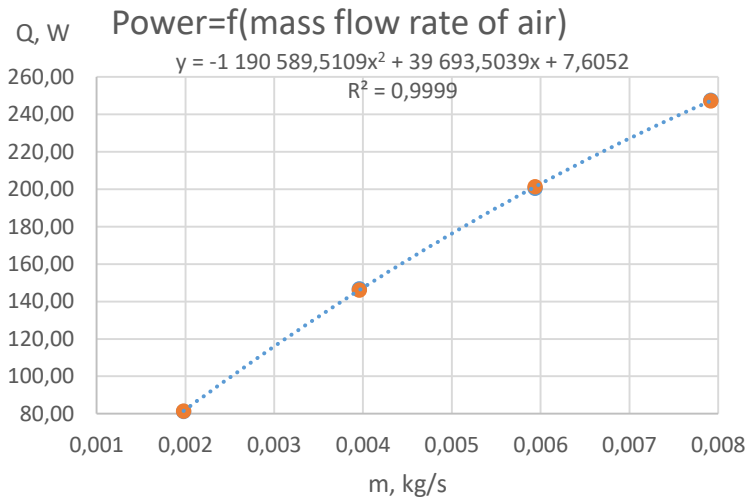

Figure 12 Correlation between power and mass flow rate of air

Similarly to mass flow rate, the quadratic trend line is matched with the correlation between power output and angle of the air flow rate entering the pipe. The lower the value of the angle the more parallel is the flow direction with respect to pipe axis and the lower is the power. Air which does not enter the pipe parallel may slide along the wall leaving the opposite wall unloaded or deflects causing more turbulent flow and giving more time for heat exchange. In such a short pipe it is very probable deflections occurred improving the power output in comparison to parallel flow. Even though the equation describing this relation looks more complicated than the first one and the range of change is smaller. Nevertheless, both parameters are considered as the basis of the final empirical equation which is described wider further in this chapter. The correlation and trend line formula are shown below in Figure 13.

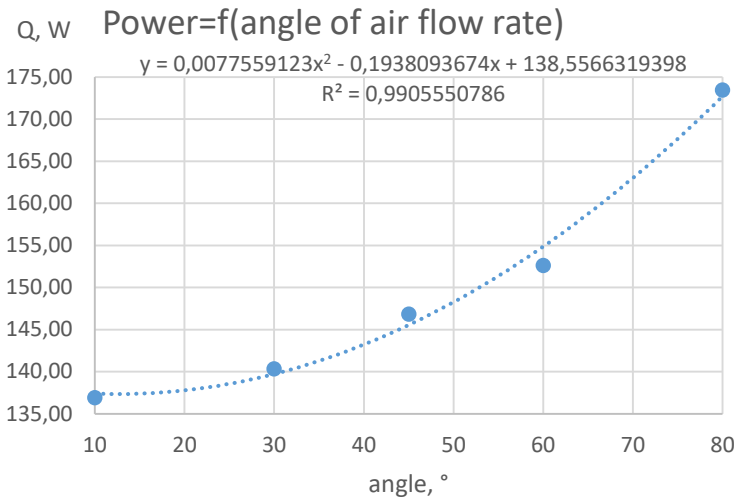

Figure 13 Correlation between power and angle of air flow rate

The rest of the parameters show linear behaviour. The increase of relative humidity (RH) of the air and steam temperature in analyzed range result in an increase of the power. In the case of the RH, the reason of such a trend is the greater specific heat value for water vapour comparing to two times smaller value of the same parameter for air. In consequence, the higher humidity in air the more heat it can take. On the other hand, mentioned increase is relatively small, almost negligible. The reason for that is that the humidity represents only a tiny part of the air. The trend line with the predicted values is shown in Figure 14.

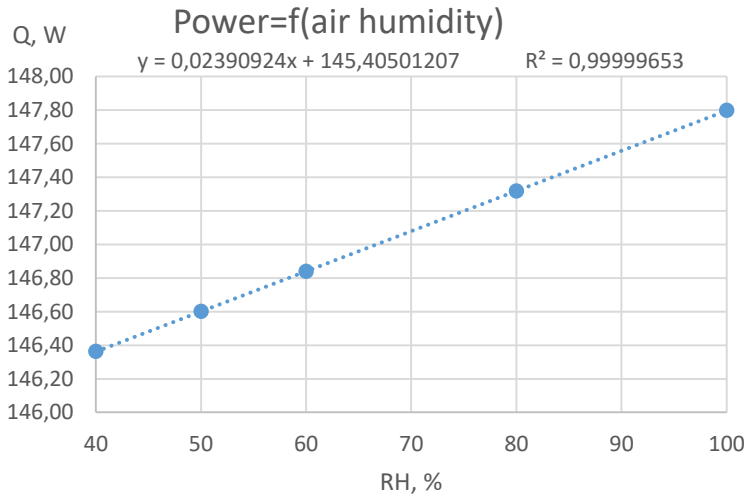

Figure 14 Correlation between power and air humidity

The increase of power with respect to steam temperature growth is related to the temperature gradient which drives the heat exchange process. The higher the temperature difference between hot and cold media would be the greater power output became. The correlation can be observed in Figure 15.

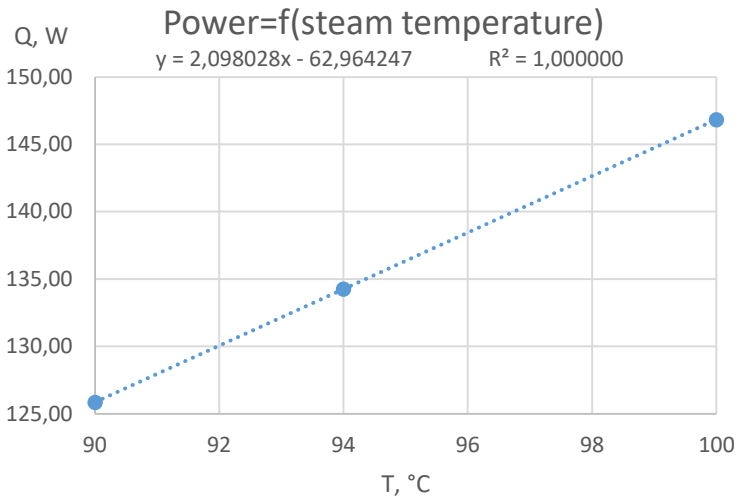

Figure 15 Correlation between power and steam temperature

Oppositely, power decreases when the temperature of the air is growing which is shown in Figure 16. The explanation is the same as for the steam temperature. Both of them contribute to the temperature gradient which increases when either hot medium temperature rises or the cold one decreases.

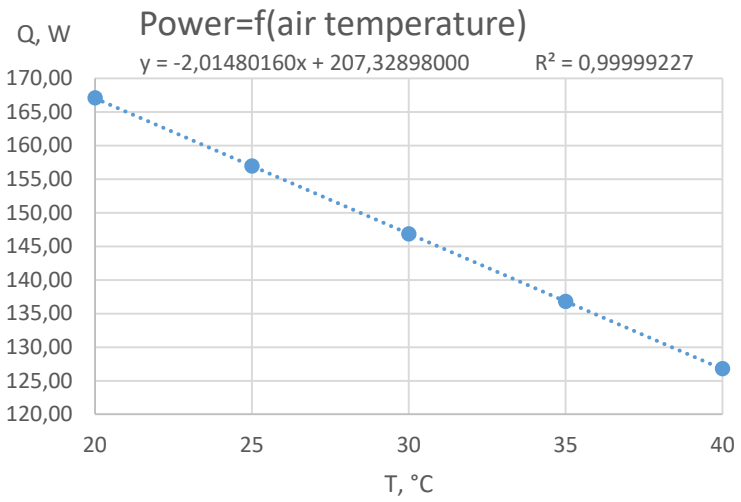

Figure 16 Correlation between power and air temperature

The trend lines correlate with cases in almost 100%. Therefore, results coming from all three parameters are decided to be used only as correction factors in the final formula. In addition, it can be observed that the humidity of the air does not influence considerably the output in comparison to the other parameters. Moreover set of variants with changed parameters and power outputs are gathered in Table 6. Each group consists of a few cases and the basic variant repeated also in the first row. The last three rows represent the control group of cases with all parameters changed during the same simulation.

Table 6 Power output from Fluent simulation for all cases

Variant name	Q_{CFD}, W	Variant name	Q_{CFD}, W	Variant name	Q_{CFD}, W
T1H3A4M3S4	167.08	T3H1A4M3S4	146.36	T3H3A1M3S4	136.93
T2H3A4M3S4	156.94	T3H2A4M3S4	146.60	T3H3A3M3S4	140.36
T3H3A4M3S4	146.84	T3H3A4M3S4	146.84	T3H3A4M3S4	146.84
T5H3A4M3S4	136.79	T3H5A4M3S4	147.32	T3H3A5M3S4	152.62
T6H3A4M3S4	126.78	T3H6A4M3S4	147.80	T3H3A6M3S4	173.45
T3H3A4M1S4	81.25	T3H3A4M3S1	125.86	T6H6A5M1S1	63.05
T3H3A4M3S4	146.84	T3H3A4M3S2	134.25	T1H1A2M5S4	266.24
T3H3A4M4S4	200.54	T3H3A4M3S4	146.84	T4H4A6M2S3	129.92
T3H3A4M5S4	247.48				

3.6. Fin efficiency analysis

Having the solutions done it is possible to check the efficiency of internally implemented fins in the pipe. The idea is to verify whether an efficiency calculated for external fins can be applied to the internal ones. If those efficiencies are nearly the same then the simpler analytical model can be applied. However, keeping in mind that the other requirement would be then to have the small influence of the inflow angle. If so, then the power of the pipe would be calculated as a function of the velocity (Re number) and surface extended with fins encompassing their efficiency.

Initially, the pipe without any fins is calculated to have the comparison whether and, if yes, how much fins improve the heat transfer from pipe to air [1]. All the dimensions, temperatures and values like convection heat coefficient for the material are assumed the same as the ones in Fluent. Below in Table 7 results for base variant are shown. For the average temperature of the air inside the pipe Prandtl number, viscosity coefficient and convection heat coefficient for the fluid are read. Furthermore, for calculated Reynolds number, the Gnieliński's equation (12) is chosen to calculate the Nusselt number. As a result h_{plane} - the heat transfer coefficient for air in the plane tube is almost 21 W/m^2-K which is reasonable for gas forced convection.

$$Nu = \frac{f}{2} \cdot (Re - 1000) \cdot Pr \cdot \left[\frac{1 + (D_i/L)^{\frac{2}{3}}}{1 + 12.7 \cdot \left(\frac{f}{2}\right)^{\left(\frac{1}{2}\right)} \cdot \left(Pr^{\left(\frac{2}{3}\right)} - 1\right)} \right] \cdot \varepsilon \tag{12}$$

$$f = (1.58 \cdot \ln Re - 3.28)^{-2}$$

$$\varepsilon = \left(t_f/t_w\right)^{0.45} \; for \; gases$$

D_i – internal diameter of the pipe m, L – length of the pipe m, f – friction coefficient, ε – coefficient for gases, Re – Reynolds number, Pr – Prandtl number, t_f – average temperature of the fluid in tube, t_w – temperature of the wall in tube

Table 7 Heat transfer coefficient for plane tube

f=	0.007965	-
ε=	0.6124	-
Nu=	21.4	-
h_{plane}=	20.6	W/m^2-K

To receive the same heat transfer coefficient but for finned pipe there is a need to read power output (Q_{CFD} in Table 6) and temperatures: of the wall and free stream from Fluent. Besides, the area of heat exchange grows up (13) because of the fins. Using, the area-weighted average-wall temperature at pipe interface for the whole area with fins (368.65 K) and mass-weighted average-static temperature at the interior of the pipe for fluid (321.25 K) the new h_{finned} for finned pipe equal to almost 46 W/m^2-K is found using formula (14).

$$A_{total} = n_{fin} \cdot A_{fin} + L \cdot (\pi \cdot D_i - n_{fin} \cdot t_{fin}) \tag{13}$$

A_{fin} – area of a single fin m^2, n_{fin} – number of fins, t_{fin} – fin thickness m

$$Q_{CFD} = A_{total} \cdot (t_{finned} - t_{fluid}) \cdot h_{finned} \tag{14}$$

Q_{CFD} – power output W, t_{finned} – area-weighted average-wall temperature at pipe interface for whole area with fins K, t_{fluid} – mass-weighted average-static temperature at interior of the pipe for fluid K, h_{finned} – heat transfer coefficient inside finned tube W/m^2-K

Knowing that the temperature distribution alongside the fin differ two lines are made in Fluent to read the area-weighted temperature just for the pipe interface base without fins taken into account. For this temperature, which is higher, the efficiency of the fin can be conducted to compensate that difference (15). Since the temperatures at the base and top of the fins are not the same the efficiency has to be lower than 100%.

$$Q_{CFD} = \left[L \cdot \left(\pi \cdot D_i - n_{fin} \cdot t_{fin}\right) + n_{fin} \cdot A_{fin} \cdot \eta_{fin}\right] \cdot \left(t_{bfinned} - t_{fluid}\right) \cdot h_{finned} \tag{15}$$

η_{fin} – efficiency of the fin, $t_{bfinned}$ – area-weighted temperature just for the pipe interface base K

Having the h_{finned} for the finned pipe the tabular efficiency for the external fin is checked. In the case of base variant, the calculated efficiency is 88% while the tabular one is 93%. Such a procedure is repeated for a couple of cases. Comparison of all proves the tables cannot be used in the case of internally installed fins and that usage of Fluent simulation is the right choice. It is so, the efficiencies differ and what is more for the internally installed fins values (82-88%) are always 5-6% lower than for externally installed ones (88-94% respectively). Combining this fact with the strong dependency of the pipe power on inflow angle indicates that the model relying solely on fin efficiency and velocity of the air is unreliable. The already existing formulas are not suitable for tubes internally finned.

3.7. Pipe equation

To compute the empirical equation for model all the cases are divided into two groups. The first one gathers most of the cases with a representative range of change within parameters. In Table 6 and

as well Table 5 those cases are at the beginning from T1H3A4M3S4 - T3H3A4M3S2. The second group stand for validation of the final equation and consists of three last cases: T6H6A5M1S1, T1H1A2M5S4, T4H4A6M2S3. Those three cases do not take part in equation creating process.

Four different variants of analytical pipe equation are proposed. Three of them use mass flow rate as the basic parameter. The reason is that mass flow rate has the biggest influence on the power of the pipe. The other parameters are scaled giving a unity when the measured parameter has the same value as in the base variant. Such a procedure makes rest of equations behave as correction factors. For the fourth one, the basic parameter is an angle because its influence on the power is nearly as big as for mass flow rate. Since the scaling factor is slightly different in case of an angle than it is for the rest of the parameters which is a result of approximation (Figure 13) two values are considered (Table 8). Last doubt is whether to incorporate humidity into the equation as it has a minor influence on pipe power.

Table 8 Comparison of empirical pipe equation variants

	variant 1	variant 2	variant 3	variant 4
Equation basis	mass	mass	mass	angle
Angle-scale value	145.5	146.8	146.8	146.8
Air RH included	no	no	yes	yes
Average error	0.56	1.18	1.20	1.20
Maximum error	1.86	2.02	1.50	1.50

Since both variants based on mass flow rate and angle are characterized by biggest average error but in general the lowest maximum error at the level of 1.5% one of them should be chosen. Keeping in mind that the increase in power is greater for the mass flow rate increase than for the change of angle finally variant based on mass flow rate correlation with air humidity taken into account is chosen. The idea is to have model equally good in the whole range of observed changes instead of very good model with some exceptions. Therefore, this equation (16) is implemented finally into the *THSC* mathematical model.

$$Q_{pipe} = (-1190589 \cdot M^2 + 39693.5039 \cdot M + 7.6052) \cdot \varepsilon_T \cdot \varepsilon_A \cdot \varepsilon_S \cdot \varepsilon_H \quad (16)$$

$$\varepsilon_T = \frac{-2.0148016 \cdot (T - 273) + 207.32898}{146.84}$$

$$\varepsilon_A = \frac{0.0077559123 \cdot A^2 - 0.1938093674 \cdot A + 138.5566319398}{146.84}$$

$$\varepsilon_S = \frac{2.098028 \cdot (S - 273) - 62.964247}{146.84}$$

$$\varepsilon_H = \frac{0.02390924 \cdot H + 145.40501207}{146.84}$$

$\varepsilon_T, \varepsilon_A, \varepsilon_S, \varepsilon_H$ – correction factors with respect to: M - mass flow rate of the air flowing through the I pipe, T - air temperature, A - angle between direction of inflowing air and central axis of pipe, S - steam temperature, H - relative humidity of air

3.8. THSC model development

The choice of Visual Basic for Application as the base for final model of *THSC* comes from the wide availability of this software. Although, Excel is widely met in industrial companies it is not a first thought engineering tool. Differently from EES, this program has no built-in tables and iterative way of computing results which causes some difficulties. The first obstacle is overcome by steam_IAPWS module implementation. This module allows reading directly input steam parameters. The non-iterative character of VBA work results in the longer process of code planning. Nevertheless, having in mind the user will not interfere inside it, there is no risk of the program to be more problematic in use.

Previously described activities in Fluent and work on the equation of pipe behaviour let the program to model the *THSC* under different conditions. To let the user change input data and show how particular modifications in parameters and construction may end up an interface with hidden condition statements and warnings has to be set. All of them make the program user-friendly without any need for deep thermodynamics knowledge.

The assumption is to create the tool which can guide its user without essential knowledge through the whole process. Therefore, at the beginning all input data values are checked whether they are from the range analyzed in Fluent. If not, there is a possibility of extrapolation of the results. After computation reaches the finish line the user is informed via activated reports of this fact. If some value drastically exceeded that range it would terminate the work of the program and point out the problem. In some situations, the model can precise the source of an error and give the hint of next step. Besides, the information is stored in help menu where one can find answers for questions about the program before initializing the calculation.

Excel, being most handful program in storing and presenting data, allows the user to reprocess given results to analyze it later. That is why in separate Worksheets, both crucial and complementary values are loaded after computation. They are sorted in the way those most valuable ones are highlighted without too many details but with guaranteed access to more of them if needed. To make it even easier VBA let create a convenient graphical interface. The procedure is very intuitive using the potential of a few GUIs shown in set order with respect to user's choices.

Mentioned GUI and reports not only minimize the number of discrepancies but in critical moments suggest where to find the source of the problem. In the GUIs, the clear difference between input and output boxes is kept. In the end, the work comes to almost mechanical activities supported by the graphical representation of *THSC*. Organization of the GUIs is described in Appendix A.

3.8.1. Heat losses

Since, the heat exchange takes place not only through described pipes, between air and steam, but also with the walls the influence of that has to be taken into account. To calculate the amount of heat lost to the environment outside EES software is used. Parameters vary depending on working conditions, and calculation of a single case may be insufficient as the effect is relatively small comparing to the amount of heat exchanged internally. That is why average values are used to check that

phenomenon with and without radiation. Namely, the final amount of lost heat between the air inside and outside through side areas A_{side}=0.072556 m^2 each, top one A_{top}=0.107040 m^2 as well as steam and air outside through backside A_{back}=0.119037 m^2 is calculated for *k*=16.27 W/m-K for 1.5 mm thick steel and three values of heat transfer coefficient. Values differ between the air inside collecting chamber (T_{air_in}=310.6 K), outside *THSC* (T_{air_out}=297.1 K), and for steam at the backside of *THSC* (T_{steam}=373.15 K) being equal to 46, 6 and 30230 W/m^2-K respectively. The surfaces taken into account are shown in Figure 17. To calculate that heat without radiation, below equations are used [11] and corresponding results are shown in Table 9.

$$Q_{lost} = q_{air} \cdot \left(2 \cdot A_{side} + A_{top}\right) + q_{steam} \cdot A_{back} \tag{17}$$

$$q_{air} = \frac{T_{air\_in} - T_{air\_out}}{R_{air}} \tag{18}$$

$$q_{steam} = \frac{S - T_{air\_out}}{R_{steam}} \tag{19}$$

$$R_{air} = \frac{1}{h_{air\_in}} + \frac{\delta}{k} + \frac{1}{h_{air\_out}} \tag{20}$$

$$R_{steam} = \frac{1}{h_{steam}} + \frac{\delta}{k} + \frac{1}{h_{air\_out}} \tag{21}$$

δ – thickness of the wall m, T_{air_in} – temperature of air inside collecting chamber K, T_{air_out} – temperature of air outside *THSC* K, h_{air_in} – heat transfer coefficient of air inside collecting chamber W/m^2-K, h_{air_out} – heat transfer coefficient of air outside *THSC* W/m^2-K, k – thermal conductivity of the wall W/m-K,

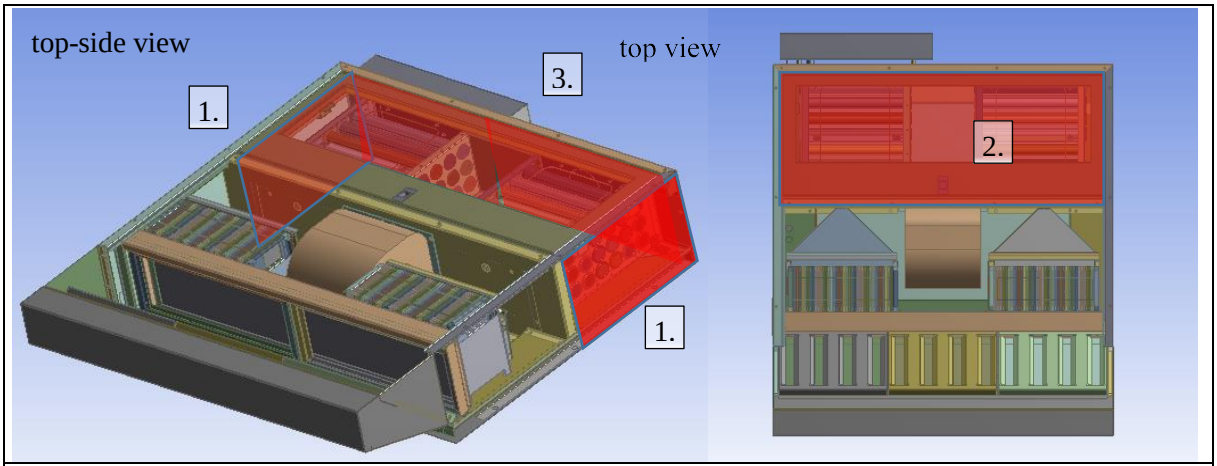

1 – side areas A_{side}, 2 – top area A_{top}, 3 – backside area A_{back}

Figure 17 Surfaces of heat loss in THSC

Table 9 Heat loss to the surrounding through external walls

R_{air}=	0.189	K-m^2/W
R_{steam}=	0.167	K-m^2/W
q_{air}=	71.44	W/m^2
q_{steam}=	456	W/m^2
Q_{lost}=	72.3	W

When taking into account the radiation, formulas have to be modified since the temperature of the external wall is not known. Therefore, iterative nature of work in EES occurs very helpful saving a lot of time. The equation for heat loss stays the same (17) but formulas for heat rates are changed from

(18), (19) into (22), (23). The heat transfer from inside to the external wall is as it has been but since radiation appeared outside the new part except convection has to be taken into account and balanced.

$$q_{air\_radiation} = \frac{T_{air\_in} - T_{wall\_air}}{\frac{1}{h_{air\_in}} + \frac{\delta}{k}} = \frac{T_{wall\_air} - T_{air\_out}}{\frac{1}{h_{air\_out}}} + \varepsilon \cdot \sigma \cdot ({T_{wall\_air}}^4 - {T_{air_{out}}}^4) \quad (22)$$

$$q_{steam\_radiation} = \frac{T_{steam} - T_{wall\_steam}}{\frac{1}{h_{steam}} + \frac{\delta}{k}} = \frac{T_{wall\_steam} - T_{air\_out}}{\frac{1}{h_{air\_out}}} + \varepsilon \cdot \sigma \cdot ({T_{wall\_steam}}^4 - {T_{air_{out}}}^4) \quad (23)$$

σ – Stefan-Boltzmann constant W/m^2-K^4, ε – emissivity of the wall surface, T_{wall_air} – temperature of side and top external wall K, T_{wall_steam} – temperature of backside external wall K,

Since the material of stainless steel is polished the amount of radiated heat is not significantly higher reaching almost 80 W which means that both approaches reach the relatively comparable level of results. Thus, the heat loss Q_{lost} to the surrounding through the walls is assumed at the level of 80 W and as the constant value it is put into the code in the *THSC* model.

According to measurements [10] about 0.126 g/s of the steam condenses on the walls of condensation chambers (surfaces visible in Figure 18) in both sections which has an influence on the results. Since that amount does not vary significantly for different operating conditions it is calculated as shown in Table 10 and finally assumed constant. Thus, there is an extra 285 W of additional power Q_{gain} according to equation (24).

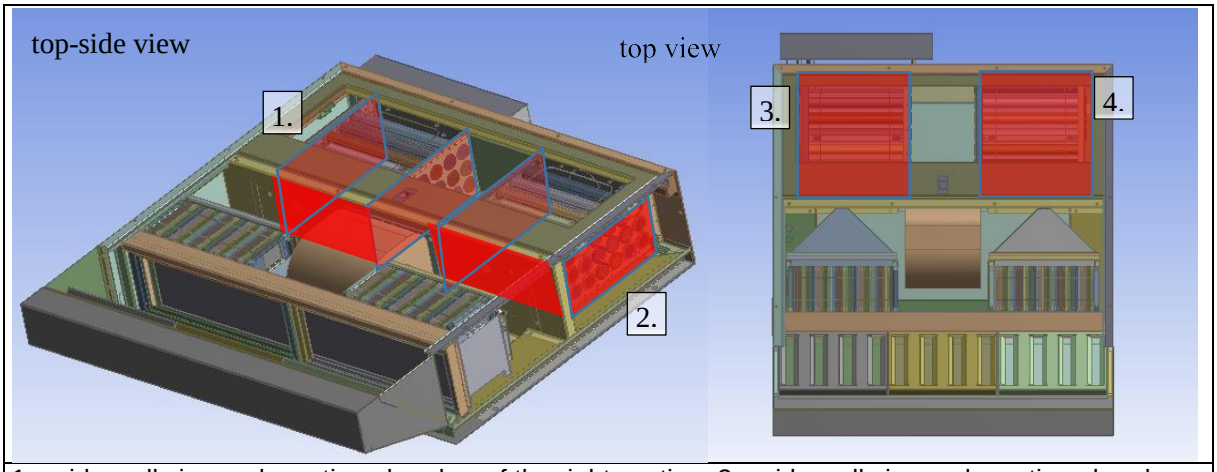

1 – side walls in condensation chamber of the right section, 2 – side walls in condensation chamber of the left section, 3 – top wall in condensation chamber of the right section, 4 – top wall in condensation chamber of left section

Figure 18 Surfaces of wall condensation in condensation chambers of THSC

$$Q_{gain} = \dot{m}_{cond} \cdot h_{fg} \quad (24)$$

$\dot{m}_{cond}$ – mass flow rate of steam condensated on the walls of condensation chambers in *THSC* kg/s

Table 10 Heat provided through the walls in condensation chambers of THSC

$\dot{m}_{cond}$=	0.1262401	g/s
h_{fg}=	2257	J/g
Q_{gain}=	284.9	W

3.8.2. Distribution of air and steam

Air total mass flow rate sucked by the fan from the surrounding is directed to the distribution chamber (4 in Figure 1) of *THSC*. In this chamber there are 48 pipes with inflows arranged on two walls perpendicularly to the outlet of the fan. In consequence, the angles and shares of total mass flow rate differ between the pipes. Although these parameters are constantly changing and their forecast is hard to model, this phenomenon has to be described. That is why, as default setup in *THSC* model there are implemented values from full CFD model [10]. However, the user is given the option to modify either particular angles or shares of inflowing mass flow rate. The way of changing these parameters is depicted in Figure 42 in Appendix A.

In the case of the steam, distribution takes place only between condensation chamber in two sections of *THSC* (5 and 6 in Figure 1). Nevertheless, according to measurements [10] the steam flow rate is not shared equally between those sections because of the narrow steam passage on the back side of the *THSC* (13 in Figure 1). Moreover, the proportion of the shares between left and right section depends on the value of total steam mass flow rate. The relation is the more steam flows into the *THSC* the more equal is the distribution up to halved steam mass flow rate since it is not feasible to have more steam flowing through the steam passage to the right section than to the left one. To reflect this correlation in the *THSC* model, the equation (25) for division controlling the amount of steam directed to the right section is implemented in the code with a condition for values of division higher than 0.5 the model assumes equal distribution of steam.

$$D_f = 7.5508 \cdot \dot{m}_{steam} + 0.3848 \tag{25}$$

D_f – the share of steam mass flow rate directed to the right section of THSC, $\dot{m}_{steam}$ – total steam mass flow rate kg/s

3.8.3. Correction factors

Direct use of single pipe model in *THSC* model as described above would lead to the maximum condensation of steam which does not coincide with the results of measurements. The reason behind is that when the amount of steam is large the pipes are fully surrounded by it. Then, the pipes work at full power. But when the steam amount goes down there are areas of the pipe without steam. The issue is lack of steam to condensate – which reduces the power of the pipe and acts as a limiting factor. Since not the whole steam can have contact with the pipes inside *THSC* the correction factors (*Eps*) are introduced to control how much of the steam can be condensed on each pipe (top, middle and bottom) in a row (1-8) depending on how much steam is left in the condenser. Therefore, from fully developed CFD model of *THSC* which is validated against measurements [10] the power values are obtained for all pipes to compare with the ones from *THSC* model. Furthermore, comparing the power outputs from both, *THSC* model is calibrated thanks to applied *Eps*. Input values taken for calibration of the outputs

Sucked air				Steam		INPUT
Air stream	Relative humidity	Temperature of the air	Pressure	Steam stream	Temperature	
kg/s	%	K	hPa	kg/s	K	
0,194983	40,1	297,35	987	0,00136	373	

Figure 19 Input data for Eps calibration

and verification of *THSC* model with the Fluent [4] are as given in Figure 19. Calibrated *THSC* model further on is validated against measurements [10].

In consequence, the limitation works only when the amount of steam is relatively small, close to or below the maximum available amount of steam condensed on the pipe. When the flow rate is much bigger, calculated limits for *Eps* are above physical limits for a single pipe and do not activate. Therefore, for a given *Eps* values gathered in Table 11 it can be observed in Figure 20 the correlation between results from Fluent (fully developed CFD model of *THSC*) [4] and mathematical *THSC* model.

Table 11 Correction factors for THSC model

		1	2	3	4	5	6	7	8	
top	Eps	0.085	0.095	0.15	0.235	0.175	0.24	0.435	0.6	LEFT
middle		0.08	0.085	0.115	0.175	0.12	0.14	0.25	0.56	
bottom		0.06	0.06	0.075	0.1	0.085	0.085	0.14	0.2	
top		0.11	0.125	0.185	0.335	0.15	0.2	0.34	0.65	RIGHT
middle		0.085	0.105	0.145	0.23	0.1	0.115	0.19	0.5	
bottom		0.045	0.05	0.065	0.1	0.08	0.075	0.105	0.28	

In Figure 20 (top view) power outputs without correction are presented. It can be observed at the beginning the *THSC* model is condensing more than according to Fluent. At some point, there is no more steam left and the power drops to zero. In addition, in the line from Fluent it is worth to notice that

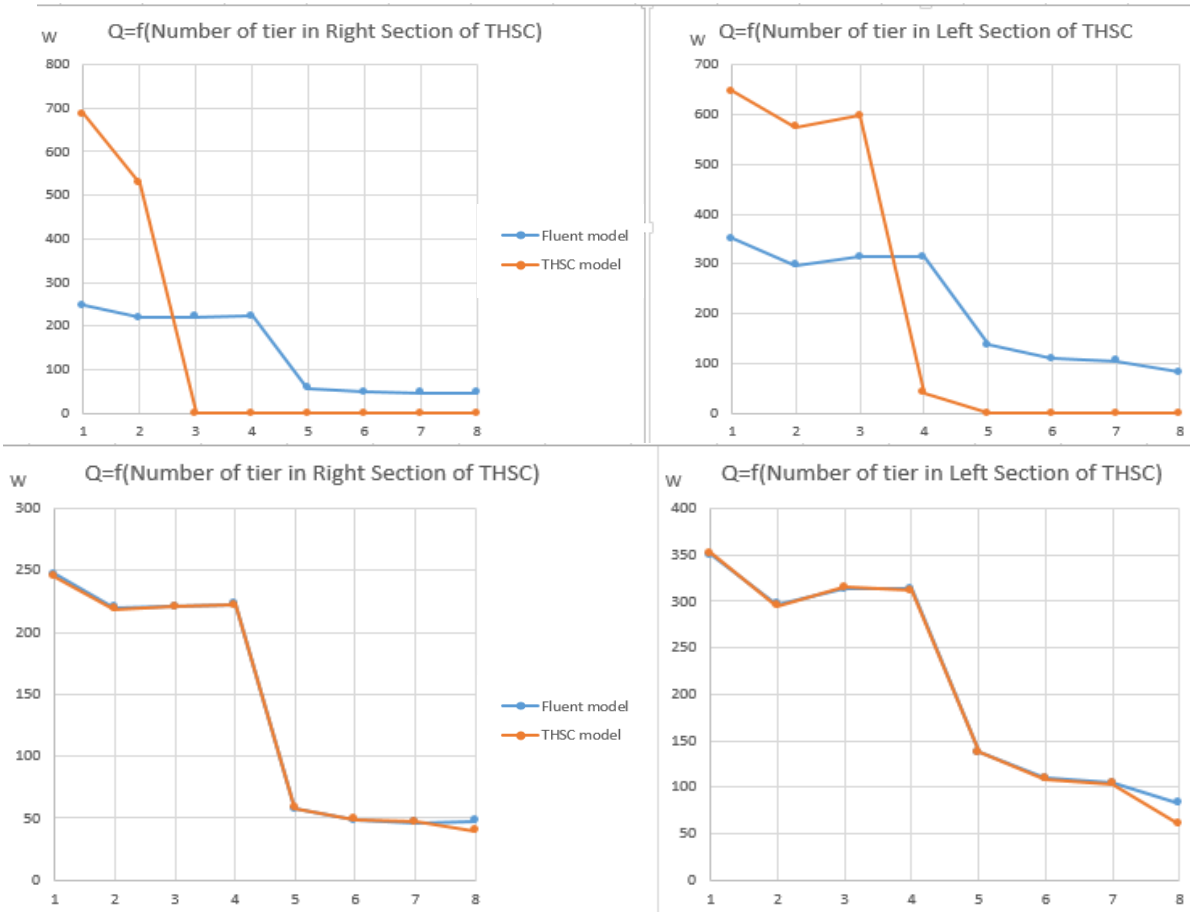

Figure 20 Comparison of power output for THSC model and Fluent without correction factors (top) and with them (bottom)

there can be distinguished two regions inside *THSC* between which power output decreases. It shows how efficient are first columns of pipes in comparison to the consecutive ones after the baffle inside. In the same Figure 20 (bottom view) after *Eps* implementation one can see how both lines correlate to each other which ends the process of model preparation. Further activities are related with verification of the model with respect to measurements.

3.8.4. Description of THSC model operations

Having all the necessary equations ready it is time to implement them into the code and specify the way of the calculations procedure. Since the assumption is to have a simple mathematical model the code consists of mostly mass and energy balances within a few areas of the *THSC*. Namely, equations are solved separately for: condensation chambers, collecting chambers, mixing chamber (5, 6, 8, 9 and 10 respectively in Figure 1) taking into account the heat gain and loss as well as steam

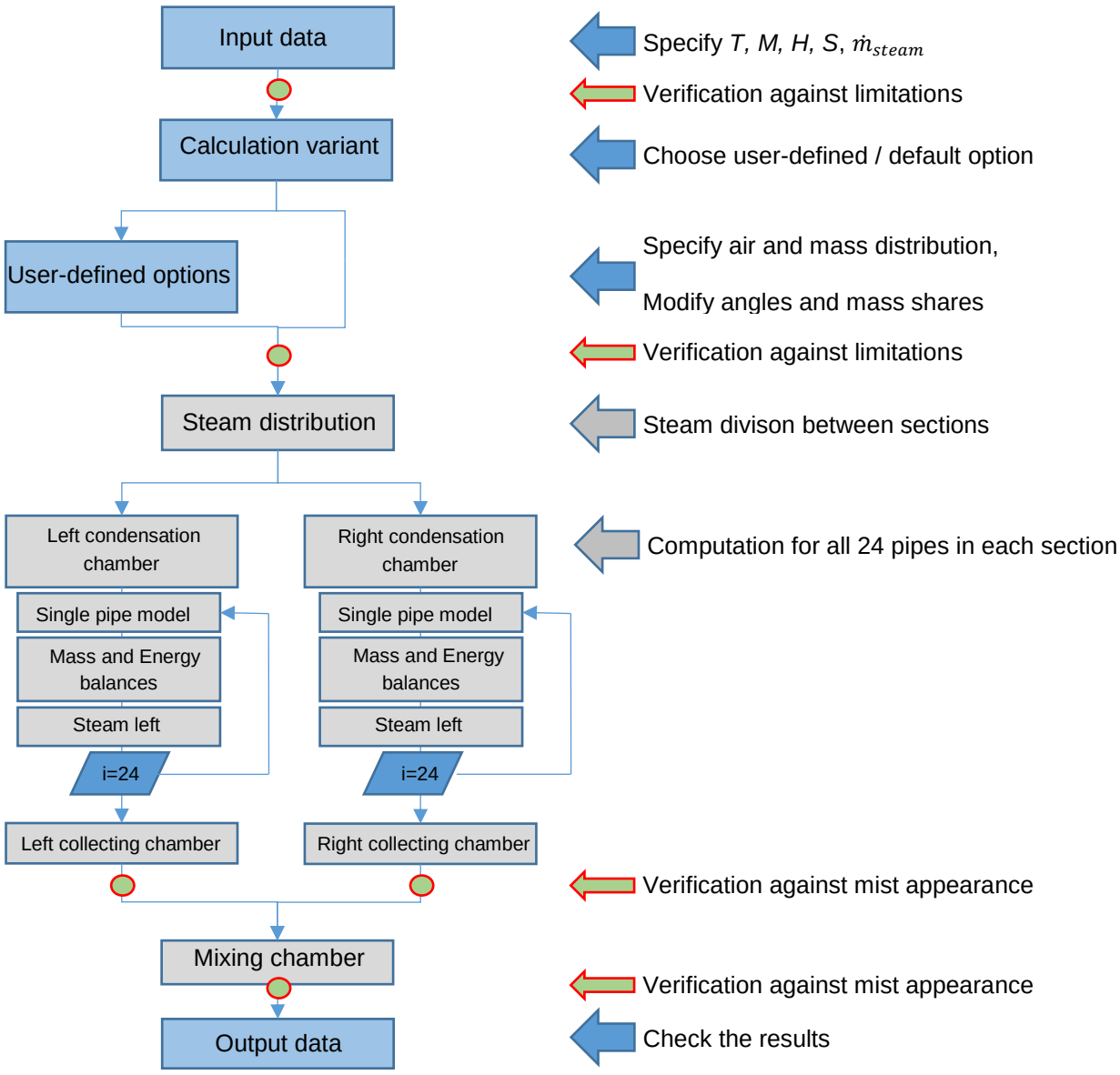

Figure 21 Flowchart of THSC model

distribution variant. The general procedure of calculation in THSC model is presented in the flowchart in Figure 21.

At the beginning one can specify the input values: temperature of the air (T), relative humidity of air (H), air mass flow rate (M) and finally steam mass flow rate ($\dot{m}_{steam}$) with its temperature ($T_{steam}, (S)$) (Block 1 in Figure 21). After verification of input data against limitations, user can choose the calculation variant (Block 2 in Figure 21): default or user-defined which influences further steps. In the case of user-defined option one can additionally specifies air inflow angle (A) and shares of air mass flow rate between the pipes as well as the way of steam and air mass flow rate distribution (Block 3 in Figure 21). If given values satisfy the limiting conditions all the values are inserted into the code and used for calculation.

First of all steam mass flow rate is divided between the left and right condensation chamber according to internal formula (25) or equally and decreased by the amount of steam condensed on the walls
(Table 10). For the air mass flow rate entering the distribution chamber (4 in Figure 1) of *THSC* the saturation pressure is read. Then the degree of humidity (26) and specific enthalpy (27) are calculated.

$$X_{in} = \frac{\frac{H_i}{100} \cdot p_{sat,in,i}}{p_o - \frac{H_i}{100} \cdot p_{sat,in,i}} \cdot \frac{M_{H2O}}{M_{da}} \tag{26}$$

$$h_{wa,in,i} = 1.005 \cdot (\mathrm{T} - 273.15) + X_{in} \cdot (1.88 \cdot (\mathrm{T} - 273.15) + 2501) \tag{27}$$

$p_{sat,in,i}$ – saturation pressure for T hPa, M_{H2O}, M_{da} – molar mass of water and dry air $kg_{H2O}/kmol_{H2O}$, $kg_{da}/kmol_{da}$, p_o – air pressure hPa

Furthermore, the calculation for left (and then right) section of condensation chamber can be done. Since in one section there are 8 columns of 3 pipes each, the calculation is repeated 24 times. Assuming none of the values exceeds the analyzed range and no unfeasible result occurs the following equations are solved. First of all for given input parameters the power of the pipe is calculated from single pipe model equation (16) and the corresponding amount of condensed steam from equation (28) shown below. The same value is validated against *Eps* (Table 11) and modified if needed.

$$\dot{m}_{cond,i} = \frac{Q_{pipe,i}}{h_{fg}} \tag{28}$$

$\dot{m}_{cond,i}$ – mass flow rate of steam condensed on the i pipe in *THSC* kg/s, i – number of calculated pipe 1-24

For the known amount of condensate (28) the specific enthalpy (29) of warmed air is calculated from energy balance. Since there is no mixing and degree of humidity (26) does not change the temperature, and relative humidity of air at the outflow are calculated using reformulated equations (27) and (26) respectively. In the end, the amount of steam left for calculation of next pipe is decreased according to equation (30).

$$h_{wa,out,i} = \frac{h_{wa,in,i} \cdot \dot{m}_{air,i} + h_{fg} \cdot \dot{m}_{cond,i}}{\dot{m}_{air,i}} \tag{29}$$

$$\dot{m}_{steam\_left,i+1} = \dot{m}_{steam\_left,i} - \dot{m}_{cond,i} \tag{30}$$

$\dot{m}_{air,i}$ – mass flow rate of the air flowing through i pipe in *THSC* kg/s, $\dot{m}_{steam\_left,i}$ – mass flow rate of steam left to be condensed on the i pipe in *THSC* kg/s

After all 24 calculations for pipes from left (then right) condensation chamber are done there is a second subpart of *THSC* to be calculated. Namely, all 24 air mass flow rates get to the collecting chamber and are mixed. Therefore, mass (31) and energy (32) balances are used to calculate the degree of humidity and specific enthalpy of air leaving the left (then right) collecting chamber.

$$X_{out,L} = \frac{\sum_{24}^{1} \dot{m}_{air,i} \cdot X_{in} + \left(\dot{m}_{steam\_left,1} - \sum_{24}^{1} \dot{m}_{cond,i}\right)}{\sum_{24}^{1} \dot{m}_{air,i}} \tag{31}$$

$$h_{wa,out,L} = \frac{\sum_{24}^{1} h_{wa,out,i} \cdot \dot{m}_{air,i} + \left(\dot{m}_{steam\_left,1} - \sum_{24}^{1} \dot{m}_{cond,i}\right) \cdot h_S}{\sum_{24}^{1} \dot{m}_{air,i}} \tag{32}$$

h_S- enthalpy of steam for $T_{steam}, (S)$ kJ/kg

Similarly, as in the case of condensation chamber now the temperature and relative humidity of mixed air flow rates at the outflow of collecting chamber are calculated with reformulated (27) and (26) respectively. In this place, it is checked for the first time whether the mist appears in the air released from left collecting chamber (then right one). To verify it the result of the degree of humidity (31) is compared with the maximum degree of humidity (33) for these conditions. If (31) is higher than (33) the temperature is found iteratively comparing (32) with equation (34) which takes into account mist in the air.

$$X_{max} = \frac{p_{sat,out,L}}{p_o - p_{sat,out,L}} \cdot \frac{M_{H2O}}{M_{da}} \tag{33}$$

$$h_{wa,out,L} = 1.005 \cdot \left(T_{out,L} - 273.15\right) + X_{max} \cdot \left(1.88 \cdot \left(T_{out,L} - 273.15\right) + 2501\right) + (X_{out,L} - X_{max}) \cdot 4.19 \cdot \left(T_{out,L} - 273.15\right) \tag{34}$$

$p_{sat,out,L}$ – saturation pressure for $T_{out,L}$ hPa, $T_{out,L}$ – temperature of mixed air flow rates at the outflow of collecting chamber K

Finally, having the results from both sections the equations for outflow of *THSC* are calculated at the end of the code. One more time the degree of humidity (35) and specific enthalpy of air at outlet (36) are calculated using mass and energy balances. For this subpart of the *THSC* also the maximum degree of humidity like in (33) is calculated and compared with (35). In case of mist appearance the

value of specific enthalpy (36) is recalculated and which is more important the user is informed about critical failure of *THSC* performance.

$$X_{out} = \frac{\sum_{48}^{1} \dot{m}_{air,i} \cdot X_{in} + \left(\dot{m}_{steam} - \dot{m}_{cond} - \sum_{48}^{1} \dot{m}_{cond,i}\right)}{\sum_{48}^{1} \dot{m}_{air,i}} \tag{35}$$

$$h_{wa,out} = \frac{\sum_{48}^{1} h_{wa,out,i} \cdot \dot{m}_{air,i} + \left(\dot{m}_{steam} - \dot{m}_{cond} - \sum_{48}^{1} \dot{m}_{cond,i}\right) \cdot h_S - Q_{lost} + Q_{gain}}{\sum_{24}^{1} \dot{m}_{air,i}} \tag{36}$$

3.8.5. Validation

Validation of the model is provided for two *THSC* working conditions. Firstly the default work is examined which means all of the pipes are active and the steam distribution is controlled internally by equation (25) dependent on its flow rate [10]. The amount of compared cases, i.e. measurements for various oven and kitchen operating conditions, is equal to 19. All the input data are gathered below in Table 12.

Table 12 Validation data of THSC model under default working condition

	Sucked air				Steam	
	Air flow rate	Relative humidity	Temperature of the air	Pressure	Steam flow rate	Temperature
	kg/s	%	K	hPa	kg/s	K
1	0.220000	31.50	300.4	987.00	0.00131	373.15
2	0.189000	29.10	298.4	987.00	0.00065	373.15
3	0.222000	31.00	299.5	987.00	0.00075	373.15
4	0.188000	27.70	299.5	987.00	0.00094	373.15
5	0.188000	33.00	299.5	987.00	0.00134	373.15
6	0.221000	33.50	299.9	987.00	0.00147	373.15
7	0.187000	29.30	299.1	987.00	0.00162	373.15
8	0.220000	29.90	300.2	987.00	0.00170	373.15
9	0.188000	32.00	299.2	987.00	0.00144	373.15
10	0.189000	27.50	299.4	987.00	0.00161	373.15
11	0.222000	25.70	298.5	987.00	0.00202	373.15
12	0.188000	31.50	299.4	987.00	0.00255	373.15
13	0.221000	29.00	300.0	987.00	0.00252	373.15
14	0.187000	29.00	300.0	987.00	0.00202	373.15
15	0.222000	21.30	298.5	987.00	0.00244	373.15
16	0.190000	33.80	298.7	987.00	0.00095	373.15
17	0.208019	40.30	297.1	987.20	0.00136	373.15
18	0.209162	41.80	297.9	987.10	0.00136	373.15
19	0.209661	43.10	297.2	987.00	0.00136	373.15

Discrepancies between measured outputs and generated in the *THSC* model are at the satisfying level. What is more important they show the right trend of changes with input values. Temperatures given by the *THSC* model are mostly higher from the measured ones by 1-3 K as can be seen in Figure 22.

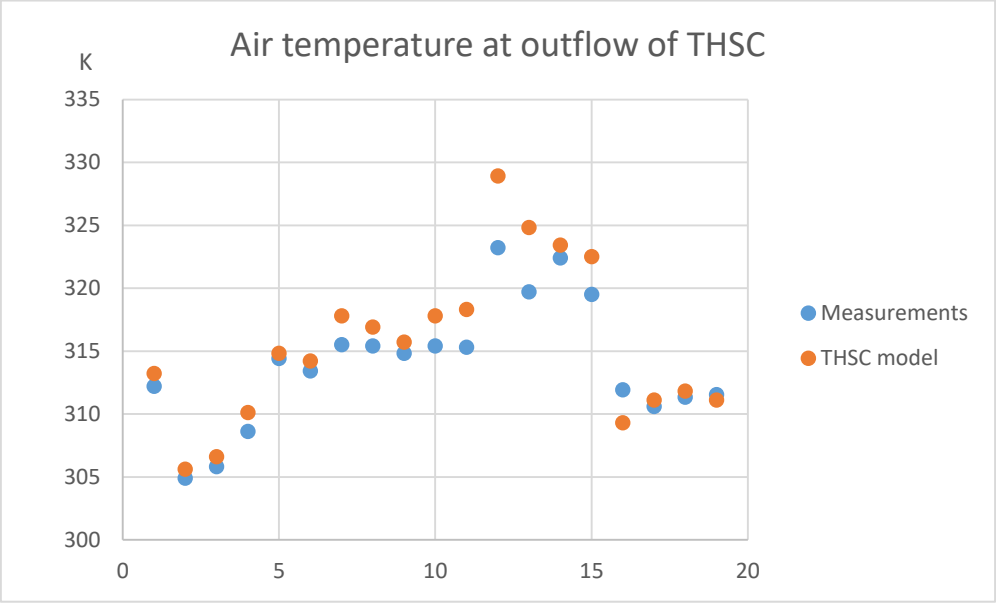

Figure 22 Temperature results from THSC model vs measurements

Logically, relative humidity given by the model is lower than measured values since those two parameters are related and change in opposite directions. Figure 23 shows all 19 compared cases.

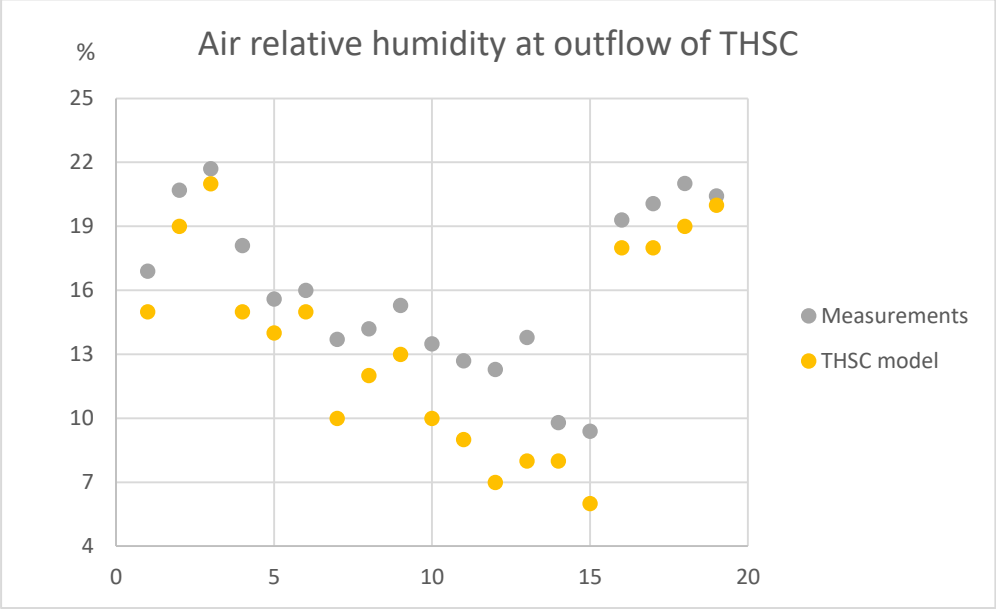

Figure 23 RH results from THSC model vs measurements

Although, air and condensed steam do not mix, crucial is the information about the condensate. The amount of condensate from *THSC* model is greater than measured one which correlates with two other parameters verifying the quality of the model. Figure 24 shows both lines correspond very well to each other with the exception of four cases (11,12,13,15), only which can be related to defective

measurements. One has to notice that for various operating conditions the relative humidity is far from mist region, which may indicate that there is a room for improvement.

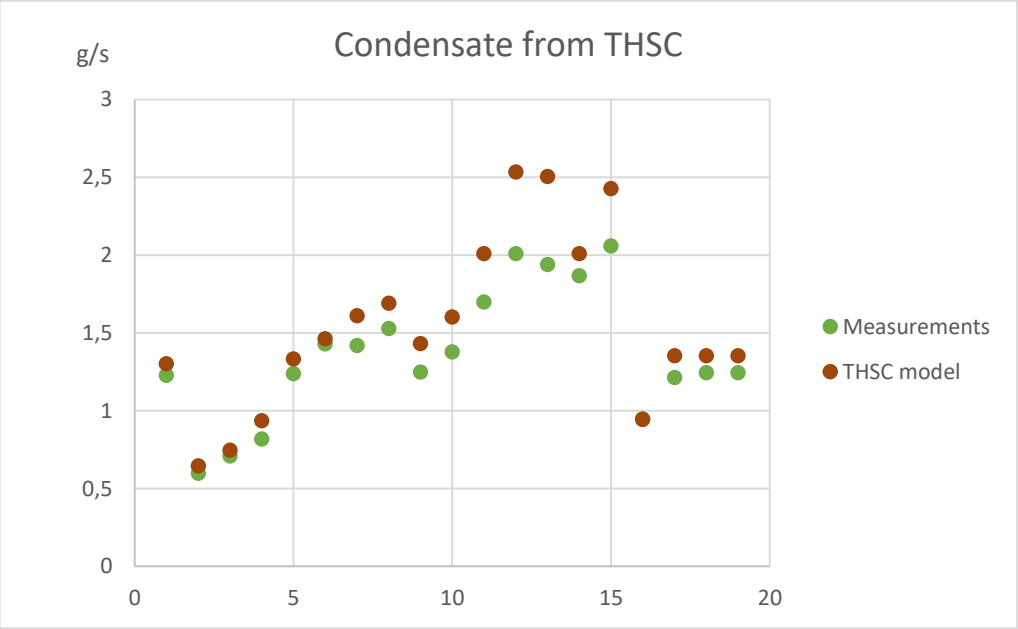

Figure 24 Condensate results from THSC model vs measurements

3.8.6. Technological modifications

Having proved the simplified model can calculate reliable results in comparison to what is measured under default working conditions, more demanding operating conditions are assumed. Namely, according to predictions it is tested how the model behaves when some of the pipes are cut off. In other words, *THSC* model is verified against measurements for a prototype of *THSC* [10] with improved construction. To simulate such a condition in the *THSC* model not only some of the pipes are

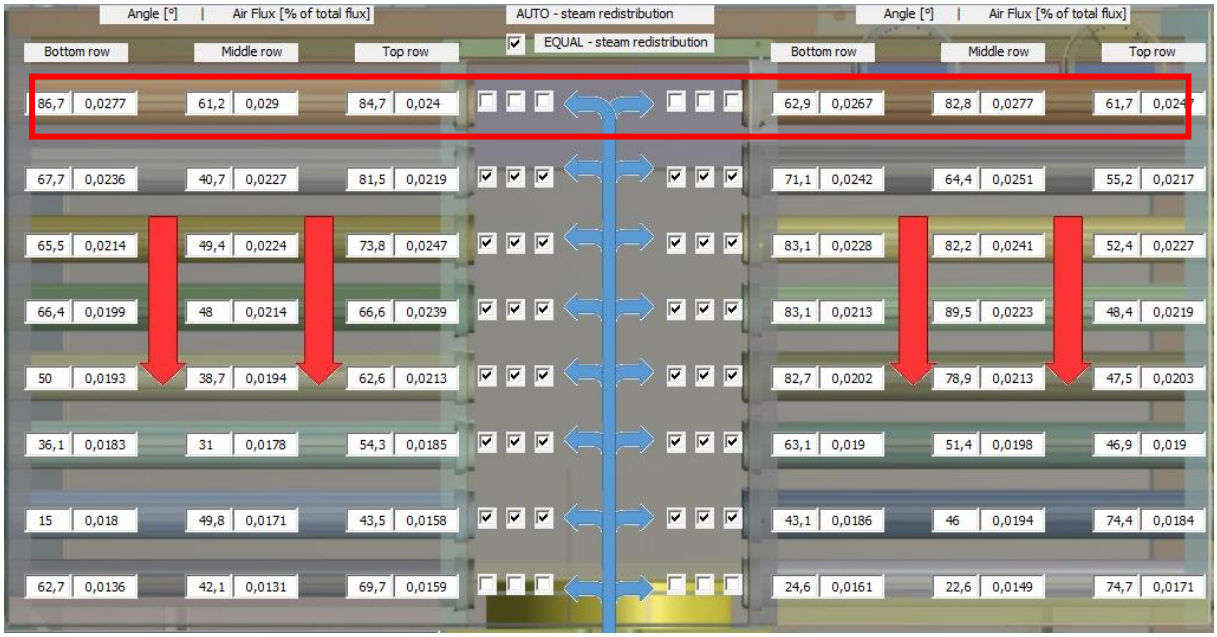

Figure 25 THSC model - enlarged steam passage

assumed with zero air flow rate going through them but also the steam distribution is changed. The latter is based on assumption when cutting first rows of pipes and enlarging the open space instead (red box in Figure 25), the steam divides no longer with formula (25) but equally (EQUAL option switched on) between both sections.

Until now, because of the very narrow passage, the right section is not enough used in comparison to the left one limiting the amount of steam for right section [10]. It may happen the left one works fully loaded along all its rows of pipes while the other one has steam only for the first few tiers. Two approaches are tested to see whether the model is sensitive for a specific choice of row number. Switching off the 1st and 8th tier in both sections as the first one and doing the same with 1st and 2nd (counting from the steam inlets side). Both of them test whether the *THSC* model can visualize the behaviour of *THSC* with changed geometry by cutting the pipes and influencing the steam distribution.

For a new prototype of *THSC* when 1st and 8th pipe are turned off the temperatures differ by maximum 2.5 K between *THSC* model and what is measured: namely the worst results are observed in cases (3, 4, 7, 9). Mostly those from *THSC* model are lower but still reach very satisfactory level of correlation differing not more than 1 K which is presented in Figure 26.

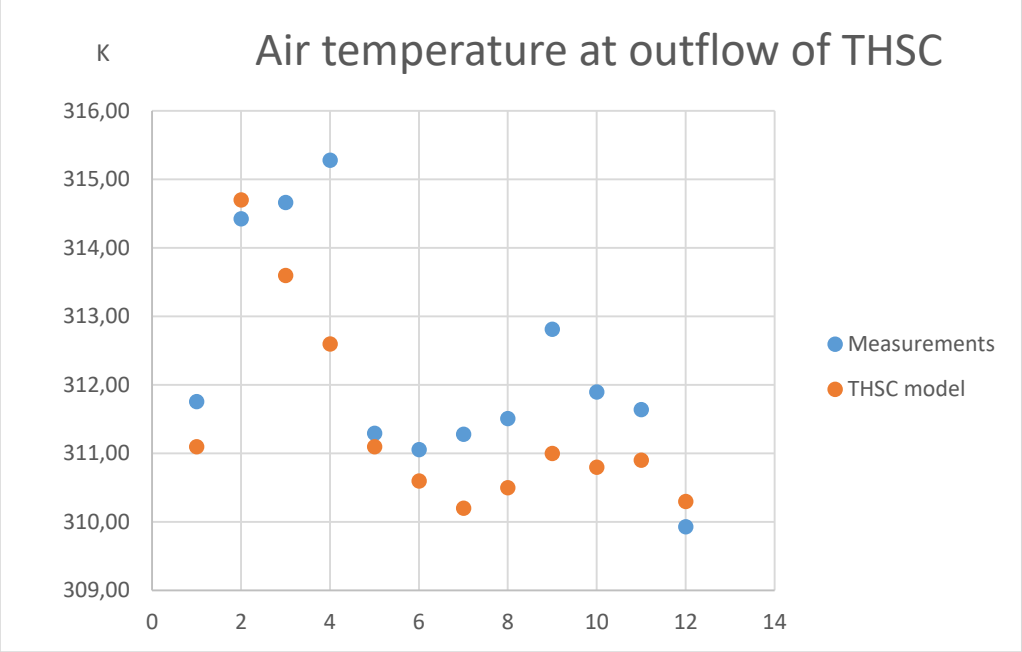

Figure 26 Temperature results from THSC model vs measurements – 1st and 8th tier switched off

For the same temperature comparison but with 1st and 2nd tier switched off *THSC* model give higher values of these parameters which results in even better solution with respect to measurement. Worse results with a difference over 1 K are for two cases (4 and 9). This increase of temperature means more condensate appears from *THSC* which is correlated with *Eps* coefficients – higher in value for consecutive rows of pipes. That is why for this case when 2nd row of pipes with worse *Eps* is turned off instead of 8th one in the model more steam is condensed. Such a trend takes place only for steam flow rate close to default one which is limited by correction coefficients. The graph is shown in Figure 27.

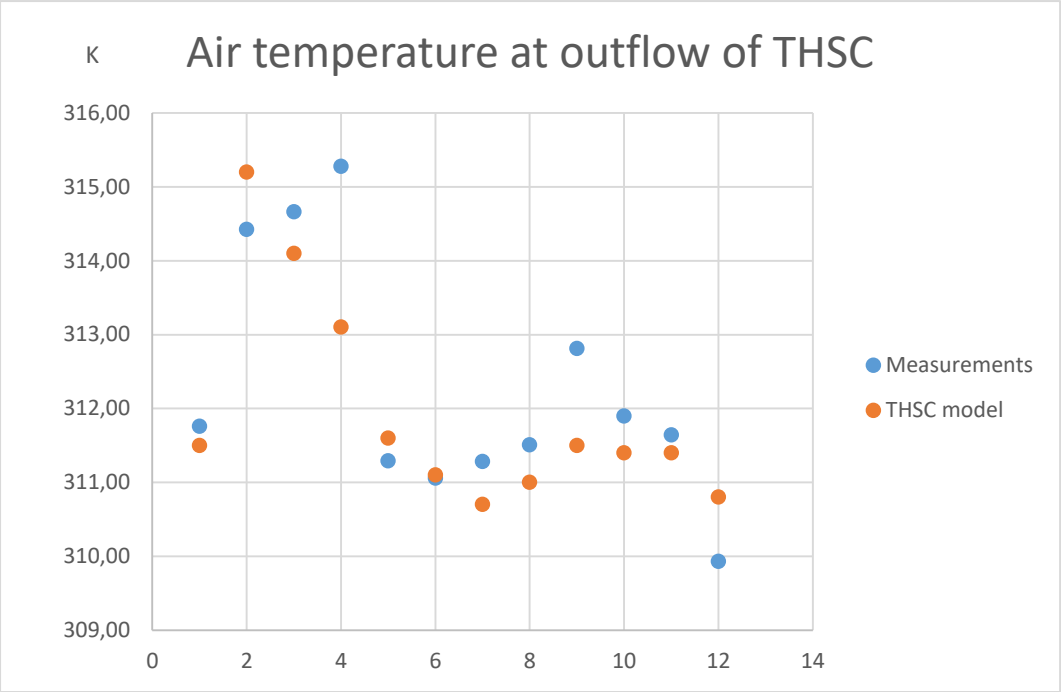

Figure 27 Temperature results from THSC model vs measurement - 1st and 2nd tier switched off

Comparing relative humidity the difference has not exceeded 4 percentage point between *THSC* model and measurements. In case of switching off 1st and 8th tier the results can be checked in Figure 28. Although having almost all temperatures from VBA lower than measured the corresponding RH values are not always higher than measured ones, namely only half of them.

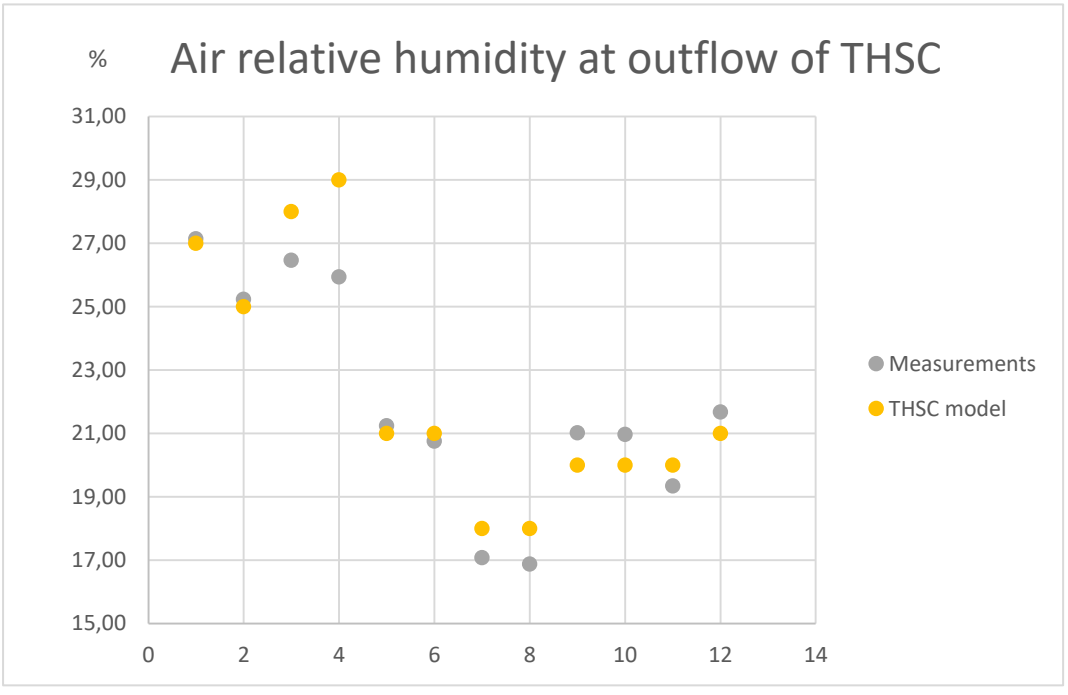

Figure 28 RH results from THSC model vs measurement - 1st and 8th tier switched off

When changing the 8th tier into 2nd one the RH decreases and since previously half of them are higher and the other half lower than measured values now most of them occurred below the measured

points. In consequence, discrepancies are higher after this change. Nevertheless, the level of difference stays below 4 percentage points which can be seen in Figure 29.

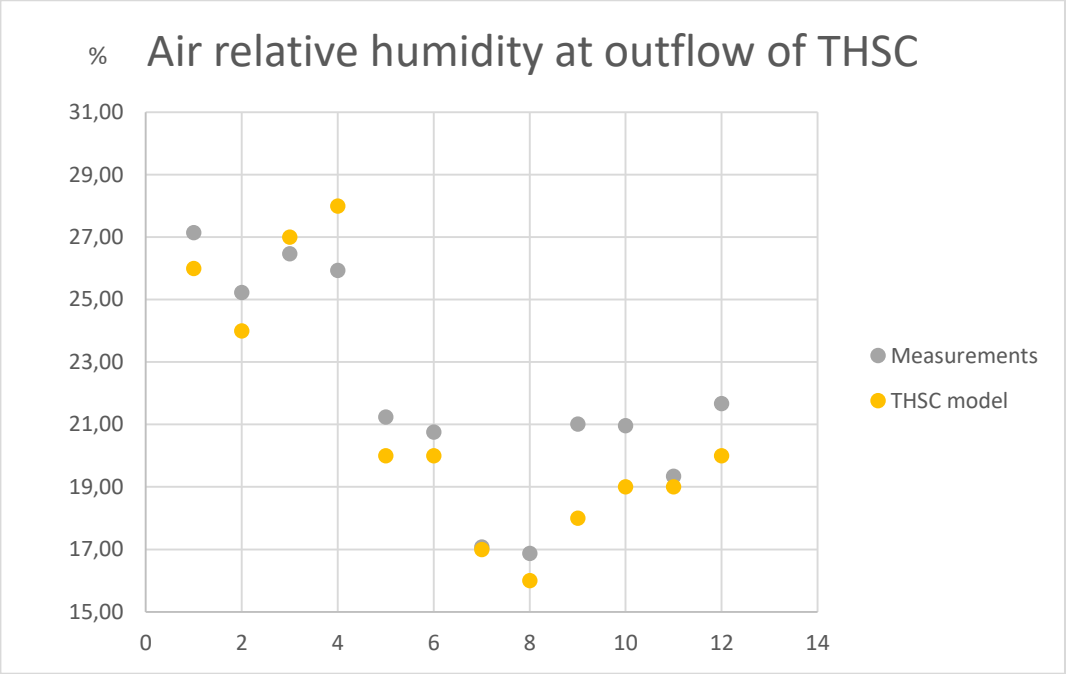

Figure 29 RH results from THSC model vs measurements - 1st and 2nd tier switched off

Looking at condensate when 1st and 8th row of pipes are turned off it can be observed in Figure 30 that values from measurements oscillate close to the ones from *THSC* model except cases 9 and 10. For those measurements there was a problem with the amount of condensate. There is no other explanation for much smaller condensation as the operating conditions are similar to case 5 and 6. Also other parameters depicted in Figures 26-29 do not exhibit such behavior. Amount of condensate calculated in *THSC* model for such a small steam flow rate is insensitive to parameters other than the order of switched off/on rows of pipes or steam flow rate itself.

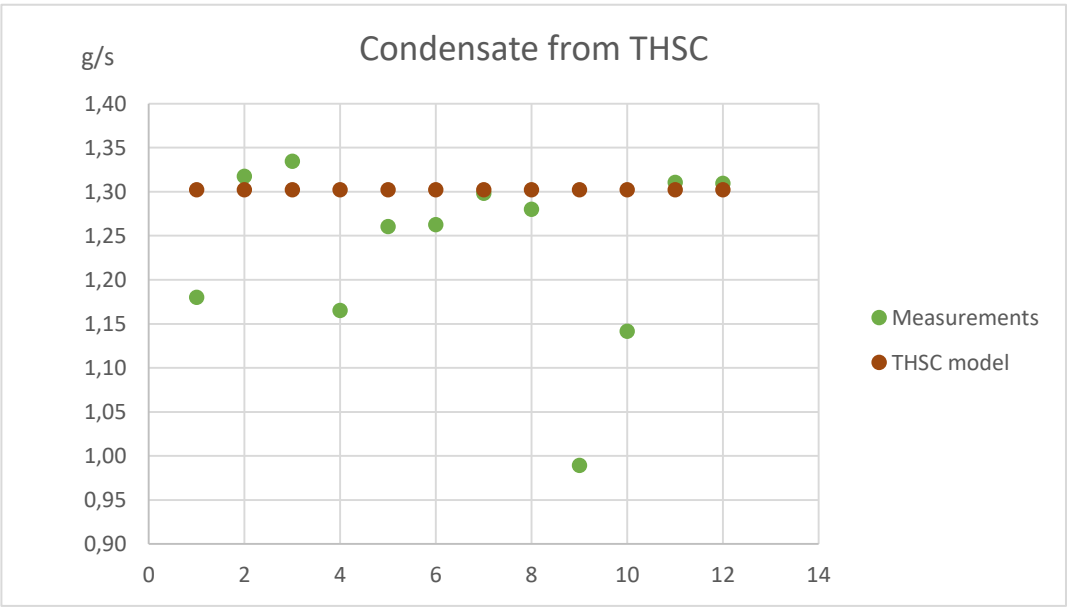

Figure 30 Condensate results from THSC model vs measurements – 1st and 8th tier switched off

When switching 1st and 2nd rows of pipes the amount of condensate from *THSC* model is each time greater than measured one which increased the average discrepancy of the results. The reason of that is Eps value for 8th row is allowing to condense more than on 2nd pipe. The results are shown in Figure 31.

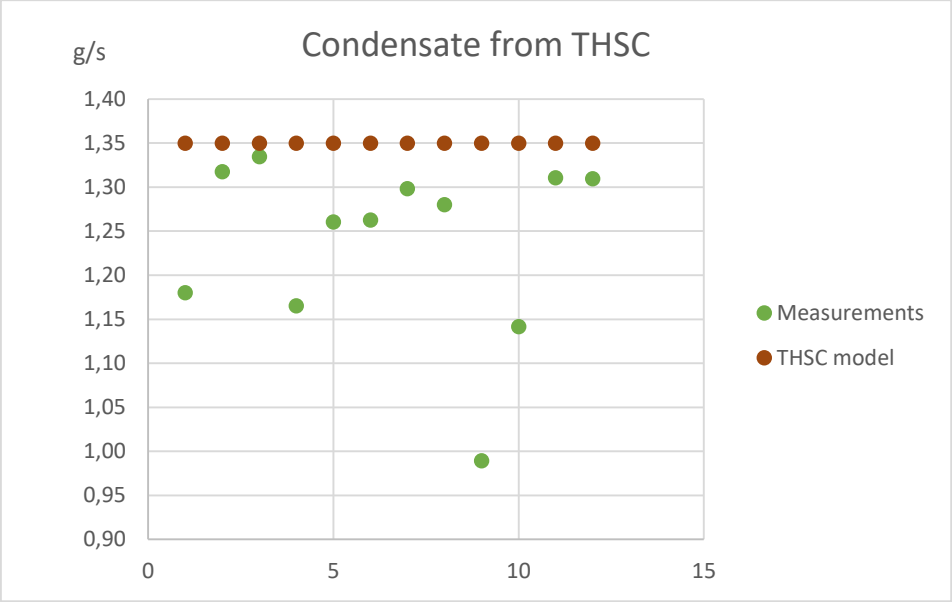

Figure 31 Condensate results from THSC model vs measurements – 1st and 2nd tier switched off

Although, temperatures and relative humidity reach the satisfactory level the comparison of condensate from *THSC* model with measured values shows it is insensitive to parameters change. Such a behavior is an influence of *Eps* correction factors. When more front rows of pipes are turned off more steam is led further and condensed there in a greater amount. Still, the difference in condensate values relates to relatively low level (low RH) far from the region at which mixture of air/water mist can appear. It has to be highlighted that above the level of limitation when the steam flow rate is high enough not only each switched off row results in decreased condensate value but also other parameters influence the results.

According to all analyses it is observed that the model is not perfectly corresponding to every measurement [10]. Nevertheless, *THSC* model according to tested cases can be assumed as an adequate tool to observe trends of change. Imperfections depending on simplification are small enough to be accepted and worth time saved in comparison to the full model. But of course, it has to be highlighted that such a model cannot be used as one and only tool for making final decisions. Any change based on *THSC* model analysis before carrying it out has to be verified in real scale prototype or at least fully developed CFD model.

4. Analysis of THSC work

The *THSC* is aimed to condensate steam and eliminate the risk of a mixture of air/water mist appearance at the outlet. Therefore, the analysis which is presented further take into account worsening conditions favourable water droplets creation at the outlet. The analysis is started for the input data from base construction for which the *THSC* model is positively validated. The values taken for calculation can

be found in row 17 in Table 12. At the beginning, it is checked whether the increase of RH of incoming air up to 100% may end up with fog at the outflow. The calculation in the model is done with default air and steam distribution option [10]. Table 13-14 and Figure 32 show input data, results and the graphical representation of the solution respectively.

Table 13 THSC work analysis – increase of RH of air

Sucked air				Steam	
Air flow rate	Relative humidity	Temperature of the air	Pressure	Steam flow rate	Temperature
kg/s	%	K	hPa	kg/s	K
0.208019	40.3	297.1	987.2	0.00136	373.15
0.208019	50.0	297.1	987.2	0.00136	373.15
0.208019	60.0	297.1	987.2	0.00136	373.15
0.208019	70.0	297.1	987.2	0.00136	373.15
0.208019	80.0	297.1	987.2	0.00136	373.15
0.208019	90.0	297.1	987.2	0.00136	373.15
0.208019	95.0	297.1	987.2	0.00136	373.15
0.208019	100.0	297.1	987.2	0.00136	373.15

Table 14 THSC work analysis - outflow results for change of RH

Right Section			Total outflow from THSC			Left Section		
Condensate	T_{air}	RH	Condensate	T_{air}	RH	Condensate	T_{air}	RH
kg/s	K	%	kg/s	K	%	kg/s	K	%
4.85E-04	307.6	22.00	1.35E-03	311.1	18.00	7.43E-04	312.6	17.00
4.85E-04	307.6	27.00	1.35E-03	311.1	23.00	7.43E-04	312.6	21.00
4.85E-04	307.5	33.00	1.35E-03	311.0	27.00	7.43E-04	312.5	25.00
4.85E-04	307.5	38.00	1.35E-03	311.0	32.00	7.43E-04	312.5	29.00
4.85E-04	307.5	44.00	1.35E-03	310.9	36.00	7.43E-04	312.4	34.00
4.85E-04	307.4	50.00	1.35E-03	310.9	41.00	7.43E-04	312.3	38.00
4.85E-04	307.4	52.00	1.35E-03	310.9	43.00	7.43E-04	312.3	40.00
4.85E-04	307.4	55.00	1.35E-03	310.8	46.00	7.43E-04	312.3	42.00

It occurs that although the air relative humidity reaches the 100% the THSC is able to deal with it and at the outflow the air has no more than 46%. In both sections, the higher is initial RH the higher is the one at the outflow, but because of temperature increase the air can accumulate more humidity in it under those changed conditions. Since the amount of steam going through the right section is lower, the amount of heat and temperature increase is lesser than in the left one. Therefore, before mixing in the right one the RH reaches greater level. Even though, the air humidity increase does not influence the amount of condensate from condenser which is equal to about 90% of initial steam flow rate. Having in mind the constant amount of steam which condenses on the walls (about 0.126 g/s) one can see almost all steam is condensed (99.2%). Correlation between amount of humid at the inlet and outlet of *THSC* is linear which is presented below in Figure 32.

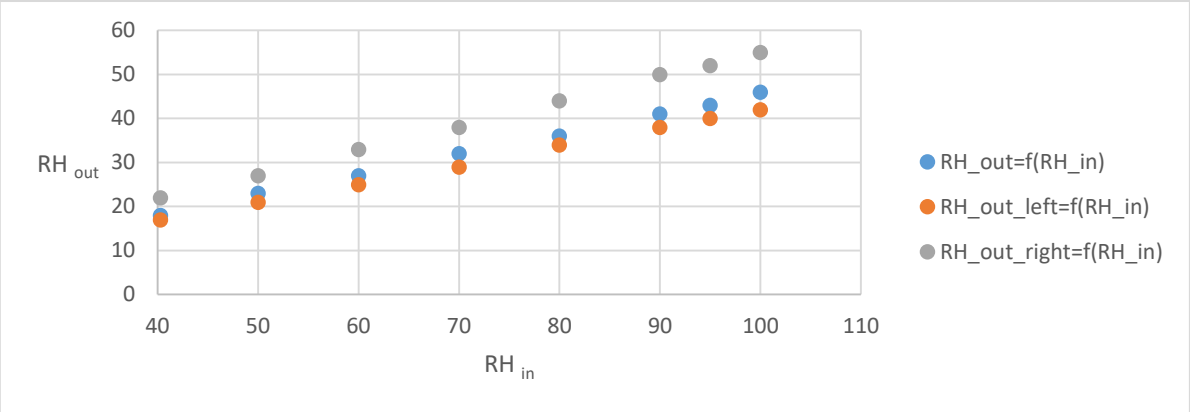

Figure 32 THSC work analysis - graph of influence of RH

The last calculated case is taken as initial one for next analysis in which temperature of input air is increased. The goal of such a test is to check whether the *THSC* can work right in an unfavourable environment where both temperature and RH are high and so the fresh air sucked inside can take less heat from the steam. Default air and steam distribution are activated once more and the range of change is assumed between 297.1 – 307 K which is shown in Table 15.

Table 15 THSC work analysis - increase of air temperature

Sucked air				Steam	
Air flow rate	Relative humidity	Temperature of the air	Pressure	Steam flow rate	Temperature
kg/s	%	K	hPa	kg/s	K
0.208019	100.0	297.1	987.2	0.00136	373.15
0.208019	100.0	299.0	987.2	0.00136	373.15
0.208019	100.0	301.0	987.2	0.00136	373.15
0.208019	100.0	303.0	987.2	0.00136	373.15
0.208019	100.0	305.0	987.2	0.00136	373.15
0.208019	100.0	307.0	987.2	0.00136	373.15

It can be observed in Table 16 that the higher the temperature is for air inflowing the condenser, the warmer is at the outflow. Furthermore, as previously the RH at the outlet increases spite of the outflowing air being warmer. Nevertheless, the amount of condensate still does not change keeping the level of about 99% of condensation efficiency taking into account the amount from walls.

Table 16 THSC work analysis - outflow results for change of temperature

Right Section			Total outflow from THSC			Left Section		
Condensate	T_{air}	RH	Condensate	T_{air}	RH	Condensate	T_{air}	RH
kg/s	K	%	kg/s	K	%	kg/s	K	%
4.85E-04	307.4	55.00	1.35E-03	310.8	46.00	7.43E-04	312.3	42.00
4.85E-04	309.3	56.00	1.35E-03	312.7	46.00	7.43E-04	314.1	43.00
4.85E-04	311.2	56.00	1.35E-03	314.6	47.00	7.43E-04	316.1	44.00
4.85E-04	313.1	57.00	1.35E-03	316.5	48.00	7.43E-04	318.0	44.00
4.85E-04	315.1	58.00	1.35E-03	318.5	48.00	7.43E-04	319.9	45.00
4.85E-04	317.0	58.00	1.35E-03	320.4	49.00	7.43E-04	321.8	46.00

Nevertheless, the initial conditions of the air do not result in fog appearance (a mixture of air/water mist) neither at the outflow nor at any of the sections. One more time, because of the same reason as previously, the temperature of the air in right section is lower. In consequence the relative humidity reaches more percentage points comparing two the left one as in Figure 33.

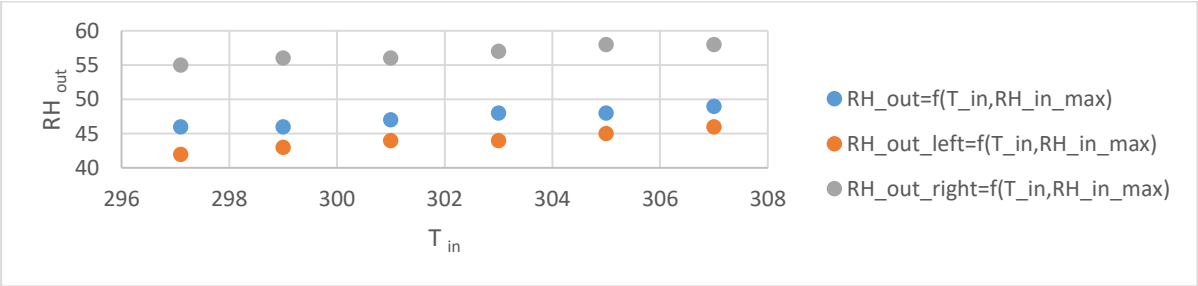

Figure 33 THSC work analysis - graph of influence of temperature

The last analysis under default option is connected with steam flow rate increase. In this case, amount of steam is the multiple of initial flow rate 0.00136 kg/s (like in first 9 rows in Table 17) until mass flow rate reaches the value 0.01224 kg/s. Next cases are calculated with the same step but starting from a doubled value equal to 0.02448 kg/s (given in 10th row which is double flow rate from 9th row).

Table 17 THSC work analysis - increase of steam flow rate

Sucked air				Steam	
Air flow rate	Relative humidity	Temperature of the air	Pressure	Steam flow rate	Temperature
kg/s	%	K	hPa	kg/s	K
0.208019	100.0	307.0	987.2	0.00136	373.15
0.208019	100.0	307.0	987.2	0.00272	373.15
0.208019	100.0	307.0	987.2	0.00408	373.15
0.208019	100.0	307.0	987.2	0.00544	373.15
0.208019	100.0	307.0	987.2	0.0068	373.15
0.208019	100.0	307.0	987.2	0.00816	373.15
0.208019	100.0	307.0	987.2	0.00952	373.15
0.208019	100.0	307.0	987.2	0.01088	373.15
0.208019	100.0	307.0	987.2	0.01224	373.15
0.208019	100.0	307.0	987.2	0.02448	373.15
0.208019	100.0	307.0	987.2	0.02584	373.15
0.208019	100.0	307.0	987.2	0.0272	373.15
0.208019	100.0	307.0	987.2	0.02856	373.15
0.208019	100.0	307.0	987.2	0.02992	373.15
0.208019	100.0	307.0	987.2	0.03128	373.15
0.208019	100.0	307.0	987.2	0.03264	373.15
0.208019	100.0	307.0	987.2	0.034	373.15
0.208019	100.0	307.0	987.2	0.03536	373.15

Increasing the amount of steam from first three cases is low enough to be limited by *Eps* coefficients. That is the reason why temperature is getting higher while the relative humidity value drops. Amount of condensate increases while increasing the steam flow rate depending on *Eps* limitation. When the same amount of steam is higher like in next rows the *THSC* works with maximum possible power since there is enough steam inside it to be sure pipes are all the time surrounded by steam.

Thenceforth, the amount of condensate does not change and each additional portion of steam results in increased humidity at the end. Although the pipes work with maximum power, condensation efficiency decreases while steam flow rate is increasing since the amount of condensate compared to enlarging amount of steam give lower percentage results. One more thing is worth underlining in this place. Since the model at the end takes into account both heat losses through the walls and the water condensed on the walls which give bigger value, the temperature at the outflow is higher than the ones from both left and right section. Particular values can be checked both in Table 18 and Figure 34-35.

Table 18 THSC work analysis - outflow results for change of steam flow rate

Right Section			Total outflow from THSC			Left Section		
Condensate	T_{air}	RH	Condensate	T_{air}	RH	Condensate	T_{air}	RH
kg/s	K	%	kg/s	K	%	kg/s	K	%
4.85E-04	317.0	58.00	1.35E-03	320.4	49.00	7.43E-04	321.8	46.00
1.04E-03	328.6	33.00	2.70E-03	334.0	26.00	1.53E-03	337.4	22.00
1.57E-03	339.5	20.00	3.45E-03	341.7	19.00	1.75E-03	342.1	20.00
1.65E-03	341.3	21.00	3.53E-03	342.8	21.00	1.75E-03	342.4	23.00
1.65E-03	341.6	24.00	3.53E-03	343.0	24.00	1.75E-03	342.6	26.00
1.65E-03	341.9	27.00	3.53E-03	343.3	27.00	1.75E-03	342.9	28.00
1.65E-03	342.1	30.00	3.53E-03	343.5	29.00	1.75E-03	343.1	31.00
1.65E-03	342.4	32.00	3.53E-03	343.80	31.00	1.75E-03	343.3	33.00
1.65E-03	342.7	35.00	3.53E-03	344.00	34.00	1.75E-03	343.5	35.00
1.65E-03	344.8	53.00	3.53E-03	345.90	50.00	1.75E-03	345.4	51.00
1.65E-03	345.1	55.00	3.53E-03	346.10	52.00	1.75E-03	345.6	52.00
1.65E-03	345.3	57.00	3.53E-03	346.30	53.00	1.75E-03	345.8	54.00
1.65E-03	345.5	58.00	3.53E-03	346.50	55.00	1.75E-03	345.9	55.00
1.65E-03	345.6	60.00	3.53E-03	346.60	56.00	1.75E-03	346.1	57.00
1.65E-03	345.8	61.00	3.53E-03	346.80	58.00	1.75E-03	346.3	58.00
1.65E-03	346.0	62.00	3.53E-03	347.00	59.00	1.75E-03	346.5	59.00
1.65E-03	346.2	64.00	3.53E-03	347.20	60.00	1.75E-03	346.7	61.00
1.65E-03	346.4	65.00	3.53E-03	347.30	61.00	1.75E-03	346.8	62.00

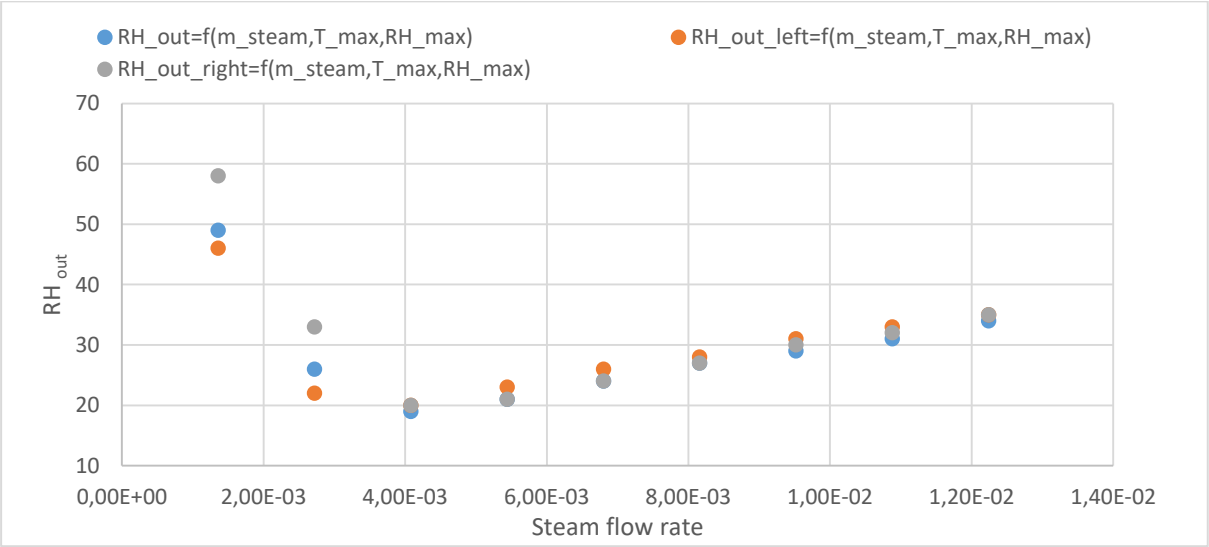

Figure 34 THSC work analysis - graph of influence of steam flow rate (rows 1-9)

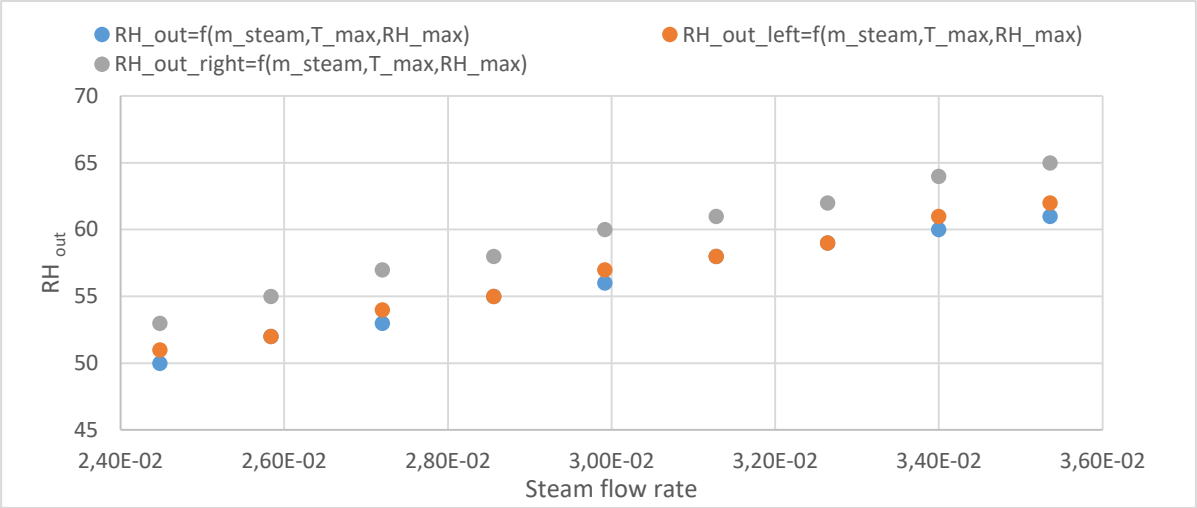

Figure 35 THSC work analysis - graph of influence of steam flow rate (rows 10-18)

Even though, the bigger amount of steam would be most probably limited in reality much earlier by fluid resistance, according to assumed values it is decided to check for what amount of steam the mixture of air/water mist appears. Tables 19-20 present cases when this phenomenon takes place.

Table 19 THSC work analysis - increase of steam flow rate (mixture of air/water mist appearance)

Sucked air				Steam	
Air flow rate	Relative humidity	Temperature of the air	Pressure	Steam flow rate	Temperature
kg/s	%	K	hPa	kg/s	K
0.208019	100.0	307.0	987.2	0.09792	373.15
0.208019	100.0	307.0	987.2	0.11016	373.15
0.208019	100.0	307.0	987.2	0.1224	373.15
0.208019	100.0	307.0	987.2	0.12512	373.15
0.208019	100.0	307.0	987.2	0.12784	373.15

Table 20 THSC work analysis - outflow results for change of steam flow rate (mixture of air/water mist appearance)

Right Section			Total outflow from THSC			Left Section		
Condensate	T_{air}	RH	Condensate	T_{air}	RH	Condensate	T_{air}	RH
kg/s	K	%	kg/s	K	%	kg/s	K	%
1.65E-03	352.1	97.00	3.53E-03	352.7	93.00	1.75E-03	352.3	94.00
1.65E-03	352.9	100.00	3.53E-03	353.4	96.00	1.75E-03	353.0	97.00
1.65E-03	354.1	100.00	3.53E-03	352.8	99.00	1.75E-03	348.8	100.00
1.65E-03	354.4	100.00	3.53E-03	360.0	100.00	1.75E-03	354.0	100.00
1.65E-03	354.7	100.00	3.53E-03	354.5	100.00	1.75E-03	354.3	100.00

Feedback given by above analysis proves the design of *THSC* can provide proper work and fulfill its task under much worse condition than commonly occurred. Therefore, it raises the question if some of the pipes were cut off would the condenser still satisfy the customer demands. Checking how much rows of pipes can be switched off the input parameters are assumed as in Table 21. Choosing

the user-defined option instead of default one the number of working pipes and fluid distribution can be controlled. Rows of pipes are counted from steam inlets to air fan (1 for top one and 8 for bottom one in Figure 42 in Appendix A). Two approaches are examined with the same, unchanged amount of inlet air which is equally redistributed between the rest off working pipes (chosen option - Assume initial air flow rate in Figure 42).

Table 21 THSC work analysis - input data for pipes modification

Sucked air				Steam	
Air flow rate	Relative humidity	Temperature of the air	Pressure	Steam flow rate	Temperature
kg/s	%	K	hPa	kg/s	K
0.208019	100.0	307.0	987.2	0.00136	373.15

Firstly, it is assumed the rows of pipes are switched off symmetrically. It means when turning off the first row of pipes in both left and right section three pipes are chosen as not working in each, which gives six pipes in total. In addition to this, the steam flow rate is distributed equally between sections starting from the case when first rows of pipes are switched off (chosen option – EQUAL in Figure 42). Such an assumption checks whether enlarging of steam passage in lieu of first rows of pipes can give satisfactory effect. From the moment when 3 or more tiers are turned off, the model informs that calculation based on air mass flow rate enters extrapolation region. Nevertheless, *THSC* works right even with only 2 last rows of pipes. When trying to switch off the 7th one model is too far from the analyzed region where power starts to be negative which is not feasible. It might be said that with no consequence the first rows of pipes can be switched off since there is no change at the outflow. Nevertheless, condensation efficiency is kept around 99% until the 4th row is switched off when condensate decreases up to 1.33 g/s. The results can be observed in Table 22.

Table 22 THSC work analysis - outflow results for change of pipes with equal distribution of steam

	Right Section			Total outflow from THSC			Left Section		
Switched off rows of pipes	Condensate	T_{air}	RH	Condensate	T_{air}	RH	Condensate	T_{air}	RH
number	kg/s	K	%	kg/s	K	%	kg/s	K	%
-	4.85E-04	317.0	58.00	1.35E-03	320.4	49.00	7.43E-04	321.8	46.00
1	6.13E-04	319.7	51.00	1.35E-03	320.3	49.00	6.13E-04	319.2	52.00
1,2	6.12E-04	319.6	51.00	1.35E-03	320.3	49.00	6.12E-04	319.2	52.00
1,2,3	6.07E-04	319.5	51.00	1.34E-03	320.3	50.00	6.10E-04	319.2	52.00
1,2,3,4	6.00E-04	319.4	52.00	1.33E-03	320.1	50.00	6.04E-04	319.1	53.00
1,2,3,4,5	5.93E-04	319.2	52.00	1.32E-03	320.0	50.00	5.98E-04	319.0	53.00
1,2,3,4,5,6	5.78E-04	318.9	54.00	1.29E-03	319.7	51.00	5.84E-04	318.7	54.00

To be sure, the steam distribution is not influencing significantly the results in the same approach the calculations are repeated with the steam flow rate distributed according to internal formula dependent on the amount of steam inflowing the *THSC* (EQUAL option is not activated). In this case, steam passage stays the same although the pipes are switched off while all the other assumptions are as those described above. The same communications about extrapolation and negative power appear

when switching off 3rd and 7th row of pipes respectively. The final result is at the same level but the disproportion of steam between sections is visible in temperature and RH difference comparing left and right section. The solution is gathered in Table 23.

Table 23 THSC work analysis - outflow results for change of pipes with internal formula for distribution of steam

	Right Section			Total outflow from THSC			Left Section		
Switched off rows of pipes	Condensate	T_{air}	RH	Condensate	T_{air}	RH	Condensate	T_{air}	RH
number	kg/s	K	%	kg/s	K	%	kg/s	K	%
-	4.85E-04	317.0	58.00	1.35E-03	320.4	49.00	7.43E-04	321.8	46.00
1	4.84E-04	317.0	58.00	1.35E-03	320.3	49.00	7.42E-04	321.7	46.00
1,2	4.83E-04	317.0	59.00	1.35E-03	320.3	49.00	7.40E-04	321.7	46.00
1,2,3	4.81E-04	316.9	59.00	1.34E-03	320.3	49.00	7.37E-04	321.7	46.00
1,2,3,4	4.74E-04	316.8	59.00	1.33E-03	320.1	50.00	7.31E-04	321.6	46.00
1,2,3,4,5	4.68E-04	316.6	60.00	1.32E-03	320.0	50.00	7.23E-04	321.5	47.00
1,2,3,4,5,6	4.58E-04	316.4	61.00	1.29E-03	319.6	52.00	6.92E-04	320.9	49.00

The second approach assumes only rows of pipes from the right section are switched off. Additionally, steam distribution is based on an internally implemented formula dependent on steam flow rate value itself. According to report, the extrapolation region is entered when turning off the 5th tier from right section but on the other hand negative power is not announced at all. On the basis of *THSC* model for assumed input data right section can be fully switched off and the left one is enough to prevent the mixture of air/water mist at the outflow. Nevertheless, condensation efficiency drops below 99% when the 4th row of pipes is switched off and for only left section working the same factor is equal to only 63.9%. Results are stored in Table 24.

Table 24 THSC work analysis - outflow results for change of pipes in right section with internal formula for distribution of steam

	Right Section			Total outflow from THSC			Left Section		
Switched off rows of pipes (right section only)	Condensate	T_{air}	RH	Condensate	T_{air}	RH	Condensate	T_{air}	RH
number	kg/s	K	%	kg/s	K	%	kg/s	K	%
-	4.85E-04	317.0	58.00	1.35E-03	320.4	49.00	7.43E-04	321.8	46.00
1	4.84E-04	318.0	56.00	1.35E-03	320.4	49.00	7.43E-04	320.6	49.00
1,2	4.83E-04	319.1	53.00	1.35E-03	320.3	49.00	7.43E-04	319.7	51.00
1,2,3	4.80E-04	320.6	49.00	1.35E-03	320.3	49.00	7.43E-04	318.7	54.00
1,2,3,4	4.74E-04	322.9	44.00	1.34E-03	320.2	50.00	7.43E-04	317.8	56.00
1,2,3,4,5	4.68E-04	326.7	36.00	1.34E-03	320.2	50.00	7.43E-04	316.9	59.00
1,2,3,4,5,6	4.47E-04	333.3	27.00	1.32E-03	320.0	50.00	7.43E-04	316.1	61.00
1,2,3,4,5,6,7	2.84E-04	338.6	26.00	1.15E-03	318.4	56.00	7.43E-04	315.3	64.00
All pipes	0.00E+00	373.0	100.00	8.69E-04	309.8	91.00	7.43E-04	314.5	67.00

It should be highlighted that, according to all analyzed cases in this chapter, *THSC* can be produced with less investment capital while keeping the same level of performance in many applications.

In other words, it is recommended to consider the production of a few versions of the same *THSC* but with a limited amount of rows of pipes inside it. Such an unsophisticated change would not influence significantly the process of either production the *THSC* or its fitting together with already produced ovens. At the same time, a removal of any number of internally finned pipes would decrease the production cost of the whole device.

Apart from this, the *THSC* model is compared with measured results and as a simplified version of fully developed CFD model it generates a solution with acceptable discrepancy taking into account the availability of the software and relatively much shorter time needed for any kind of analysis done by the user.

5. Conclusions

Within the framework of this thesis, a top hood steam condenser mathematical model is developed. Its final version written in Visual Basic for Application in Excel satisfies the Retech company needs to have software for private use free of paid license and straightforward for users without specific technical background. Satisfying all the demands there are required not only global mass and energy balances but also an empirical equation of a single pipe and other correlations.

Work on the full steam condenser model consists of several stages starting from CFD simulation, through GUI creation and implementation of developed single pipe thermal response model up to validation the *THSC* model against measurements and preliminary analysis of possible change.

The first conclusion is related to building a geometry and a mesh of the single pipe which has to be fully structural hexahedral one. If non-structural or mixed mesh appeared the quality of solution would be significantly decreased and influence final results [3]. Based on that, it is crucial to create the mentioned geometry that consisted of only separate, replicated quadrilateral sketches.

Furthermore, the mesh aimed at solving the heat transfer phenomena can be simplified. Indeed, all the chamfers and filletings are eliminated improving the feasibility of the numerical solution in Fluent [3]. From the heat transfer point of view that change has negligible influence and that is why it is accepted without any hazard for results.

Another limitation, which strongly influences the development of single pipe model, is to use a student Ansys license which allows for usage of only half of a million elements mesh. Such model is successfully validated against benchmark prepared with the full version of the Fluent. The goal is achieved by refining the mesh inside and nearby the fins where the heat transfer is intense at the cost of the elements in the core of the pipe. The right approach to mesh creation and specific settings with chosen models in Fluent plays crucial role from the technical point of view.

Nevertheless, one of the most important conclusions of the thesis is that usage of tabular efficiencies for fins would negatively affects the results. At first sight, values computed for externally finned pipes can be applied for this rare situation of internally mounted fins. Such an approach would be wrong if it were accepted. According to heat transfer coefficient from a few cases calculated in Fluent, the efficiencies for internal and external fins on the same geometry are compared. Each time the efficiency of the internally installed fins is 5 to 6 percentage points lower than for tabular ones, which are very accurate. Lack of correspondence between efficiencies proves different behaviours depending on the place of fins mounting. Thus, decision of single pipe modeling in Fluent in this particular case is reasonable.

Since each simulation in Fluent lasts relatively long time and it is impossible to check all configurations the representative amount of cases is chosen to cover the widest possible distribution of the parameters within variants. Influence of five chosen factors on the power of the pipe is analyzed and used as the basis for formula implemented to VBA code. From the simulation, it occurs that the power in single pipe grows mostly along with mass flow rate of air. More important is the fact, for values greater

than 0.0167 kg/s the behaviour is inversed with decreasing power trendline. Since this is unacceptable it is limited by internal conditions in *THSC* model. For the rest of the factors such a phenomenon does not appear and so they can be limited within the just feasible range of input data.

An empirical equation is developed after testing four different approaches. The chosen one is based on air mass flow rate as the most influential factor. For all of them, Excel coefficients are taken from trendlines. Except air mass flow rate parameter other four are treated as correction factors in equation (16). Such a decision is made with respect to the smallest maximum error (1.5%) comparing all variants. The final empirical equation aim is assumed to model the single pipe work equally good within the whole range of solutions. That is why other variants having smaller average errors with some exceptions reaching 2% or even more are rejected.

As it is already mentioned the user should not be obliged to know either the fundamentals of heat transfer phenomenon or use sophisticated CFD simulation software. Therefore, widely available Excel with VBA is chosen to create the fully developed model. The interface connecting the user with the software is designed with transparent GUIs which guide him through the whole procedure of data implementation. Mistakes like wrong format or values entering the extrapolation region are verified by conditions embedded in the model. Such an approach minimizes user errors since model helps to localize the source of the problem or eliminates them fully. Such a user-friendly model let the process of usage acceptable for any employee being its huge asset from the company point of view.

Assumed simplifications and built-in equations like the one for the power and Eps correction factors result in some discrepancies comparing results from the model to the measured ones [10]. Nevertheless, the model allows the user to observe right trends of changes and results at satisfactory level. On the other hand, computing power and time needed for calculation in *THSC* model is orders of magnitude smaller than using the whole *THSC* Fluent model. It is worth mentioning that the single change in the Fluent model of *THSC* may take from a few hours to weeks to converge the model while work with the *THSC* model is limited to a couple of seconds. Taking into account all the aspects the existence of such a tool facilitates preliminary analysis with a much lower cost both human power and monetary.

The last but not least conclusion comes from the analysis carried out with the *THSC* model. The analysis is aimed to verify whether the considered design of *THSC,* which is on sale in a single variant, is over-scaled in many appliances and demonstrate the theory that there is the margin for optimization. According to received results it occurs the *THSC* is most probably overscaled since even much worse operating conditions do not result in a mixture of air/water mist appearance at the outflow which is a disqualifying factor. Nevertheless, the amount of condensate decreases and so, related with it, condensation efficiency of a device also decreases.

For a relative humidity of inlet air equal to 100%, the RH of the outflowing air reaches maximum of 46%. Adding to this the inlet air temperature increase up to 307 K results in only 3 more percentage point in RH at the outflow. The condensation efficiency in both cases does not drop below 99% (taking into account that constant value of 0.126 g/s of steam which is condensed on the walls). Keeping those two parameters and increasing the steam mass flow rate, the amount of humidity does not exceed the

saturation point unless the mass flow rate is 94 times greater (0.12784 kg/s) than default one (0.00136 kg/s), but condensation efficiency gets worse from 99.26% down to 2.76%. Such a huge flow rate most probably would not flow through a device without any change in fluid resistance, which is not taken into account in the *THSC* model. Nevertheless, that wide range of operating condition under which *THSC* can still play its role proves the device can handle much worse conditions than those commonly operated.

The previously observed behaviour of the condenser highlights that there is an opportunity to drag the production cost down considering different applications. For those ovens where steam flow rate rarely reaches higher values than the default ones it is checked how much fewer pipes can be mounted inside *THSC,* keeping the same performance. Three different approaches are verified turning off the rows of pipes in both sections either with symmetrical distribution or dependent on internal formula and finally switching off only rows of pipes from the right section with the distribution of steam contrrolled internally.

First and second approach differ only by the method of steam flow rate redistribution between sections [10]. In the former, it is assumed that in the place of removed pipes the steam passage connecting two sections is enlarged. Thanks to that, the steam flow rate spreads equally between left and right sections. The latter, in opposition, does not take into account any change and the share of steam depends only on steam flow rate itself. Even though, in the second approach less steam is directed to the right section because of the narrow connecting passage. But the final results are the same. In both cases, model allows to switch off 6 rows of pipes before entering the extrapolation region where power value is negative because of too big air flow rate going through the single pipe. Relative humidity is 51% and 52% and temperature 319.7 K and 319.6 K respectively. Looking at the condensation efficiency the level of 99% is kept one more time in both cases until 4^{th} rows of pipes are turned off with preceding ones. For all 6 rows of pipes switched off the same factor drops to the level of 94-95% depending on the approach.

The last approach assumes internally controlled steam distribution and switching off only pipes from right section, since there is a suspicion that *THSC* can work with only one section. Indeed, with those operating conditions and all right section pipes turned off, the mixture of air/water mist does not appear yet at the outflow and the condensation efficiency drops up to the level of 63.9%. The condensation efficiency is kept at the level of 99% until a 4^{th} row of pipes in right section is switched off. This analysis confirms the hypothesis that the number of pipes mounted inside *THSC* may be cut down. In these particular analysis the results prove user can eliminate first 3 rows of pipes with no consequence for the *THSC* performance.

Since *THSC* is only a subpart of greater and more expensive device, which is a large scale cooking oven in this case, its modification with respect to global geometry and size is complicated. Knowing that internally finned pipes are unusual and in consequence generate higher production cost it is highly recommended to consider a few customized versions of *THSC*. Depending on designed operating conditions the amount of mounted inside pipes may differ. Such a possibility may decrease the investment cost for some applications and does not influence the production process significantly.

Moreover, this kind of change does not hamper the fitting of *THSC* as subpart with the more expensive product - oven.

One of the main aims of the thesis is to find out whether the *THSC* model with implemented CFD single pipe model may correlate with the actual *THSC*. Successfully accomplished goal saves time and human power being used by Retech company for improvements of the device. For this particular model, it can be checked how the changes in working conditions and geometry influence the performance of *THSC*. Results comparing to measurements reach a satisfactory level of accuracy. Nevertheless, future work in this field is required in order to extend the possible range of analyzed operating conditions. In addition, other approaches to correction factors can be used to develop the model and for improvement of the overall results quality. What is more, the same idea of the model can be used for other equipments if needed since the Retech company produces a dozen of similar devices. The process of their development, as well as the one considered in this work, would proceed more efficiently when combined with user-friendly software. Easy to access, *THSC* models without huge investment costs can lead to better device performance and reduced expenditures thanks to quickly forecasted results of changes. The same model can allow a higher level of device customization which makes both the product more desirable from the customer point of view and saves raw materials if not needed for production which makes the process more eco-friendly.

References

[1] Yunus A. Çengel, Afshin J. Ghajar, “Heat and Mass Transfer. Fundamentals and Applications, Fourth Edition in SI Units”, McGraw-Hill, 2011

[2] Kevin W. Linfield, Robert G. Mudry, “Pros and Cons of CFD and Physical Flow Modeling”, A White Paper of Airflow Sciences Corporation, 2008

[3] Joel H. Ferziger, Milovan Peric, “Computational Methods for Fluid Dynamics, 3rd Edition”, Springer, 2001

[4] Retech – technical documentation of the THSC (personal information)

[5] Chris Long, Naser Sayma, “Heat Transfer”, Ventus Publishing ApS, 2009

[6] E. Bari, J.-Y. Noel, G. Comini G. Cortella, “Air-cooled condensing systems for home and industrial appliances”, Applied Thermal Engineering, Volume 25, Issue 10, July 2005, Pages 1446-1458

[7] Thomas G. Lestina, Robert W. Serth, “Process Heat Transfer. Principles, Applications and Rules of Thumb”, Book, 2nd Edition Elsevier, 2014, Pages 431-508

[8] W.F. He, Y.P. Dai, J.F. Wang, M.Q. Li, Q.Z. Ma, ”Performance prediction of an air-cooled steam condenser using UDF method”, Applied Thermal Engineering, Volume 50, Issue 1, 10 January 2013, Pages 1339-1350

[9] Dawid Taler, “Mathematical modeling and experimental study of heat transfer in a low duty air-cooled heat exchanger”, Energy Conversion and Management, Volume 159, 1 March 2018, Pages 232-243

[10] Documentation and results of the project POIR.03.02.01-18-0019/15-00 „Wdrożenie do produkcji nowej generacji pochłaniaczy pary do pieców konwekcyjno-parowych” (Implementation to production of a new generation of top hood steam condensers for the convection-steam ovens) in the frame of the 3.2.1 Action of Intelligent Development for 2014-2020 „Badania na rynek” (Research for the market) - in Polish

[11] John H. Lienhard IV, John H. Lienhard V, “A Heat Transfer Textbook, 3rd edition”, Phlogiston Press, 2008

[12] Manual for EES software, website: http://www.fchart.com/, (11.03.2018)

[13] W. M. Rohsenow, “Film Condensation”, In Handbook of Heat Transfer, ed. W.M. Rohsenow and J.P. Hartnett, McGraw-Hill, 1973

Appendix

Appendix A

Starting the model user enters the first Worksheet “Input_Output” shown in Figure 36. In this one main results are stored after the computation. To ease the analysis through the same Worksheet all the parameters for calculation can be given and saved. Both input and output are stored in the same row and using save button replicated downwards. Therefore, when needed data from previous cases can be just copied and pasted.

	A	B	C	D	E	F	G	H
1	Sucked air				Steam		INPUT	START
2	Air stream	Relative humidity	Temperature of the air	Pressure	Steam stream	Temperature		SAVE
3	kg/s	%	K	hPa	kg/s	K		CLEAN
4	0,21	100,00	307,0	987,20	0,03400	373		
5								
6								
7	Sucked air				Steam		D - Default / UD - User-de	
8	Air stream	Relative humidity	Temperature of the air	Pressure	Steam stream	Temperature	Date of save	
9	kg/s	%	K	hPa	kg/s	K		
10	0,208019	40,3	297,1	987,2	0,00136	373	2018-03-09	D
11	0,21	50,00	297,1	987,20	0,00136	373	2018-03-16	D
12	0,21	60,00	297,1	987,20	0,00136	373	2018-03-16	D

Figure 36 Worksheet "Input_Output" in the THSC model - Inputs

It can be observed in Figure 37 data are presented for the whole *THSC* as well as for both sections of it. From this place using the Start button, one can open the first GUI. After computation inside this and the second “Complementary_data” Worksheets there appear values representing a particular solution. If needed, the numbers are possible to be saved into the other place since each time all the values are overwritten. Besides, all previously saved cases with a solution can be deleted using the clean button.

H	I	J	K	L	M	N	O	P	Q	R	S	T	U
START	OUTPUT	Right Section				Total outflow from THSC				Left Section			
SAVE		Condensate	Efficiency	Temperature of the air	Relative humidity	Condensate	Efficiency	Temperature of the air	Relative humidity	Condensate	Efficiency	Temperature of the air	Relative humidity
CLEAN		kg/s	%	K	%	kg/s	%	K	%	kg/s	%	K	%
		1,66E-03	7,6	311,2	100,00	3,43E-03	10,1	295,5	100,00	1,77E-03	14,5	364,2	24,00
		SAVED DATA											
ault / UD - User-defined		Right Section				Total outflow from THSC				Left Section			
Date of save		Condensate	Efficiency	Temperature of the air	Relative humidity	Condensate	Efficiency	Temperature of the air	Relative humidity	Condensate	Efficiency	Temperature of the air	Relative humidity
		kg/s	%	K	%	kg/s	%	K	%	kg/s	%	K	%
2018-03-09	D	4,94E-04	80,5	308,2	24,00	1,24E-03	90,9	311,4	19,18	7,43E-04	99,5	312,6	17,00
2018-03-16	D	4,94E-04	80,5	308,1	30,00	1,24E-03	90,9	311,2	23,68	7,43E-04	99,5	312,4	21,00
2018-03-16	D	4,94E-04	80,5	308,0	35,00	1,24E-03	90,9	311,2	28,21	7,43E-04	99,5	312,4	25,00

Figure 37 Worksheet "Input_Output" in the THSC model - Outputs

Anytime, but just for the last calculated case if needed more detailed data are kept in the mentioned “Complementary_data” Worksheet. One more time, all the values were divided with respect to sections where the right one looking at the backside of *THSC* (further from steam channels) is for first twelve columns. Analogically the next 12 columns are showing results from left section. To make it easier next to the tables the visualization of *THSC* either right or left section was placed respectively.

Here, one can find a specific pipe with a dedicated output. In Figure 38, the organization of the Worksheet is shown.

Q_pipe W			Efficiency %		
Bottom	Middle	Top	Bottom	Middle	Top
231	207	204	100	100	100
183	158	186	100	100	100
167	161	196	100	100	100
158	154	183	100	100	100
143	138	164	100	100	100
131	126	141	100	100	100
125	129	118	100	100	100
113	101	134	100	100	100
Condensate g/s			**Temperature of air K**		
Bottom	Middle	Top	Bottom	Middle	Top
0,1025	0,0918	0,0906	344,1	338,7	344,9
0,0809	0,07	0,0826	341,4	337,9	344,8
0,074	0,0713	0,0868	341,7	339	342,2
0,0701	0,0684	0,0813	342,3	339,1	341,1
0,0634	0,0613	0,0726	340	338,7	341,2
0,058	0,056	0,0623	338,8	338,6	340,8
0,0555	0,0573	0,0525	337,9	340,6	340,3
0,0501	0,0446	0,0593	344	341,2	344,4

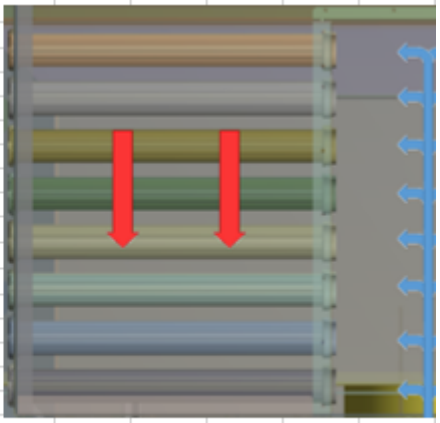

Figure 38 Worksheet "Complementary_data" in the THSC model - sample detailed data for right section of THSC

There is also the last Worksheet, namely “Saves” which play the role of a source for the program. Here, the user can find values for angles and percentage shares of air mass flow rates within all pipes. Moreover, the coefficients responsible for pipes' heat exchange efficiency (orange background) and factors depending on OFF/ON stage (green background) were located there. Most of them keep default data and are locked against any external modification. From this place, parameters can be only loaded using the button from one of the GUI. Nevertheless, the first table of factors might be (but it is not necessary) used as an input place for the model since there are kept last saved inputs. Figure 39 presents the layout of this Worksheet.

		Angle			Flux (% of total flux)			Angle			Flux (% of total flux)			Turned OFF/ON Pipe			Turned OFF/ON Pipe			last saved input for user-defined case
		Bottom	Middle	Top	Bottom	Middle	Top	Bottom	Middle	Top	Bottom	Middle	Top	Bottom	Middle	Top	Bottom	Middle	Top	
1	1	86,7	61,2	84,7	0,0277	0,029	0,024	62,9	82,8	61,7	0,0267	0,0277	0,0247	0	0	0	-1	-1	-1	
2	2	67,7	40,7	81,5	0,0236	0,0227	0,0219	71,1	64,4	55,2	0,0242	0,0251	0,0217	0	0	0	-1	-1	-1	
3	3	65,5	49,4	73,8	0,0214	0,0224	0,0247	83,1	82,2	52,4	0,0228	0,0241	0,0227	0	0	0	-1	-1	-1	
4	4	66,4	48,0	66,6	0,0199	0,0214	0,0239	83,1	89,5	48,4	0,0213	0,0223	0,0219	0	0	0	-1	-1	-1	
5	5	50,0	38,7	62,6	0,0193	0,0194	0,0213	82,7	78,9	47,5	0,0202	0,0213	0,0203	0	0	0	-1	-1	-1	
6	6	36,1	31,0	54,3	0,0183	0,0178	0,0185	63,1	51,4	46,9	0,019	0,0198	0,019	0	0	0	-1	-1	-1	
7	7	15,0	49,8	43,5	0,018	0,0171	0,0158	43,1	46,0	74,4	0,0186	0,0194	0,0184	0	0	0	-1	-1	-1	
8	8	62,7	42,1	69,7	0,0136	0,0131	0,0159	24,6	22,6	74,7	0,0161	0,0149	0,0171	0	0	0	-1	-1	-1	

	Default settings												
ROW	Angle			Flux (% of total flux)			Angle			Flux (% of total flux)			Default input for "back to default" button and default case window
	Bottom	Middle	Top	Bottom	Middle	Top	Bottom	Middle	Top	Bottom	Middle	Top	
1	86,7	61,2	84,7	0,0277	0,029	0,024	62,9	82,8	61,7	0,0267	0,0277	0,0247	
2	67,7	40,7	81,5	0,0236	0,0227	0,0219	71,1	64,4	55,2	0,0242	0,0251	0,0217	
3	65,5	49,4	73,8	0,0214	0,0224	0,0247	83,1	82,2	52,4	0,0228	0,0241	0,0227	
4	66,4	48,0	66,6	0,0199	0,0214	0,0239	83,1	89,5	48,4	0,0213	0,0223	0,0219	
5	50,0	38,7	62,6	0,0193	0,0194	0,0213	82,7	78,9	47,5	0,0202	0,0213	0,0203	
6	36,1	31,0	54,3	0,0183	0,0178	0,0185	63,1	51,4	46,9	0,019	0,0198	0,019	
7	15,0	49,8	43,5	0,018	0,0171	0,0158	43,1	46,0	74,4	0,0186	0,0194	0,0184	
8	62,7	42,1	69,7	0,0136	0,0131	0,0159	24,6	22,6	74,7	0,0161	0,0149	0,0171	

top	Eps	0,085	0,095	0,15	0,235	0,175	0,24	0,435	0,6	LEFT
middle		0,08	0,085	0,115	0,175	0,12	0,14	0,25	0,56	
bottom		0,06	0,06	0,075	0,1	0,085	0,085	0,14	0,2	
top		0,085	0,09	0,12	0,165	0,055	0,06	0,065	0,075	RIGHT
middle		0,07	0,08	0,1	0,135	0,04	0,035	0,04	0,05	
bottom		0,035	0,04	0,045	0,06	0,035	0,025	0,025	0,035	

Figure 39 Worksheet "Saves" in the THSC model - parameters for calculation

Knowing all the Worksheets it is possible to describe the GUI which will appear further. To call the first interface the mentioned Start button (Figure 36) has to be pressed. Firstly, if not given in the

Worksheet then here the Inputs can be specified or modified. Moreover, before calculation necessary is to decide whether the VBA should use the default values or the user is willing to specify more details. In Figure 40, the first GUI is presented.

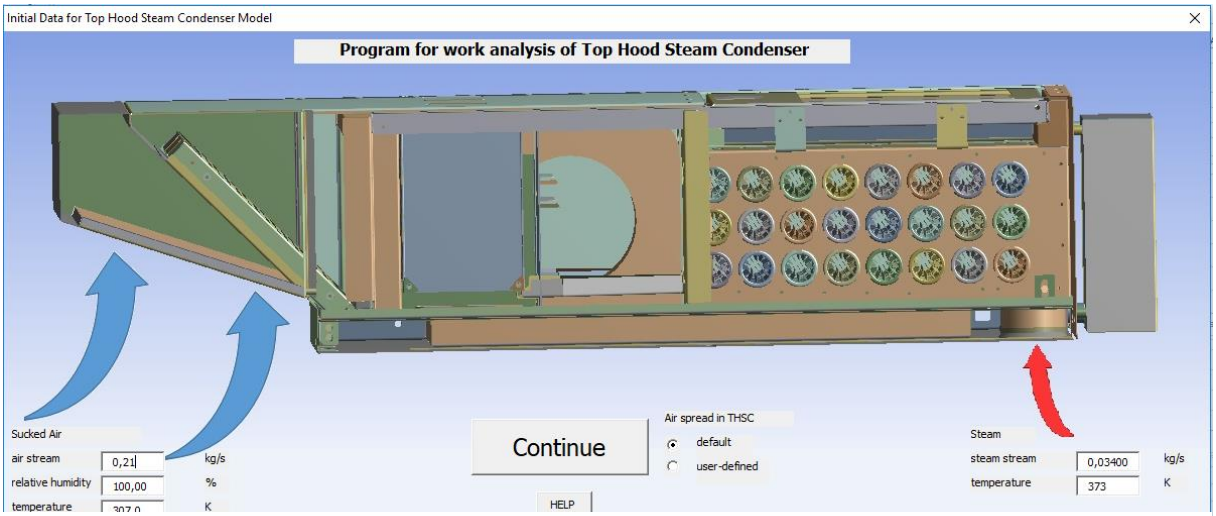

Figure 40 GUI1 - Initial Data for Top Hood Steam Condenser

Units and last used values for both air and steam set an example of a possible input to be entered. If not enough then user can find a wider explanation by clicking Help button (Figure 40). There one can find also a description of two possible options of calculation, the feasible, recommended ranges and crucial tips. How the Help GUI looks like can be observed in Figure 41.

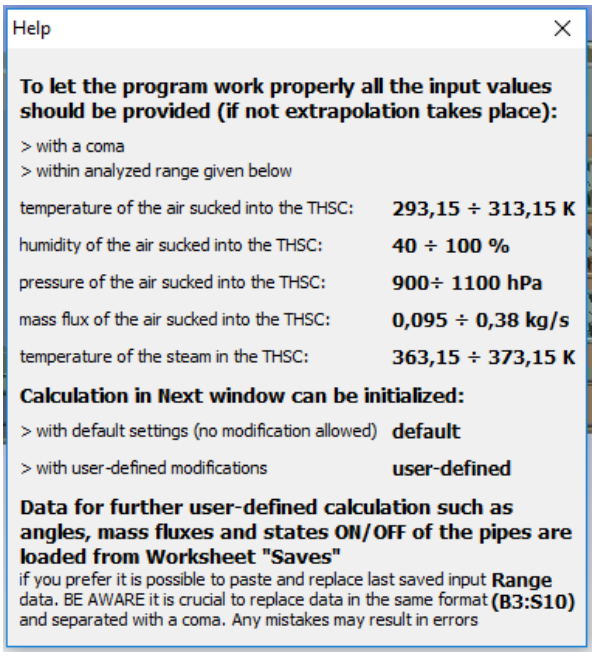

Figure 41 GUI1 - Help

Assuming the default option was to be used the next GUI would show the pre-defined angles and air flow rate shares with visualization of internal distribution [10]. At this stage, the user can accept the conditions as they are or go back and decide on user-defined working conditions. The same window would appear for a user-defined option with additional options. Therefore, in Figure 42, the presented interface is not the one for basic, default model but the second in which user can implement changes.

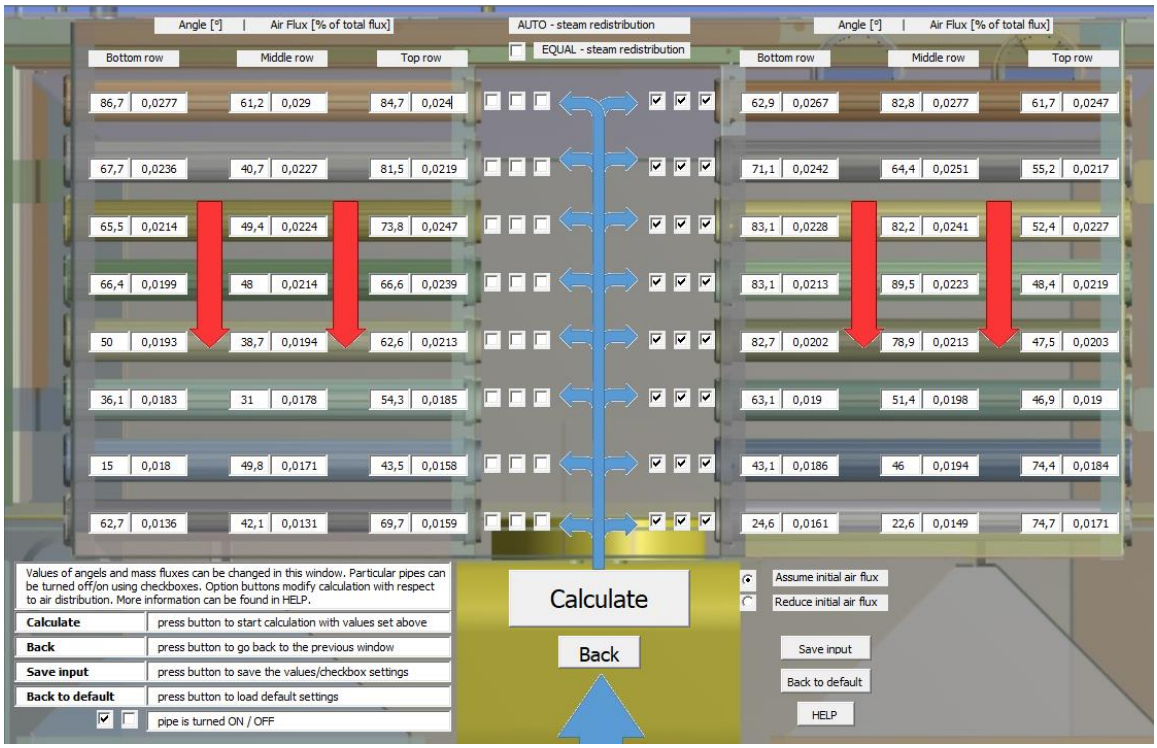

Figure 42 GUI2 - user-defined options

Each angle and flow rate value can be changed in the box or the pipe can be fully turned on/off. Before pressing Calculate it is wise to check the inputs but the program has built-in limits according to which user can be informed whether some of the solutions enter the extrapolation region or cannot be even initialized because of some errors. The sample information (Figure 43) might appear when the sum of flow rate shares does not equal unity or the air flow rate value is not in acceptable range. The user can decide whether let the software to correct it or not and do it personally in the first case. The second type of communicate deal with limiting errors and then the program is not initiating calculation before correction.

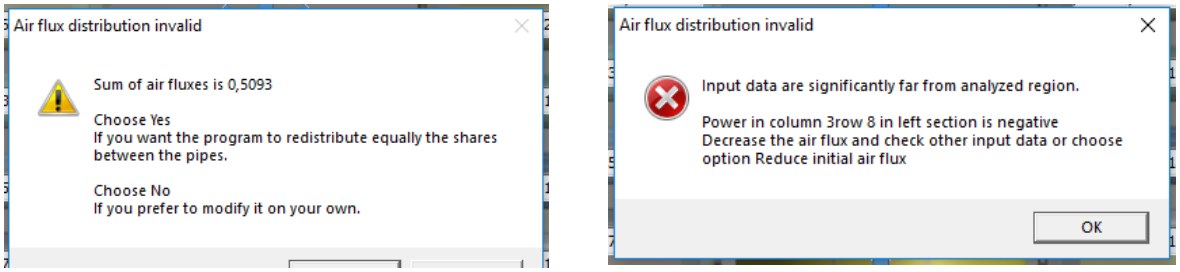

Figure 43 Warning communicates - choice window (left) and error window (right)

In the situation of pipes turning off the user should decide whether the air volume would stay the same (redistributed within still left pipes) or be reduced. Similar choice relates to the steam flow rate which by default is shared between sections according to internal formula. For analysis, especially the ones where first rows of pipes are cut it was enabled to choose equal redistribution by marking EQUAL box. In addition to these, there were two more buttons implemented in this interface. The first one is used for saving the given output. It is useful for repeating the calculation not to type the same values a few times. The second one lets the user come back to default options.

One more time, the user is informed which values can be modified and what kind of conditions can be switched on/off for calculation. Some of the details are highlighted in the left, bottom corner. For more information, the user has to activate Help interface showed in Figure 44.

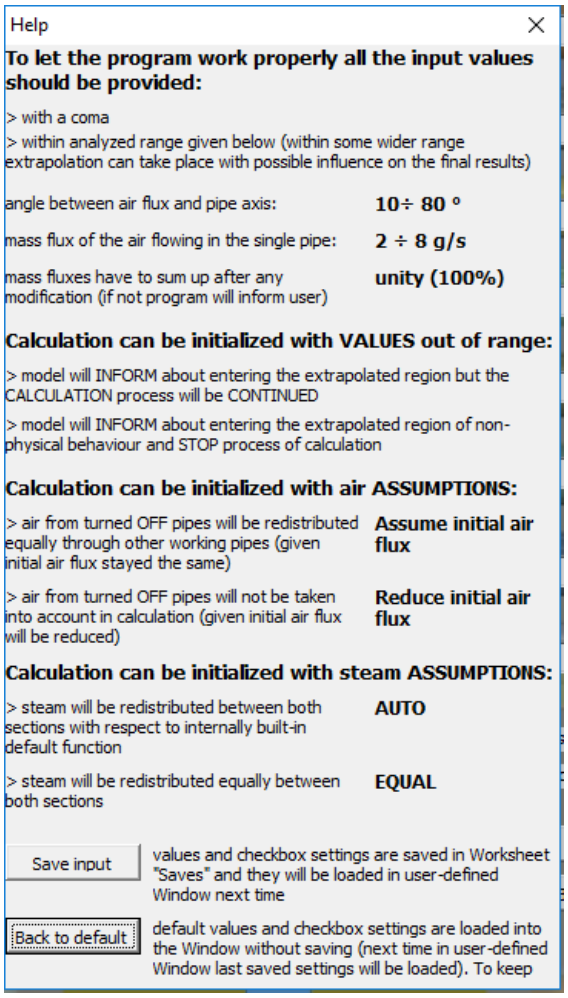

Figure 44 GUI2 - Help

When choosing Calculate (Figure 42) program will show final GUI with main outputs – the same which then could be found in first Worksheet “Input_Output”. In the same interface may appear communicate when the fog appears at the outlet of *THSC.*

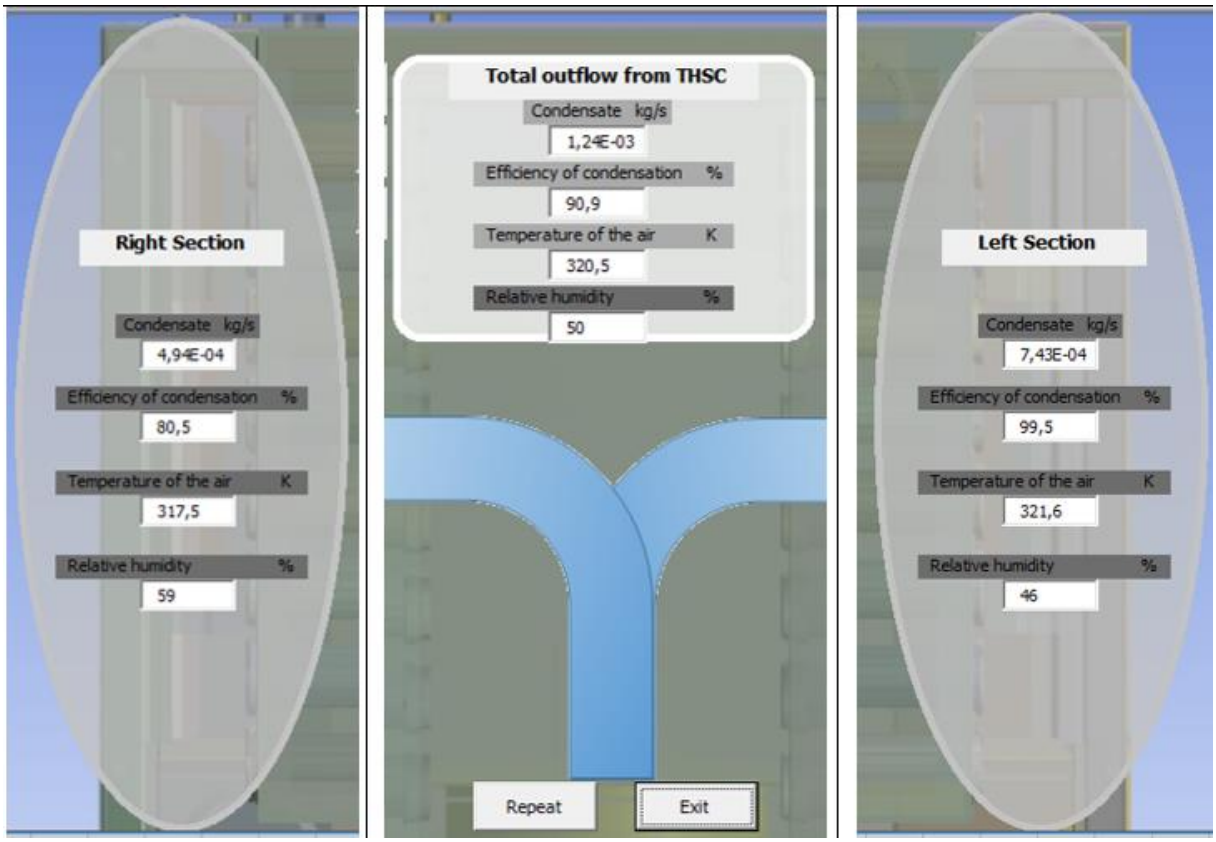

Figure 45 GUI4 - Results

From this place, the user can decide to close the window and work with the Excel file e.g. to save and analyze the results (Figure 36) or to repeat the procedure going directly to the first GUI (Figure 40). How the last GUI looks like is visible in Figure 45.

Appendix B

Table 25 Set of all meshes and benchmark

K- ω models														
mesh name		**benchmark**	**I**	**II**	**III**	**IV**	**V**	**VI**	**VII**	**VIII**	**IX**	**X**	**XI**	**XII**	**XIII**
surface integrals															
report type	**Surface***	**velocity values [m/s]**													
mass-weighted average	air cross-section	11.03	10.68	10.72	10.73	11.02	11.01	10.96	11.01	10.97	10.97	11.01	11.09	11.22	11,27
	fin&air cross-section	11.09	10.38	11.28	11.55	12.15	12.08	12.20	12.07	12.21	11.88	12.07	12.09	11.97	12,17
	outlet air	11.28	10.91	10.99	11.02	11.07	11.04	11.07	11.05	11.08	11.07	11.04	11.10	11.14	11.17
report type	**surface**	**temperature values [K]**													
mass-weighted average	air cross-section	309.27	311.23	311.31	310.15	309.67	309.33	309.53	309.31	309.55	309.45	309.27	309.10	308.36	308,30
	fin&air cross-section	311.32	316.11	311.64	307.86	305.97	305.00	304.34	305.00	304.33	306.24	305.00	305.49	306.12	305,23
	outlet air	331.11	333.54	334.09	331.05	334.06	331.34	331.33	331.34	331.32	331.34	331.35	331.30	331.27	331.28
fluxes															
mass flow rate net results [kg/s]		3.7E-17	-1.7E-17	0.0E+00	0.0E+00	6.9E-18	7.8E-18	-2.3E-17	-3.5E-18	-5.2E-18	2.6E-18	8.7E-18	-3.1E-17	-2.6E-18	-1.4E-17
total heat transfer rate net results [W]		-4.8E-13	6.2E-12	-1.2E-11	-1.6E-12	-2.6E-11	-8.2E-08	1.2E-08	6.8E-13	1.2E-12	-2.3E-12	1.5E-08	-2.2E-12	4.7E-12	6.2E-12
edge sizing* **		**number of elements**													
air top/bottom between fins (1)		16	6	8	8	10	10	10	10	10	10	10	12	14	16
air between fins side (2)		23	10	12	13	14	14	14	14	15	13	13	15	16	16
fin top/bottom side (3)		4	2	3	3	3	3	3	3	3	3	3	3	3	3
inside square side (4)		40	24	33	33	20	20	20	20	20	20	20	20	20	20
between arcs side (5)		8	4	6	6	6	6	6	6	6	6	6	6	6	6
pipe side (along the pipe)		200	100	110	120	100	120	130	130	130	140	140	114	95	88